NIST SPECIAL PUBLICATION 400-82

U.S. DEPARTMENT OF COMMERCE/National Institute of Standards and Technology

Semiconductor Measurement Technology:

Database for and Statistical Analysis of the Interlaboratory Determination of the Conversion Coefficient for the Measurement of the Interstitial Oxygen Content of Silicon by Infrared Absorption

A. Baghdadi, R. I. Scace, and E. J. Walters, Editors

NATIONAL INSTITUTE OF STANDARDS & TECHNOLOGY
Research Information Center
Gaithersburg, MD 20899

The National Institute of Standards and Technology[1] was established by an act of Congress on March 3, 1901. The Institute's overall goal is to strengthen and advance the Nation's science and technology and facilitate their effective application for public benefit. To this end, the Institute conducts research to assure international competitiveness and leadership of U.S. industry, science and technology. NIST work involves development and transfer of measurements, standards and related science and technology, in support of continually improving U.S. productivity, product quality and reliability, innovation and underlying science and engineering. The Institute's technical work is performed by the National Measurement Laboratory, the National Engineering Laboratory, the National Computer Systems Laboratory, and the Institute for Materials Science and Engineering.

The National Measurement Laboratory

Provides the national system of physical and chemical measurement; coordinates the system with measurement systems of other nations and furnishes essential services leading to accurate and uniform physical and chemical measurement throughout the Nation's scientific community, industry, and commerce; provides advisory and research services to other Government agencies; conducts physical and chemical research; develops, produces, and distributes Standard Reference Materials; provides calibration services; and manages the National Standard Reference Data System. The Laboratory consists of the following centers:

- Basic Standards[2]
- Radiation Research
- Chemical Physics
- Analytical Chemistry

The National Engineering Laboratory

Provides technology and technical services to the public and private sectors to address national needs and to solve national problems; conducts research in engineering and applied science in support of these efforts; builds and maintains competence in the necessary disciplines required to carry out this research and technical service; develops engineering data and measurement capabilities; provides engineering measurement traceability services; develops test methods and proposes engineering standards and code changes; develops and proposes new engineering practices; and develops and improves mechanisms to transfer results of its research to the ultimate user. The Laboratory consists of the following centers:

- Computing and Applied Mathematics
- Electronics and Electrical Engineering[2]
- Manufacturing Engineering
- Building Technology
- Fire Research
- Chemical Engineering[3]

The National Computer Systems Laboratory

Conducts research and provides scientific and technical services to aid Federal agencies in the selection, acquisition, application, and use of computer technology to improve effectiveness and economy in Government operations in accordance with Public Law 89-306 (40 U.S.C. 759), relevant Executive Orders, and other directives; carries out this mission by managing the Federal Information Processing Standards Program, developing Federal ADP standards guidelines, and managing Federal participation in ADP voluntary standardization activities; provides scientific and technological advisory services and assistance to Federal agencies; and provides the technical foundation for computer-related policies of the Federal Government. The Laboratory consists of the following divisions:

- Information Systems Engineering
- Systems and Software Technology
- Computer Security
- Systems and Network Architecture
- Advanced Systems

The Institute for Materials Science and Engineering

Conducts research and provides measurements, data, standards, reference materials, quantitative understanding and other technical information fundamental to the processing, structure, properties and performance of materials; addresses the scientific basis for new advanced materials technologies; plans research around cross-cutting scientific themes such as nondestructive evaluation and phase diagram development; oversees Institute-wide technical programs in nuclear reactor radiation research and nondestructive evaluation; and broadly disseminates generic technical information resulting from its programs. The Institute consists of the following divisions:

- Ceramics
- Fracture and Deformation[3]
- Polymers
- Metallurgy
- Reactor Radiation

[1]Headquarters and Laboratories at Gaithersburg, MD, unless otherwise noted; mailing address Gaithersburg, MD 20899.
[2]Some divisions within the center are located at Boulder, CO 80303.
[3] Located at Boulder, CO, with some elements at Gaithersburg, MD.

Semiconductor Measurement Technology:

Database for and Statistical Analysis of the Interlaboratory Determination of the Conversion Coefficient for the Measurement of the Interstitial Oxygen Content of Silicon by Infrared Absorption

Aslan Baghdadi, Robert I. Scace, and E. Jane Walters, Editors

Semiconductor Electronics Division
Center for Electronics and Electrical Engineering
National Engineering Laboratory
National Institute of Standards and Technology
Gaithersburg, MD 20899

July 1989

NOTE: As of 23 August 1988, the National Bureau of Standards (NBS) became the National Institute of Standards and Technology (NIST) when President Reagan signed into law the Omnibus Trade and Competitiveness Act.

U.S. DEPARTMENT OF COMMERCE, Robert A. Mosbacher, Secretary
NATIONAL INSTITUTE OF STANDARDS AND TECHNOLOGY, Raymond G. Kammer, Acting Director

Library of Congress Catalog Card Number: 89–600739
National Institute of Standards and Technology Special Publication 400-82
Natl. Inst. Stand. Technol. Spec. Publ. 400-82, 179 pages (July 1989)
CODEN: NSPUE2

U.S. GOVERNMENT PRINTING OFFICE
WASHINGTON: 1989

For sale by the Superintendent of Documents, U.S. Government Printing Office, Washington, DC 20402–9325

PREFACE

This report contains complete supporting information on a worldwide interlaboratory experiment to determine the conversion coefficient relating infrared (IR) measurements of interstitial oxygen in silicon to absolute measurements (charged particle activation analysis, photon activation analysis, inert gas fusion analysis). The interstitial content of silicon wafers destined for integrated circuit manufacture is tightly specified by process engineers because precise knowledge of the oxygen content is required in order to design the fabrication process. Controlled precipitation of oxygen during processing creates gettering centers within the bulk of the silicon, which serve to trap fast-diffusing impurities such as iron, nickel, and cobalt. Infrared measurements, since they are nondestructive, quick, and inexpensive, are routinely used to monitor the oxygen content of production wafers. However, the infrared measurements are relative measurements only. The infrared technique must be calibrated by other methods which are capable of measuring the oxygen content of silicon directly. These absolute measurements are destructive and expensive, so they cannot be used to monitor production wafers, but are used in this study to calibrate the infrared measurements.

A number of workers have reported values for this conversion coefficient in recent years; most of them are in general agreement with one another but differ significantly from the value required by ASTM and DIN standards. The present work, in which all of the recent workers in the subject were participants, was done to establish this important relationship as carefully as possible. The result is being incorporated in revised ASTM standards. A description of the experiment is being published*. It should be read as a necessary adjunct to this report, which does not repeat much of the published information. A preprint appears as Appendix C.

This report contains many details of the work, including the complete set of data obtained in the study (Appendices A and B), that could not be included in a journal article for space reasons. The report makes this information available to any interested persons, including the participants. It also makes the IR database accessible for the future, if it should become possible to realize a substantial improvement in the accuracy and statistical distribution of the absolute methods, which accounts for most of the uncertainty in the conversion coefficient. The material specimens are being retained at the National Institute

* Baghdadi, A., Bullis, W. M., Croarkin, M. C., Li, Y., Scace, R. I., Series, R. W., Stallhofer, P., and Watanabe, M., Interlaboratory Determination of the Calibration Factor for the Measurement of the Interstitial Oxygen Content of Silicon by Infrared Absorption, *J. Electrochem. Soc.* **136**, 2015-2024 (July 1989).

of Standards and Technology (formerly National Bureau of Standards) and could be used for further study.

The experimental design is detailed in the *Journal of the Electrochemical Society* paper and described briefly in section 1 of this report. It is a complex design, intended to allow a large number of IR laboratories (18) to participate in parallel over a reasonably short period of time. Eight sets of virtually identical specimens were cut from 20 specially grown silicon ingots. Seven sets were circulated for IR measurements, each accompanied by a "zero-oxygen" reference specimen and a sapphire plate used in an instrumental check. Charged particle activation analysis measurements were made following the IR measurements on some of these sets. The photon activation and inert gas fusion analyses were made on larger pieces taken from a neighboring part of the ingots. Over 2500 IR measurements and 235 absolute measurements were reported and are included in this report.

The price of complexity in experimental design is difficulty in statistical analysis. M. C. Croarkin, whose report is in section 4, participated in the design of the experiment and was the principal statistical consultant. A second approach was contributed by J. Mandel, author of section 5, who is well known for his work on methods for analyzing data from interlaboratory experiments. The two analyses take quite different approaches, but yield comparable (though slightly different) results. Croarkin's analysis focuses on the main bodies of data, one from the IR work and the other from the absolute measurements, to seek the conversion coefficient as the relating constant between them. Her work uses methods perhaps more familiar to most researchers. Mandel, on the other hand, looked for relationships, laboratory by laboratory, to see whether or not one can find useful information on within-laboratory and between-laboratory differences. We have chosen to take as the result for publication the one from Croarkin, in part because the effects of possible material inhomogeneities can be assessed more clearly from her approach. The fact that the two approaches, using significantly different methods, yield similar results lends considerable credence to both and to the work as a whole.

Table of Contents

List of Figures

List of Tables

1. INTRODUCTION

A. Baghdadi and R. I. Scace

This Special Publication* contains the data collected for the worldwide, double-round-robin determination of the conversion coefficient used to calculate the interstitial oxygen content of silicon from infrared absorption measurements. It also contains detailed statistical analyses of those data. A paper describing the results of this study is being published by the *Journal of the Electrochemical Society.*† It should be considered the official result of the study. The approach taken to determine the conversion coefficient was to conduct interlaboratory round robins for both the infrared measurements and the absolute measurements. The infrared measurements were carried out at 18 laboratories in China, Europe, Japan, and the United States (see table 1-1), using either dispersive infrared (DIR) or Fourier transform infrared (FTIR) spectrometers. The absolute measurements were carried out at eight laboratories in Europe, Japan, and the United States, using either charged-particle activation analysis (CPAA), photon activation analysis (PAA) or inert gas fusion analysis (IGFA).

Table 1-1 outlines the experimental plan for this study. It can be used to follow any test set throughout the study. For example, test set 2 was measured by IR at Toshiba, Nippon Telegraph and Telephone, Komatsu, Hitachi, and then Toshiba again. After the IR measurements, it was measured by CPAA.

The sample sets were produced specifically for this project by eight leading producers of semiconductor silicon. The samples were cut from 20 different 100-mm-diameter silicon crystals with room-temperature free-carrier concentrations of less than 2×10^{15} cm^{-3}. The crystals were grown so that the IR absorption coefficient at 1107 cm^{-1} due to oxygen for all the slices were distributed relatively uniformly from about 0.9 cm^{-1} to about 5 cm^{-1}.

Each laboratory contributing specimens cut a 120-mm-long section from each crystal. Two 2-mm-thick slices, a 10-mm-thick slug, and then two more 2-mm slices were cut from the end of this section, as shown in figure 1-1a. The 2-mm slices were polished on both sides. The 10-mm-thick slug was reserved for PAA or IGFA measurements. Samples for the destructive PAA and IGFA measurements were cut from the 10-mm slugs as they were

---

* Certain commercial equipment, instruments, or materials are identified in this paper in order to adequately specify the experimental procedure. Such identification does not imply recommendation or endorsement by the National Institute of Standards and Technology, nor does it imply that the materials or equipment identified are necessarily the best available for the purpose.

† Baghdadi, A., Bullis, W. M., Croarkin, M. C., Li, Y., Scace, R. I., Series, R. W., Stallhofer, P., and Watanabe, M., Interlaboratory Determination of the Calibration Factor for the Measurement of the Interstitial Oxygen Content of Silicon by Infrared Absorption.

Table 1-1. Experimental plan[a]

JEIDA SETS			TEST SETS[b]						
J-1	J-2	J-3	1	2	3	4	5	6	7
TOS			TOS	TOS					TOS
NTT	NBS		NBS	NTT	NBS				NBS
KOM				KOM					
HIT	MON	WAC	WAC	HIT	MON	WAC			WAC
TOS	SIL			TOS	SIL				
CPAA		TFK		CPAA		TFK			
NBS[c]	NBS				NBS				
CPAA	RSR		RSR	TOS[c]	CPAA		RSR		RSR
WAC[c]		WAC				WAC			
	MUL			NBS[d]	NBS[d]		MUL		
CPAA	GEC	SIM	SIM			CPAA	GEC	SIM	SIM
WAC[c]	RSR	DNS				WAC[c]	RSR		
CPAA	TOS[d]	TEM	NBS[d]				DNS	TEM	NBS[d]
		ZJU					ENS[e]	ZJU	
		SSS						SSS	
		SIM				CPAA		SIM	
TOS[d]		TOS[d]				NBS[d]	NBS[d]	NBS[d]	

[a] 10-mm slugs cut from ingots were used for destructive PAA measurements in UK and Germany, as well as for IGFA in Germany

[b] Test set 8 was reserved for high-temperature anneal and remeasure for total oxygen

[c] Transit only, no measurements

[d] Home location

[e] ENS measured only specimens from ingots 2101-05 to 2109-05

Participating laboratories (Regional coordinators in boldface followed by standards organization):

TOS **Toshiba Ceramics, JEIDA**
HIT Hitachi
KOM Komatsu Electronic Metals
NTT Nippon Telegraph and Telephone

NBS **National Bureau of Standards (U.S.), ASTM**
MON Monsanto
SIL Siltec Silicon

WAC **Wacker Chemitronic, DIN**
TFK Telefunken

RSR **Royal Signals and Radar Establishment (U.K.)**
DNS Dynamit Nobel Silicon
ENS École Normale Superiéure, Université Paris VII, France
GEC General Electric Company, Ltd.
MUL Mullards, Ltd.

SIM **Shanghai Institute of Metallurgy (Academia Sinica)**
SSS Shanghai Second Smelting Plant
TEM Tianjin Electronic Materials Research Institute
ZJU Zhejiang University

needed. Two of the four 2-mm slices were used for the IR and CPAA measurements. The remainder of each crystal was set aside for future or follow-up experiments.

The nominal oxygen concentration was measured by the silicon producers. They measured the IR absorption at least three times at each of four positions on each slice 90 deg apart located 18.5 $\pm$ 1.0 mm from the center of the slice, with one measurement on each of the four radii at 45 deg to the bisector of the primary flat. The oxygen concentration reported was the average of these measurements. The maximum difference in the IR absorption coefficient due to oxygen in slices cut from either side of the 10-mm slug was less than 0.06 cm^{-1}. These measurements were used to qualify the test sets prior to the round robin.

Four squares, 25 $\pm$ 1 mm on a side, were cut from the center of each of 2 slices from each of the 20 crystals, as shown in figure 1-1b. Each square was laser marked or scribed in the corner nearest the center of the slice with a three-part code which identified the preparing organization, the set number from that organization, and the square number. There were eight squares, marked 1 through 8, prepared from each crystal. Thus there were 8 essentially equivalent test sets of 20 squares each specially prepared for this study. In addition to these 8 sets of 20 squares, 3 sets of 7 samples each were supplied by the Japan Electronic Industry Development Association (JEIDA). The eight test sets prepared for this study were designated Test Sets 1 through 8, and the JEIDA test sets were designated JEIDA Sets 1 through 3. Test sets 2 through 6 also included an oxygen-free float-zoned (FZ) reference square, and a sapphire filter to be used in an instrumental check.

The thicknesses of the test and reference squares were measured at the National Institute of Standards and Technology (formerly National Bureau of Standards), Toshiba Ceramics, Wacker Chemitronic, and the Shanghai Institute of Metallurgy. All replicate thickness measurements agreed to within $\pm$0.05%.

Section 2 of this publication describes the procedural instructions given to the infrared laboratories. Since the methodology for each of the absolute measurements was developed individually at each of the absolute laboratories, section 3 consists of separate reports from each of the laboratories describing the techniques they used.

The statistical analysis used to obtain the conversion coefficient quoted in the paper submitted to the *Journal of the Electrochemical Society* was carried out by M. Carroll Croarkin of the Statistical Engineering Division at the National Institute of Standards and Technology. This analysis is described in section 4. The general methodology used for this analysis was to develop an empirical straight line fit relating the oxygen content as determined by the absolute laboratories to the infrared absorption coefficient as determined by the IR laboratories. The slope of the straight line is the conversion coefficient. The analysis accounts for the fact that there is random error in both the absolute and IR measurements.

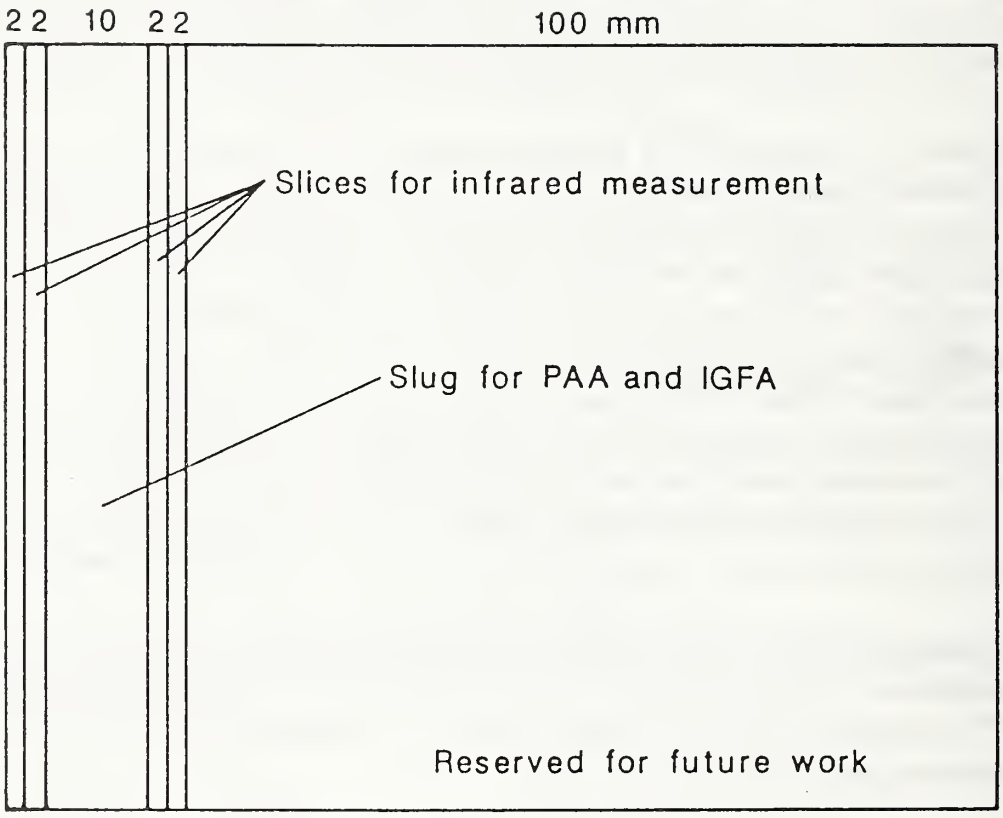

Figure 1-1a. Schematic of 100-mm-diameter silicon crystal showing four 2-mm-thick slices for infrared absorption and CPAA measurements, a 10-mm-thick slug for PAA and IGFA measurements, and the 100-mm-wide section reserved for future work.

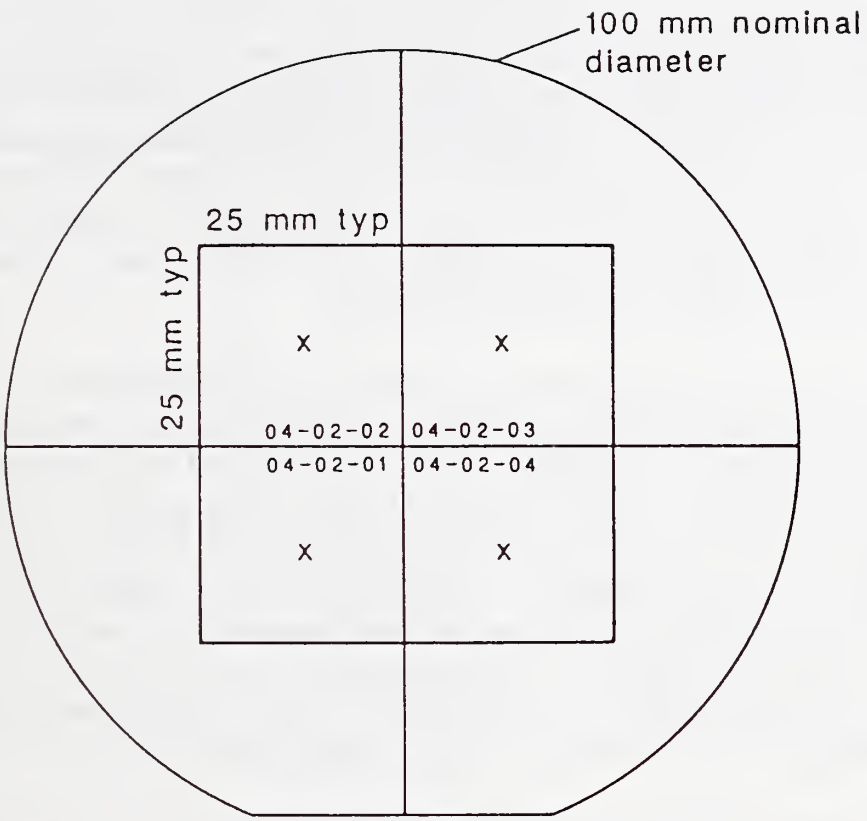

Figure 1-1b. Diagram of 2-mm-thick slice, showing test squares 1 to 4, 25 mm on a side; identification markings (04-02-0x); and the location of the infrared measurements (x). A second similar slice contains test squares 5 to 8.

The data from the 18 IR laboratories were all consistent with each other, and therefore data from all the IR laboratories were included in the final computation of the conversion coefficient.

The data from the absolute laboratories were not as consistent. Significant "outliers" were identified and excluded. After their exclusion, the data from each of the absolute laboratories were further analyzed to decide whether to include that laboratory's data in the final computation. Since the IR data were consistent with each other, they were used as the baseline for evaluating the results from the absolute laboratories. The absolute results were tested by determining whether, when plotted against the IR data, they fit the model of a straight line with a zero intercept. The data from five of the eight laboratories fit this model. The data from three laboratories did not fit the model and were, therefore, excluded in the final computation of the conversion coefficient. The conversion coefficient was calculated by pooling absolute data on the test sets as a single data set and fitting a zero-intercept straight line to the average of the infrared data. Absolute data on the JEIDA sets were used to corroborate the results.

An alternative analysis of the data was carried out by John Mandel of the National Measurement Laboratory of the National Institute of Standards and Technology. This analysis is described in section 5. This analysis also concluded that the data from the same three laboratories should be excluded. Mandel's analysis differed from Croarkin's analysis in many respects. The most important difference was that, while Croarkin pooled all the absolute data into a single data set, Mandel obtained a slope from each individual absolute laboratory by fitting its data to a straight line against the average of the IR data for each ingot. Mandel assigned a weighting factor to the slope obtained from each of the absolute laboratories, based upon the quality of fit for each laboratory's data, and used that weighting factor in calculating the final value for the conversion coefficient.

Croarkin's analysis yielded a conversion coefficient of 6.28 ± 0.18 ppma/cm^{-1}, and Mandel's analysis yielded a conversion coefficient of 6.03 ± 0.108 ppma/cm^{-1},* with limits to random errors in both analyses estimated as twice the standard deviation of the estimated conversion coefficient. Random errors are due to nonreproducibility among and between the different laboratories. Systematic error, as estimated by Croarkin, is due to possible inhomogeneity in the sample set. The fact that two fundamentally different analytical approaches yield results in reasonable agreement with each other shows that the data are "robust," i.e., data that are not sensitive to the particular analytical approach used in evaluating it. The two analyses essentially differ on how the data from the different absolute laboratories, which used different methodologies, should be combined. Croarkin's analysis placed all the individual data points on an equal footing. Mandel's analysis eval-

* Mandel's result here is quoted in ppma/cm^{-1} to allow a direct comparison with Croarkin. His calculations in section 5 use μg/g as the unit of concentration.

uated each of the absolute laboratories based upon the quality of the fit of its data to the model, and then assigned weights to each of the laboratories accordingly in combining the data. Mandel's analysis thus rests upon the assumption that all the errors in each absolute laboratory would affect the quality of the fit to the model. That ignores the possibility of systematic errors that are proportional to the oxygen content. Croarkin's analysis makes no such explicit assumption. All three absolute analytical methods used in this study rely upon several calibration steps. Any error in one of these steps would result in a systematic error proportional to the oxygen content of the sample.

Appendices A and B contain data obtained by the infrared laboratories and from the absolute laboratories, respectively. Appendix C is a preprint of the results of this study, to be published in the *Journal of the Electrochemical Society.*

2. INFRARED ABSORPTION TEST METHOD

Instructions to the Participating IR Laboratories

Make IR absorption measurements by the difference method using the oxygen-free FZ reference supplied. Single- or double-beam techniques may be used with either FTIR or dispersive IR spectrophotometers. In either case, report measurement conditions and instrument used to your coordinating laboratory on the data cover sheet supplied.

Immediately prior to the initial measurement in any laboratory, etch the silicon test squares (including the reference specimen) in HF to remove any surface oxide. Record spectra over the wavenumber range from 450 to 1350 cm^{-1}. Use the following test conditions:

Resolution: 4 cm^{-1} at 1107 cm^{-1}

Number of scans: Minimum of 64 (Note: For dispersive instruments which do not have an averaging capability, use an equivalent scan speed.)

Measurement location: Center of square

Detector: Tri-Glycerine Sulfide (TGS), if available

Perform the following instrumental checks immediately prior to each set of measurements using the measurement conditions outlined above (except where noted otherwise in 2 and 5):

1. Establish the 100% baseline. On double-beam instruments, record the transmittance spectrum with the sample and reference beams both empty. On single-beam instruments, obtain the ratio of two spectra taken with the reference specimen in the sample beam; after taking the first reference spectrum, wait for a time equivalent to that which will be required to collect the sample spectra in the measurement sets before taking the second reference spectrum. Provide a hard copy of the 100% line over a wavenumber range which includes 900 to 1300 cm^{-1}; use an expanded transmittance scale, a scale from 97 to 103% with an interval of at least 1%/inch (0.5%/cm is preferred).

2. Establish the 0% line (dispersive instruments only). With the sample beam blocked, record the instrument zero over the range 900 to 1300 cm^{-1}. Provide a hard copy of the 0% line over this wavenumber range on an expanded transmittance scale.

3. Determine whether stray light is present. Run an air-reference transmittance spectrum using the sapphire cut-off filter supplied. Provide a hard copy of the spectrum

over the range 900 to 1300 cm^{-1} on an expanded transmittance scale, with an interval of at least 1%/inch (0.5%/cm is preferred).

4. Determine mid-scale linearity. Run an air-reference transmittance spectrum using the reference specimen over the wavenumber range 450 to 4000 cm^{-1}. Report the transmittance at both 1107 and 4000 cm^{-1} and provide a hard copy of the transmittance spectrum.

5. Establish the throughput characteristics (FTIR instruments only). Record a background spectrum with the sample beam empty over the wavelength range from 450 to 4000 cm^{-1} and provide a hard copy of this spectrum.

Measure the test samples at least three (3) times over a three- (3-) or more day period. Before measuring the samples, allow them to come to thermal equilibrium near the spectrometer. Supply the infrared spectra as ratioed transmittance spectra. For measurements on double-beam (dispersive) instruments, the oxygen-free reference should be in the reference beam and the oxygen-containing sample should be in the sample beam. For measurements on single-beam (FTIR) instruments, the transmittance spectrum should be obtained from the ratio of the transformed emission spectrum of the oxygen-containing sample to the transformed emission spectrum of the oxygen-free reference. Supply a hard copy of each ratioed spectrum together with the results of the instrumental checks.

Forward all data to your coordinating laboratory, which will forward a complete set to Aslan Baghdadi at the National Bureau of Standards.

Supplementary Instructions for Toshiba Ceramics, NBS, and Wacker: Please measure or verify the thickness of all test and reference squares sent to you and report the results of the thickness measurements to Aslan Baghdadi at NBS.

3. ABSOLUTE TEST METHODS: REPORTS FROM THE LABORATORIES

This section was compiled from reports submitted by each of the absolute laboratories describing the procedures they used to measure the oxygen content of the test specimens.

The charged particle activation analysis method was used by five laboratories, the photon activation analysis method was used by two laboratories, and one laboratory used inert gas fusion analysis.

Centre de Recherches Nucleaires, Strasbourg
Report from Dr. J. Stoquert

A. METHOD

1. Irradiation:

The samples are irradiated by the ^{3}He beam of the tandem Van de Graaff accelerator of the Centre de Recherches Nucleaires. The beam passes through aluminum and silicon absorbers before irradiating the samples. The oxygen is activated through the reaction:

$$^{16}\mathrm{O}(^3\mathrm{He},p)^{18}\mathrm{F} \xrightarrow{\beta^+(T_{0.5}=110min)} {}^{18}\mathrm{O}\ .$$

After irradiation, the Si samples are etched to avoid errors due to surface contamination and recoil implantation.

Typical values of the experimental conditions are:

incident ^{3}He^{++} beam energy, before absorbers: 20 MeV.
beam current: 150 nA (20 nA for Al_2O_3 reference)
absorber thicknesses: Al: 50 μm Si: 85 μm
etched thickness: 15 μm
effective ^{3}He energy E_i at the entrance of the sample, after etching, is 11.92 MeV.

The sample and the two absorbers were fixed in a Faraday cup and the total charge integrated for each run:

irradiation time 30 min (30 s for Al_2O_3 reference).

B. ACTIVITY MEASUREMENT

The β^+ spectrometer consists of two NaI γ-ray detectors (2×2 inches) at 180 deg from each other. They detect in coincidence the two γ-rays emitted at 180 deg during the positron annihilation. A classical fast-slow double-coincidence circuitry screens out the background γ-rays. The fast coincidence windows are 15 ns; the slow coincidence window is centered on the 511-keV peak. The background counting rate (without any source between detectors) is 1.2 counts per minute.

The activity curve is registered on a multiscale analyzer (2 min/channel) which counts the number of disintegrations as a function of time.

One activated isotope (example: O in Al_2O_3):

$$N = N_o e^{-\lambda t}$$

where N_o counts/channel at the end of the irradiation.

$\lambda = \frac{ln2}{T_{0.5}}$ where $T_{0.5}$ is the period, and N_o is determined by a least-squares fit of the experimental data (λ fixed).

C. POSSIBLE INTERFERENCES

Several isotopes are activated by the ^{3}He beam by the reactions

$$^{28}\mathrm{Si}(^3\mathrm{He}, p)^{30}\mathrm{P} \quad \overset{\beta^+, 2.5min}{\longrightarrow} \quad ^{30}\mathrm{Si}$$

and

$$^{12}\mathrm{C}(^3\mathrm{He}, ^4\mathrm{He})^{11}\mathrm{C} \quad \overset{\beta^+, 20min}{\longrightarrow} \quad ^{11}\mathrm{B} \ .$$

The total count is given by:

$$N = N_1 e^{-\lambda_1 t} + N_2 e^{-\lambda_2 t} + N_3 e^{-\lambda_3 t} + N_4 \ .$$

The experimental data are fitted by least squares to determine N_1, N_2, N_3 with

$$T_1 = \frac{ln2}{\lambda_1} = 2.5 \ min$$

$$T_2 = \frac{ln2}{\lambda_2} = 20 \ min$$

$$T_3 = \frac{ln2}{\lambda_3} = 110 \ min$$

$N_4 = 2.4$ counts per channel .

For each irradiation, the quantity A is calculated:

$$A = \frac{N_3}{Q} \frac{\lambda t_{irr}}{(1 - e^{-\lambda t_{irr}})(1 - e^{-\lambda t_{count}})} ,$$

where Q is the charge, t_{irr} is the irradiation time (30 min for Si), and t_{count} is the counting time per channel.

D. CONCENTRATION CALCULATION

The number n of atoms/cm^3 is given by

$$n = \frac{A}{\int_{E_g}^{E_i} \frac{\sigma(E)}{S(E)} dE} ,$$

where E_g is the threshold energy; E_i is the incident energy; $\sigma(E)$ is the reaction cross-section; and $S(E) = \frac{dE}{dx}$ is the stopping power.*

E. ERRORS

a) E_m:

Ishii *et al.* showed that errors $\frac{\Delta E_m}{E_m} = \pm 5\%$ at $E_i \approx 12$ MeV do not introduce significant errors in F (see fig. 1 of their paper; F is the relative content of a given isotope). That error is therefore neglected, and only errors due to the measurements of A and E_i are considered.

b) A and E_i:

$$\frac{dn}{n} = \frac{dA}{A} - \frac{\sigma(E_i)S(E_m)}{\Sigma(E_i)S(E_i)} dE_i$$

$$= \frac{dA}{A} - \frac{\sigma(E_i)}{\Sigma(E_i)} S(E_m) dx ,$$

* For a detailed discussion of the average stopping power method, see Ishii et al., The Average Stopping Power Method for Accurate Charged Particle Activation Analysis, *Nucl. Instr. Meth.* **150**, 213 (1978).

where dx is the error in absorber thickness and etched thickness measurement contributing to an error of E_i (effective incident energy).

The random error in the measurement, estimated from these factors, is 4%, when the same absorber is used for both the specimen and the reference measurements. A higher error,* however, was estimated for the silicon reference sample, which had a very low oxygen content.

c) Possibility of Systematic Errors:

Errors due to interfering reactions are minimized by the choice of an incident beam energy $E_i \approx 12$ MeV. There is a low probability for significant interfering reactions at this energy. The Al absorber is chosen so as to limit the recoil implant of other ions into the silicon. Carbon deposition during irradiation is observed and evaluated by the $T_{0.5} = 20$ min component of the decay curve. Correlation with etching thickness and total irradiation time is clearly seen, but no effect on the oxygen concentration is seen when the specimens are correctly etched.

Two possible errors may be due to absorption. The ^{3}He intensity diminution in Si and Al absorbers is neglected. The γ-ray at 511-keV absorption in the samples is taken into account using tables from J. H. Hubbell, *Applied Radiation & Isotopes* **33**, 1269 (1982).

The stopping power calculation data are taken from ^{4}He tables of J. F. Ziegler, *Helium: Stopping Power and Ranges in All Elemental Matter* (Pergamon Press, New York, 1977). The Bragg additivity rule was used for Al_2O_3.

The cross-section values for $^{16}O(^3He,p)^{18}F$ were taken from Hahn and Ricci, *Phys. Rev.* **146**, No. 3, 650 (1966), for energies below 10 MeV; and from Markovitz and Mahony, *Analytical Chemistry* **34**, No. 3, 32 (1982), for energies from 10 to 14 MeV.

* Regolini, Stoquert, et al. (ref. 15, Appendix C) estimate an error of $\pm 20\%$ in their measurement of low oxygen content silicon. [Note added by the editors.]

Institute for Nuclear Sciences, Rijksuniversiteit Gent
Report from Dr. K. Strijckmans

METHOD

Charged particle activation analysis is applied using the $^{16}O(^{3}He,p)^{18}F$ ($Q > 0$) reaction (^{18}F : $t_{0.5}$ = 109.8 min; β^+-emitter).

SAMPLE AND STANDARDS

Silicon samples were provided by P. Stallhofer, Wacker-Chemitronic. The surface of the silicon samples was rough on receipt. Quartz was used as an oxygen standard.

EXPERIMENTAL

Samples and standard, placed behind a copper foil serving as beam intensity monitor and an aluminium foil, were irradiated with 20 MeV ^{3}He particles. After irradiation, the samples were chemically etched in a mixture of concentrated $HNO_3/HF/CH_3COOH$ (68/9/23, v,v,v) to remove a 5.2 to 6.2 mg/cm^2 surface layer. No interference from surface oxygen occurs for a chemical etch exceeding 3 mg/cm^2 as experimentally determined. Samples and standards were measured repeatedly with $\gamma - \gamma$ coincidence set-up with two NaI(Tl) detectors at 180 deg to obtain the decay curve.

ANALYSIS

The decay curve was analyzed using the CLSQ program of Cumming.* The best fit for the half-life of ^{18}F yielded 110.4 $\pm$ 1.7 min (mean $\pm$ standard deviation for 17 decay curve analyses of the Si samples), which agrees with the literature value of 109.8 min.

To correct for the different stopping power of standard versus sample, the numerical integration method† was applied, using the stopping power data of Ziegler‡ and the excitation function data of Vandecasteele et al.§.

The method is interfered with by F and Na to an extent of 5% for equal concentrations. The analyzed mass is $\approx$20 mg. One sample was analyzed for each irradiation campaign and it yielded a standard deviation of 13%, which corresponds with the reproducibility attainable with this method at this concentration level.

---

* J. Cumming in *Applications of Computers to Nuclear and Radiochemistry,* G. O'Kelley, Ed., NAS-NS 3107 (1963).

† C. Vandecasteele and K. Strijckmans, *J. Radioanal. Chem.* **57**, 121 (1980).

‡ J. F. Ziegler, *Helium: Stopping Power and Ranges in All Elemental Matter* (Pergamon Press, New York, 1977).

§ C. Vandecasteele, F. Adams, and J. Hoste, *Anal. Chim. Acta* **71**, 67 (1974).

Max-Planck-Institut für Metallforschung, Dortmund
Report from Dr. E. Grallath

SPECIMEN PREPARATION

The specimens were cleaned prior to analysis according to the procedure of the BCR: etch 1 to 1.5 m in a mixture of 3:5:3 v/v/v HF (40%) : HNO_3 (d=1.4) : acetic acid (96%) at room temperature; wash three times in water; wash three times in methanol; dry in a warm air stream. During etching and rinsing, an ultrasonic bath was used. The samples were stored dustfree before analysis (maximum 2 h).

ANALYTICAL APPARATUS

Oxygen determination by the carrier-gas fusion extraction process was done with a Leybold-Heraeus NOA 2003 nitrogen-oxygen analyzer. Helium was the carrier gas. In contrast with the usual apparatus of this type, the equipment is fitted with a more sensitive CO detector (IR absorption, 5000 ppm BINOS). It also has the capability for heating the specimen in a graphite crucible under temperature program control. A Leco double crucible was used. In this arrangement, the outer crucible is heated directly by the passage of electric current. The inner crucible, which contains the specimen, is only indirectly heated; it thus has a more uniform temperature distribution.

ANALYTICAL PROCEDURE

About 1 g nickel is placed in the inner crucible and heated gas-free to about 2000 °C for 1.5 min. After the temperature is reduced to about 1500 °C (temperature program), the prepared specimens (three to four pieces per analysis) are dropped into the nickel bath through an airlock. At the same time, the temperature program starts a linear heating of the crucible up to about 1800 °C within 10 s. The oxygen present in the specimen (and on the surface) is set free as CO by melting of the specimen, is carried by the carrier gas to the CO detector, and measured. A Spectra-Physics SP 4200 computing integrator at the output of the detector is used for evaluating the signal. A new crucible is used for each analysis.

CALIBRATION

Calibration of the equipment is done with a calibration gas. This is done by introducing, with a built-in thermostated dosing apparatus, 536 μL of a calibration gas mixture (29.86 $\pm$0.12 vol% CO, 20.23 $\pm$ 0.15 vol% N_2, balance He; from Messer Griesheim) dynamically diluted 10:90 with He into the carrier gas stream of the apparatus. This calibration procedure passes a dose of 9.8 μg of oxygen as CO over the hot crucible.

CALCULATIONS

A blank value of 0.1-μg oxygen per cm^2 of specimen surface is subtracted from the gross measured value. This correction value was determined from 13 blank determinations with specimens 3R, 133R, 137R, and 256R provided by the BCR as "zero material." From the value for $\hat{x}_b$ of 0.35 μg O (s=0.15 μg O), and under the assumption that practically the entire blank value rises from the specimen surface, a residual surface oxygen content of 0.1 $\mu g/cm^2$ follows. From the blank value scatter, the detection limit (3 s) of the procedure is calculated to be 0.45 μg.

Bundesanstalt für Materialprüfung (BAM), Berlin
Report from Dr. B. F. Schmitt

METHOD

The method used was photon activation analysis of oxygen.

SPECIMENS

The specimens were rectangular parallelopipeds 5 by 5 by 8 mm^3. The reference used was BeO. The specimen mass was about 880 mg, and the reference specimen's mass was about 28 mg. The specimens and reference specimens were wrapped in Al foil.

ACTIVATION

The maximum electron energy was 30 MeV. The electron current was 100 μA. The specimens were irradiated for 4 min, except for specimen 10/4, which was irradiated for 10 min. The specimens were rotated during activation in the photon stream.

ETCHING

After irradiation, specimens were etched in concentrated HF-HNO_3 for about 10 s. Etch loss was about 30 to 50 mg.

HEAT EXTRACTION

Heat extraction was carried out in a graphite crucible at 2020 °C, with a helium carrier gas stream at 0.2 liters per minute, and 1.3 g iron as the bath metal. The CO was oxidized to CO_2 by Schütze reagent. The CO_2 was absorbed by ascarite (sodium asbestos).

ANALYSIS

The ^{15}O concentration was determined from coincidence measurement of annihilation radiation of positron decay. Final results were determined by calculation programs DKLIE and KNOFB.

Institut für Kernphysik, Wolfgang Goethe Universität, Frankfurt
Report from Dr. K. Bethge

METHOD

The method used was charged particle activation analysis, based upon the reactions

$$^{16}\mathrm{O}(^{3}\mathrm{He},p)^{18}\mathrm{F}$$

and

$$^{16}\mathrm{O}(^{3}\mathrm{He},n)^{18}\mathrm{Ne} \longrightarrow ^{18}\mathrm{F} \longrightarrow ^{18}\mathrm{O}\ .$$

The irradiation energy was 10-MeV $^{3}He^{++}$ particles. After irradiation, the surface was removed by etching of 16 μm. Thereafter, the irradiating energy was 8.8 MeV. The difference is due to the energy loss of the $^{3}He^{++}$ in the surface region.

ETCHING

The specimens were etched after irradiation for 90 s in 30 mL of etching agent. The etch used was HF:HNO_3 in a 1:5 ratio by volume. Approximately 16 μm of silicon on the surface was etched away.

MEASUREMENT

Two NaI detectors were arranged in opposition with a small gap between them, into which the specimens were inserted. The detectors were used in coincidence. The background counting rate was 0.05 counts per second, which was subtracted from the starting counting rate. There is no known interfering half-life for oxygen in silicon ($t_{0.5}$=109.7 min). Carbon, with a half-life of 20.3 min, can easily be distinguished. The estimated error for a single measurement is approximately $\pm$16%. The statistical error depends upon the counting rate.

CALIBRATION

As standard, an SiO_2 target was used for measuring the excitation function of the nuclear reaction.

CALCULATIONS

The oxygen concentrations were calculated using known cross sections σ(E) and known ranges of ^{3}He ions in silicon.

AERE Harwell, Oxfordshire
Report from Drs. J. Hislop and D. Wood

METHOD

The method used was photon activation analysis, based upon the reaction

$$^{16}\mathrm{O}(\gamma,n)^{15}\mathrm{O}\ ,$$

as described previously in J. Hislop et al., *J. Electrochem. Soc.* **133**, 189 (1986).

The potential interfering reactions are

$$^{19}\mathrm{F}(\gamma,nt)^{15}\mathrm{O}$$

and

$$^{28}\mathrm{Si}(\gamma,f)^{15}\mathrm{O}\ .$$

Both these reactions are considered negligible under the irradiation conditions used.

The γ rays are bremsstrahlung from 32-MeV electrons colliding with a 3-mm-thick tungsten target. Integrated current is 6 to 7 μA, as measured on the tungsten converter with sample rotation during irradiation.

ETCHING

After irradiation, the specimens were etched twice using a mixture of HF/HNO_3/glacial HAc. Approximately 2% by weight was removed from the surface.

SAMPLES

The samples were 6 mm by 6 mm by 2 mm of silicon.

CALIBRATION

$Li_2B_4O_7$ pellets were used as the standards, without radiochemical separation.

MEASUREMENT

The oxygen was first separated from the silicon using inert gas fusion at 2000°C with a copper/graphite powder flux. $C^{15}O$ was adsorbed on "Hopcalite." Recovery is estimated to be greater than 95%, based upon analyses of SiO_2 layers of known thicknesses.

The concentration of ^{15}O was measured using β^+ annihilation radiation in NaI coincidence counters.

Institute of Physical and Chemical Research (RIKEN), Wako, Saitama
Report from Dr. T. Nozaki*

METHOD

The method used was charged particle activation analysis, based upon the reaction ^{16}O ($^{3}He, p$) ^{18}F. There are practically no interfering reactions for the semiconductor silicon matrix in the procedure described below.

ACTIVATION

The samples were bombarded behind a 50-μm-thick aluminum foil. The acceleration energy of the ^{3}He particles was 18 MeV, and the energy on the sample is estimated at 15 MeV. The incident particle flux was 2 to 4 μA and was kept as constant as possible in each bombardment, which was continued for 10 or 20 min.

ETCHING

From the bombarded sample, a surface layer of 23 $\pm$ 1 μm in thickness was removed by etching with HF-HNO_3 (1 vol : 3 vol).

MEASUREMENT

The annihilation radiation was usually measured a Ge(Li) detector. A polyethylene plate was inserted between the detector and the bombarded side of the sample plate in contact with both, for the minimization of the bremsstrahlung due to ^{31}Si formed from the matrix silicon. The measurement was initiated at about 1 h from the end of bombardment and usually repeated four times with about 1-h intervals, with each measurement continuing 200 s or 4 min. The γ-ray spectrum was analyzed by a microcomputer for the removal of the bremsstrahlung interference, and the result was often checked by manual analysis. For the sample of the lowest oxygen content, the annihilation radiation was measured by two BGO detectors operated in coincidence. This detection is of higher efficiency but is more sensitive to minute geometrical variation than the Ge(Li) counting.

CALIBRATION AND CALCULATION

A silica plate covered with a 20-μm aluminum foil was bombarded with a lower flux for a shorter time (3- to 6-μC fluence) for use as a standard. The aluminum foil is almost equivalent in ^{3}He energy loss to the sample surface removed by etching. Eight such sil-

* Present address: Kitasato University, Sagamihara, Kanagawa 228, Japan

ica standard plates were bombarded in a 20-h cyclotron machine time to ascertain the reproducibility.

The following relation was used for the calculation of oxygen content:

$$[\text{O Content of Si (wt fraction)}] = 0.4904 \frac{[^{18}\text{F Sat. Act. in Si}]}{[^{18}\text{F Sat. Act. in SiO}_2]} ,$$

where $[^{18}\text{F Sat. Act.}]$ is the ^{18}F saturation activity for 1-μA bombardment of the given sample. The factor 0.4904 was obtained by graphical integration from the excitation function of the $^{16}\text{O}(^3\text{He,p})\ ^{18}\text{F}$ reaction* and the stopping powers of the two matrices.†

REPRODUCIBILITY

From 1982 to 1985, the oxygen content of a silicon plate of presumably uniform oxygen content was determined repeatedly by the above procedure. The results were 9.86, 9.71, 10.05, 9.87, 10.20, 10.08, 10.13, and 10.28 μg/g ([mean] = 10.04, σ = 0.18). In the present work, each sample was analyzed at least twice. When the two results deviated more than 5% from each other, the analysis was repeated further.

* T. Nozaki et al., *Int. J. Appl. Radiat. Isotopes* **25**, 393 (1974).

† J. F. Ziegler, *Helium: Stopping Power and Ranges in All Elemental Matter* (Pergamon Press, New York, 1977).

Center for Chemical Characterization and Analysis, Texas A & M University
Report from Dr. E. Schweikert

METHOD

The method used was charged particle activation analysis, based upon the reactions

$$^{16}\mathrm{O}(^{3}\mathrm{He},p)^{18}\mathrm{F}$$

and

$$^{16}\mathrm{O}(^{3}\mathrm{He},n)^{18}\mathrm{Ne} \longrightarrow ^{18}\mathrm{F}\ .$$

There are two possible interfering reactions:

$$^{19}\mathrm{F}(^{3}\mathrm{He},\alpha)^{18}\mathrm{F} \quad \text{and} \quad ^{28}\mathrm{Si}(^{3}\mathrm{He},x)^{18}\mathrm{F}\ .$$

ETCHING

3 mg/cm^2 were removed from the surface.

IRRADIATION

The maximum energy of the beam produced by the Cyclotron was 18 MeV. After passing through an Al monitor foil and accounting for the 3 mg/cm^2 removed from the surface after irradiation, the energy of the beam actually impinging upon the measured specimen was 14.3 MeV.

CALIBRATION

Three Si samples with oxygen levels at 9.8, 6.7, and 14.3 ppm (weight), respectively, were used for standards. These Si standards were determined by French colleagues using triton activation $\left[^{16}O(^{3}H,n)^{18}F\right]$.

Muscovite $\left[KAl_2Si_3AlO_{10}(OH)_2\right]$ standards were also used, with agreement in the specific activities from the muscovite as well as from the silicon standards.

MEASUREMENT

The comparator method described in *Anal. Chem.* **42**, 1525 (1970) was also used.

4. STATISTICAL ANALYSIS RELATING THE INFRARED MEASUREMENTS TO THE ABSOLUTE MEASUREMENTS

by
M. Carroll Croarkin
Statistical Engineering Division

4.1 PURPOSE OF THE ANALYSIS

The purpose of the analysis is to develop a conversion coefficient for relating infrared (IR) measurement of the net absorption coefficient of oxygen in silicon wafers to the absolute determination of oxygen concentration by charged particle activation analyses (CPAA), photon activation analyses (PAA), and inert gas fusion analysis (IGFA). The data amassed by the study came from eighteen IR laboratories, four CPAA laboratories, two PAA laboratories, and one IGFA laboratory.

4.2 ARTIFACTS FOR THE STUDY

Twenty silicon ingots with varying concentrations of oxygen were specifically prepared for the study. A 10-mm slug was cut from each ingot and prepared for PAA and IGFA. Two slices, intended for IR analysis and CPAA, were cut from segments adjacent to each slug so as to minimize the effect of material inhomogeneities on the study. The slices were then quartered with the specimens from the first slice designated as test specimens 1 to 4 and the specimens from the second slice designated as test specimens 5 to 8. Eight test sets, each made up of 20 specimens (one specimen from each ingot), were then packaged for circulation to the IR laboratories and CPAA laboratories. Test set 8 was reserved for other evaluations.

Additional sets of test samples, supplied by JEIDA, were also circulated to the laboratories participating in this study. However, the data obtained on the JEIDA samples were only used to confirm the results obtained in this study. They were not used in the computation of the conversion coefficient itself.

4.3 GENERAL METHODOLOGY

The general methodology is to develop an empirical calibration curve which relates absolute determinations to net IR absorption coefficients. If the empirical curve has a zero intercept, then the slope of the empirical curve is the conversion coefficient from net absorption coefficient to oxygen concentration. In the analysis we account for the fact that there are random errors in both the IR measurements and the measurements made by absolute methods. Detailed consideration is given to several assumptions that are critical to the validity of the results, including: 1) ingot homogeneity; 2) linearity of absolute

determinations relative to IR determinations; 3) zero intercept; and 4) agreement among absolute methods.

4.4 ABSOLUTE MEASUREMENTS BY CPAA, PAA, AND IGFA

Charged particle activation analyses were performed on test sets 2, 3, and 4 after IR measurements on these test sets were completed. Results are reported in micrograms of oxygen per gram (μg/g) of silicon. One laboratory measured test set 2; between two and four independent measurements were reported for each specimen. One laboratory measured test set 3; one measurement was reported for each specimen. Two laboratories measured test set 4; the first laboratory made 3 independent measurements on each specimen, and the second laboratory made a single measurement on 10 of the specimens in the test set and 2 measurements on 5 of the specimens.

Photon activation and inert gas fusion analyses on the slugs provided for that purpose were reported by three laboratories.

Test sets measured by each absolute laboratory

Method	Laboratory ID	Test Set ID
CPAA	21	2
CPAA	22	3
CPAA	23	4
CPAA	26	4
PAA	25	10-mm slug
PAA	24	10-mm slug
IGFA	28	10-mm slug

4.5 POTENTIAL PROBLEMS

The interlaboratory study lacks closure because artifacts were generally measured by both IR and CPAA only within a national region. Thus, there is closure within a region but not from region to region. This inadequacy is immaterial if test specimens within an ingot are equivalent with respect to oxygen concentration. This premise is examined in sections 4.9 and 4.12 of this report.

Consistency within individual IR laboratories must be demonstrated, meaning that each IR laboratory must produce net absorption coefficients which are a linear function of oxygen concentration. Consistency of measurements for absolute laboratories must also be demonstrated in the sense that different absolute measurement methods must agree. These issues are examined in sections 4.7, 4.12, and 4.14.

4.6 INFRARED MEASUREMENTS

Five IR laboratories, designated as coordinating laboratories within a country or region, and 13 auxiliary IR laboratories participated in the study. Test sets 1 and 7 were circulated among the coordinating laboratories. No other laboratories measured these test sets. Test sets 2 through 6 were circulated according to the scheme shown in table 4-1. Circulation for each of test sets 2 through 6 was generally restricted to a single country or region.

Participants in the study were asked to provide data from triplicate runs on each specimen from the test set. Coordinating laboratories were asked to provide both "before" and "after" triplicate measurements on the test set.

In order to assign equal weight to each IR laboratory, only data on test sets 2 through 6 are used for developing the calibration curves. Data on test sets 1 and 7 were used for diagnostic purposes.

Table 4-1. Design for infrared measurements

	Test Sets						
	1	2	3	4	5	6	7
Lab							
1						X	
2						X	
3						X	
4					X		
5					X		
6		X					
8		X					
9			X				
10					X		
11	X		X				X
12		X					
13	X				X		X
15			X				
16	X					X	X
17	X	X					X
18				X			
19	X			X			X
31					X		

4.7 VALIDATION OF THE INFRARED DATABASE

In order to validate the extraction of transmission data from graphs to the database, the range (difference between the largest and smallest of the triplicate net absorption coefficients) was examined for each specimen and each laboratory. Coefficients with large ranges were checked for mis-recordings. Approximately 30 mis-recordings were identified in this manner and corrected. Large ranges which could not be accounted for by the transmission data were flagged as outliers. Measurements on 12 specimens were flagged in this manner.

Consistency of infrared measurements within individual IR laboratories is illustrated in figures 4-1a through 4-1h where, for each specimen, differences for each laboratory from the mean of all laboratories are plotted versus oxygen concentration. The plots also illustrate that there are systematic differences among the IR laboratories and that these differences are a function of oxygen concentration. The plots also identify as outliers three groups of triplicate measurements (see test set 4) which are not consonant with the other measurements.

4.8 PRECISION OF INFRARED MEASUREMENTS

Two levels of measurement precision are identified in this study. The first is related to the ability of the IR laboratories to make repeated measurements in the short run and is quantified by a within (laboratory) standard deviation. The absorption coefficients *for a single test set* are denoted by X_{ijk} where X_{ijk} denotes the k^{th} measurement for the j^{th} laboratory on the i^{th} specimen.

For the i^{th} specimen and the j^{th} laboratory, a within standard deviation from r measurements is defined as

$$s_{ij} = \left(\frac{1}{r-1} \sum_{k=1}^{r} (X_{ijk} - X_{ij.})^2 \right)^{1/2} \qquad (4-1)$$

with degrees of freedom $\nu_{ij} = (r-1)$ and where

$$X_{ij.} = \frac{1}{r} \sum_{k=1}^{r} X_{ijk} \ .$$

A pooled within standard deviation is defined for the j^{th} laboratory over the n specimens by the general formula

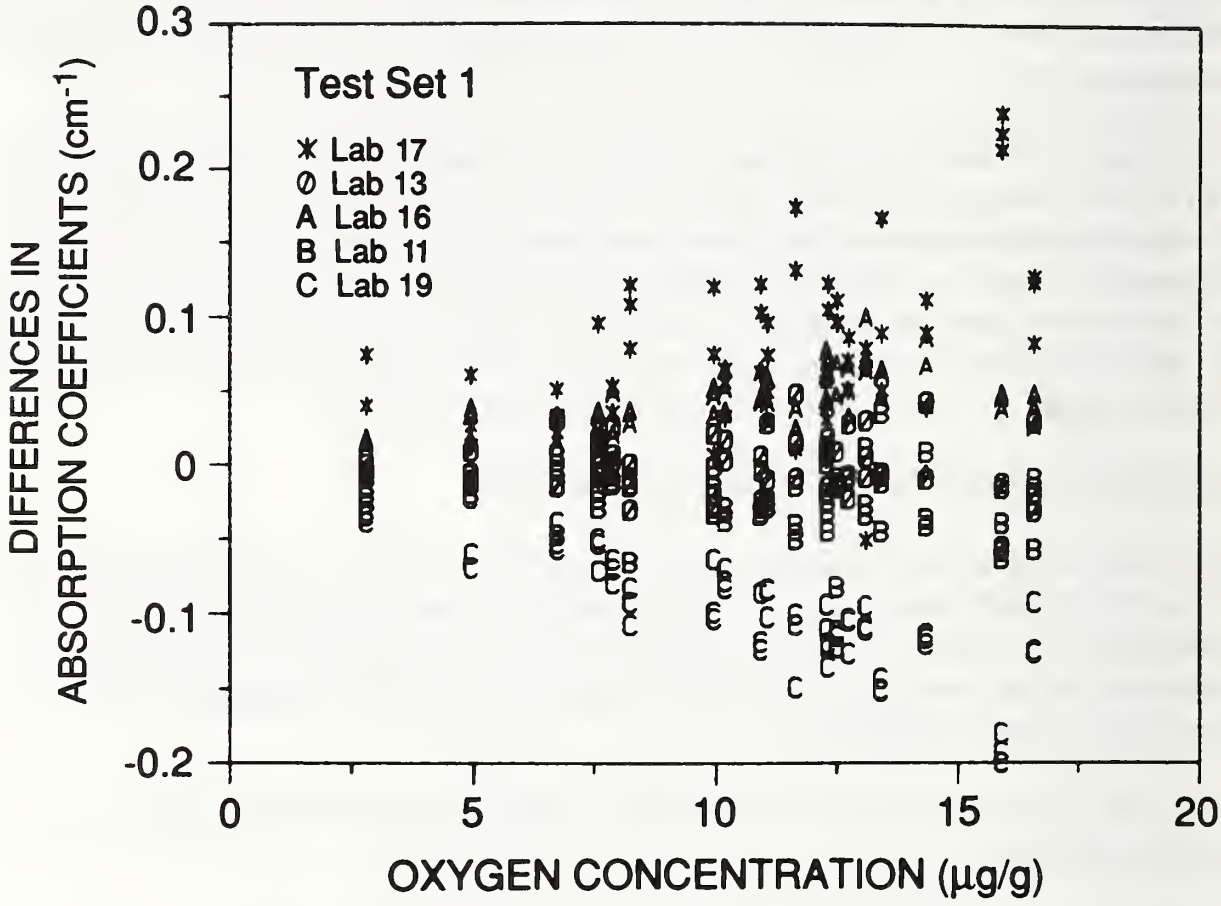

Figure 4-1a. For test set 1, differences of each laboratory's triplicate measurements from the mean of IR laboratories vs. oxygen concentration showing systematic errors among IR laboratories.

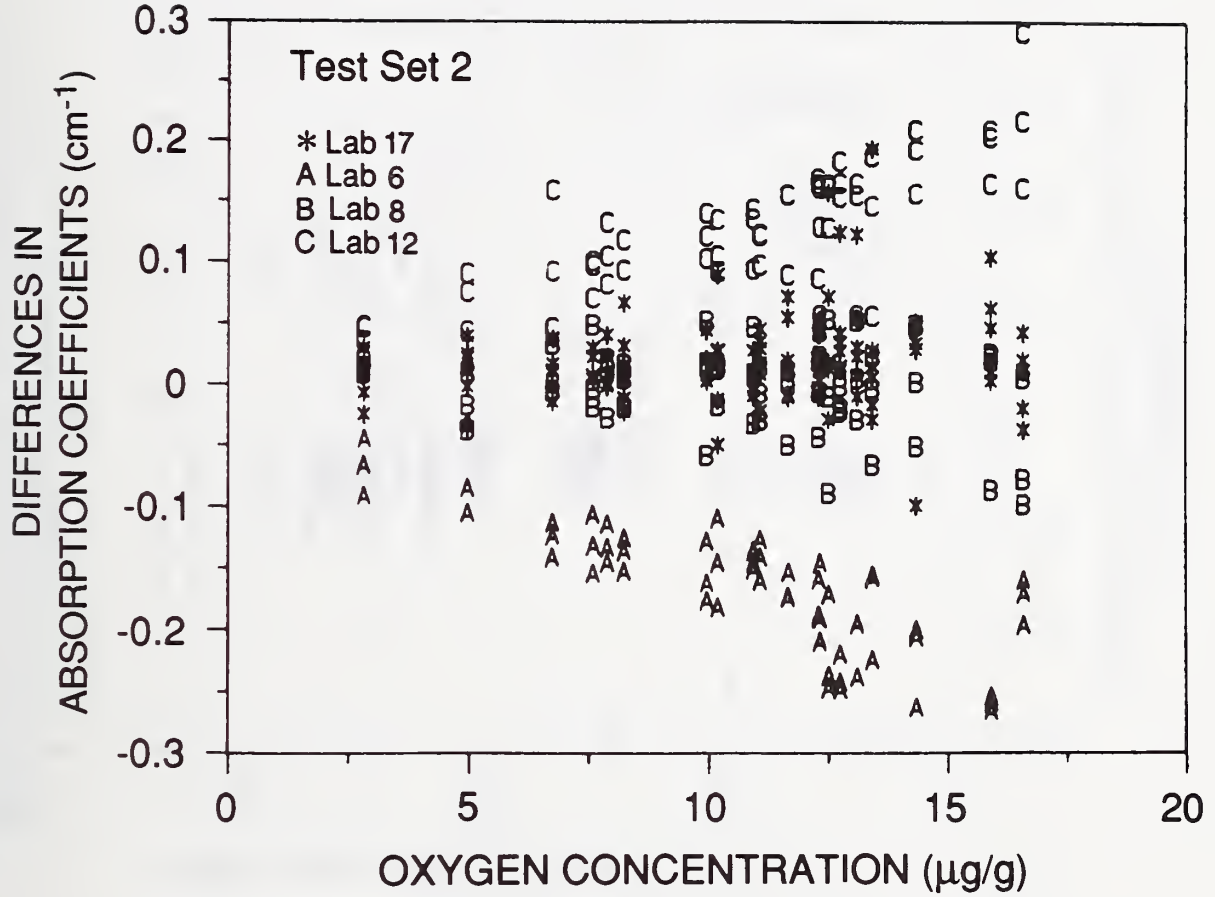

Figure 4-1b. For test set 2, differences of each laboratory's triplicate measurements from the mean of IR laboratories vs. oxygen concentration showing systematic errors among IR laboratories.

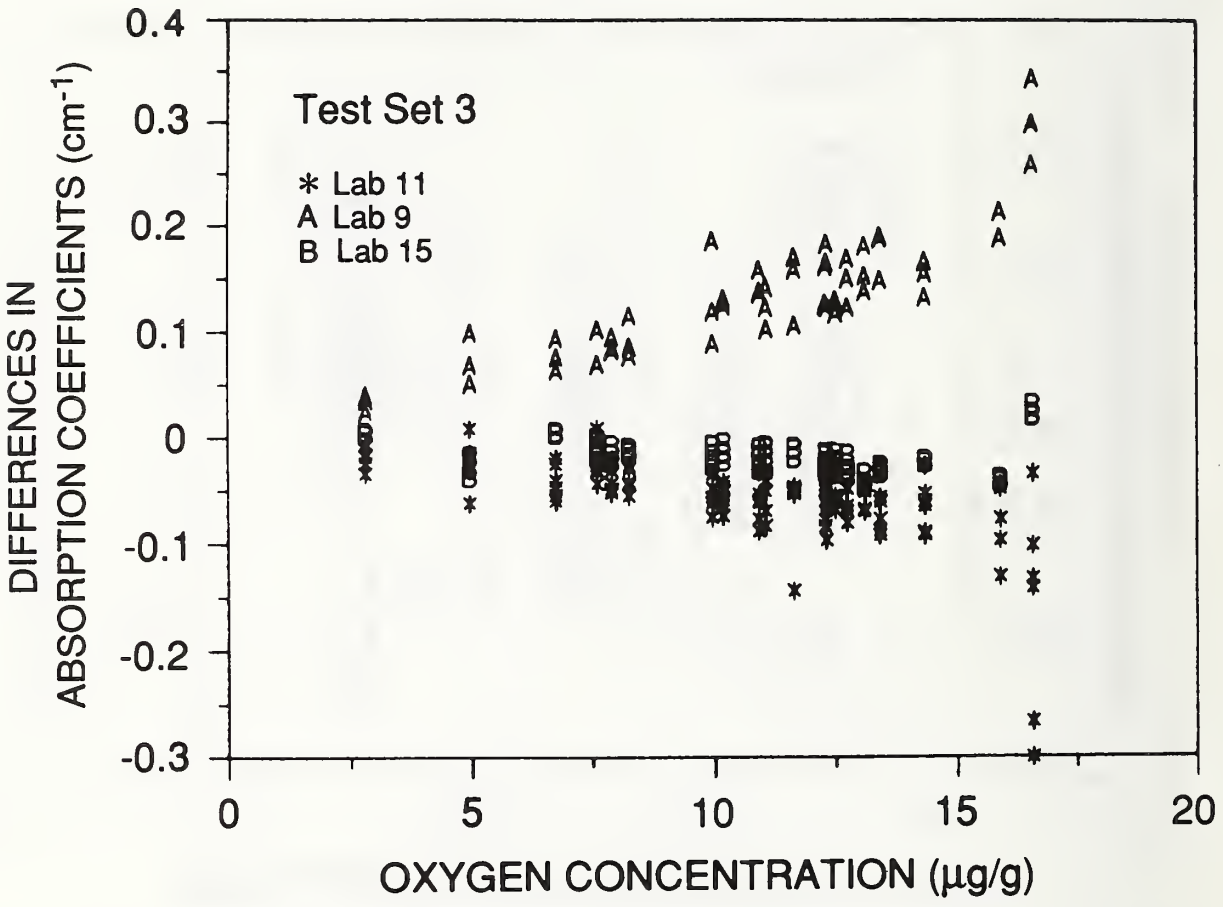

Figure 4-1c. For test set 3, differences of each laboratory's triplicate measurements from the mean of IR laboratories vs. oxygen concentration showing systematic errors among IR laboratories.

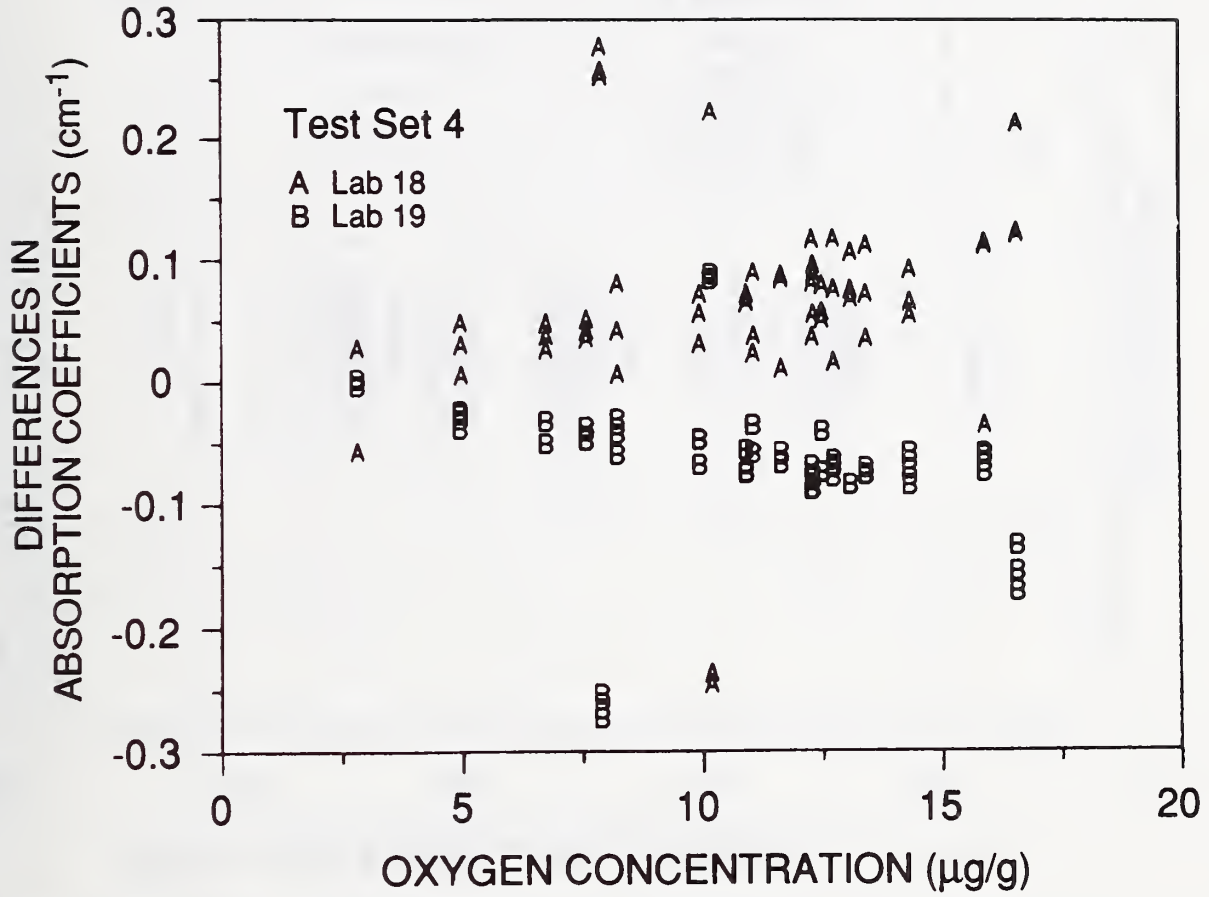

Figure 4-1d. For test set 4, differences of each laboratory's triplicate measurements from the mean of IR laboratories vs. oxygen concentration showing systematic errors among IR laboratories.

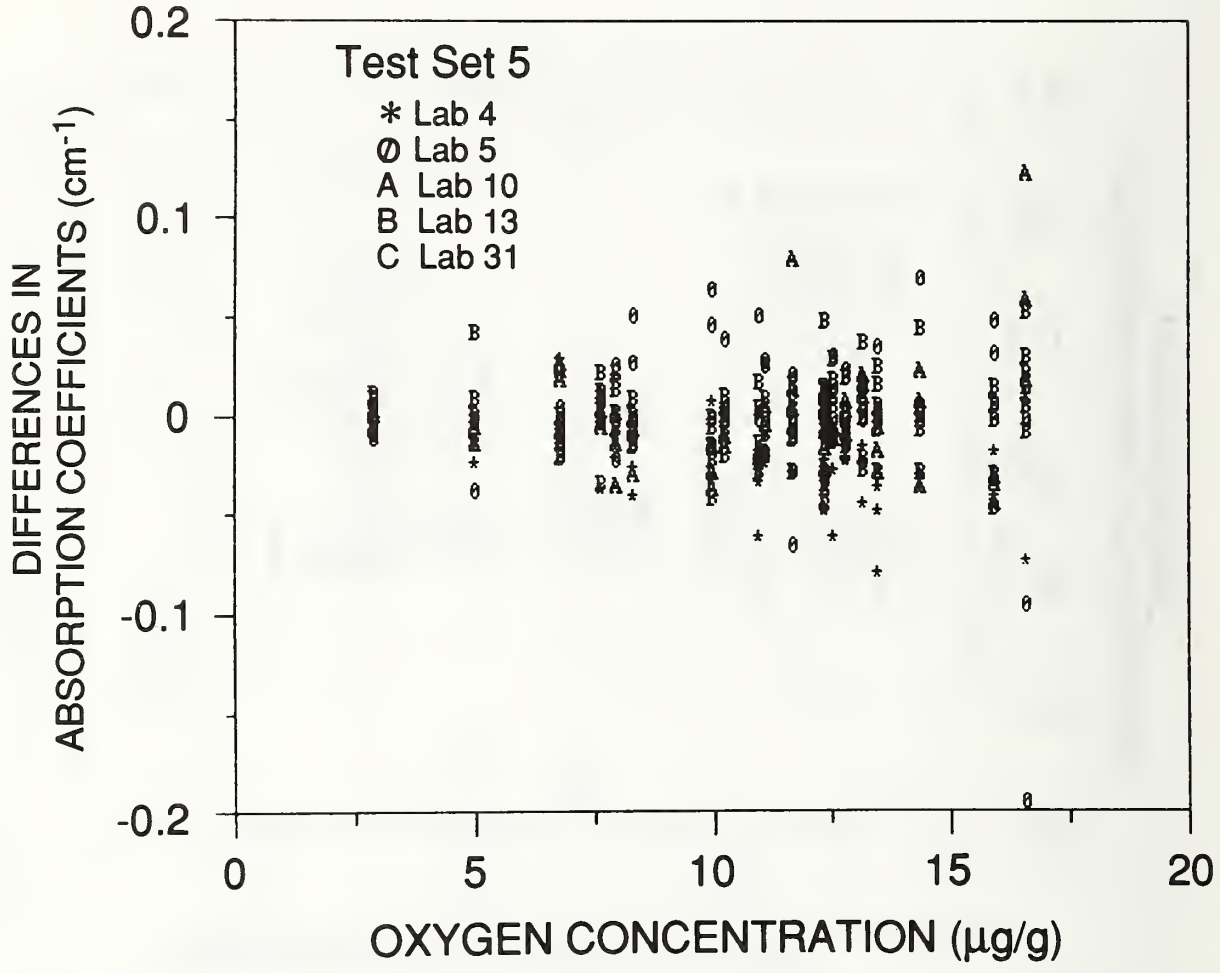

Figure 4-1e. For test set 5, differences of each laboratory's triplicate measurements from the mean of IR laboratories vs. oxygen concentration showing systematic errors among IR laboratories.

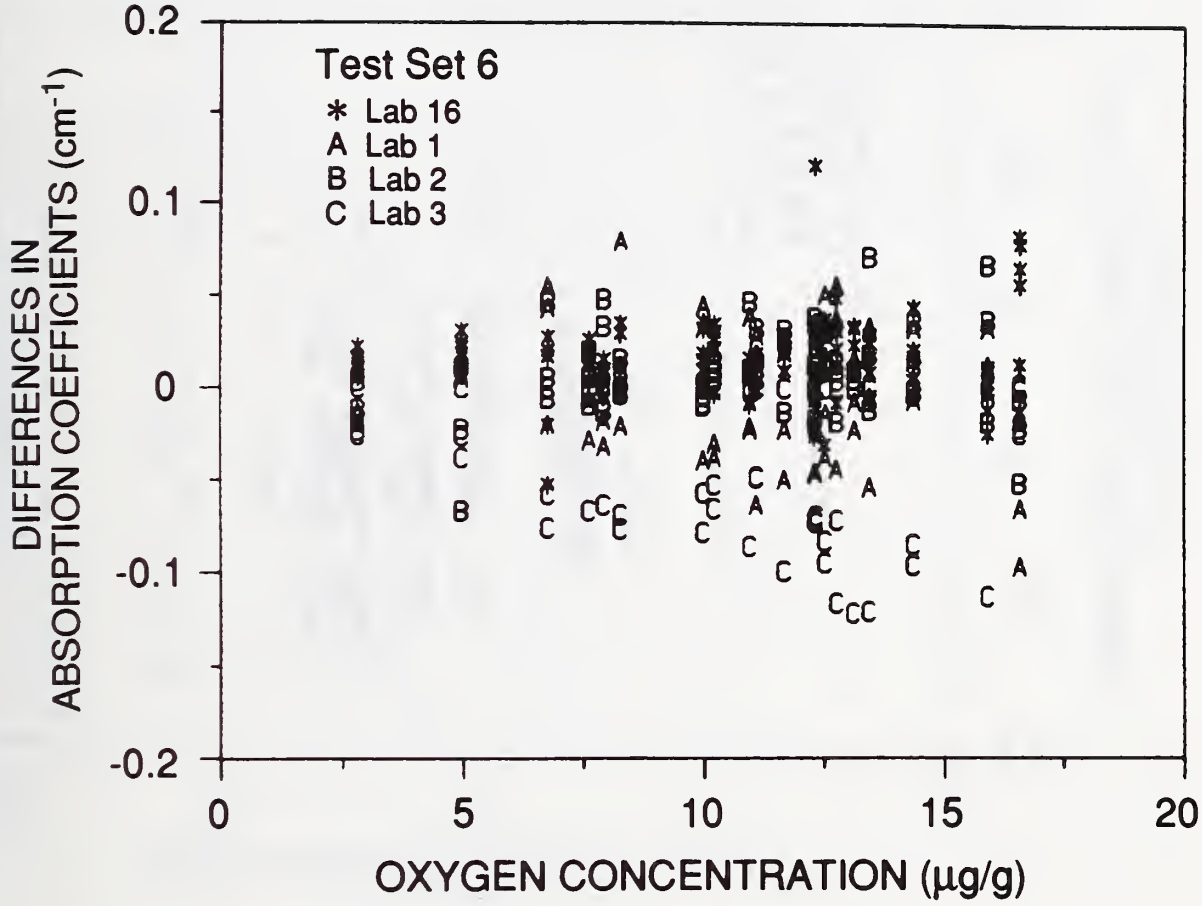

Figure 4-1f. For test set 6, differences of each laboratory's triplicate measurements from the mean of IR laboratories vs. oxygen concentration showing systematic errors among IR laboratories.

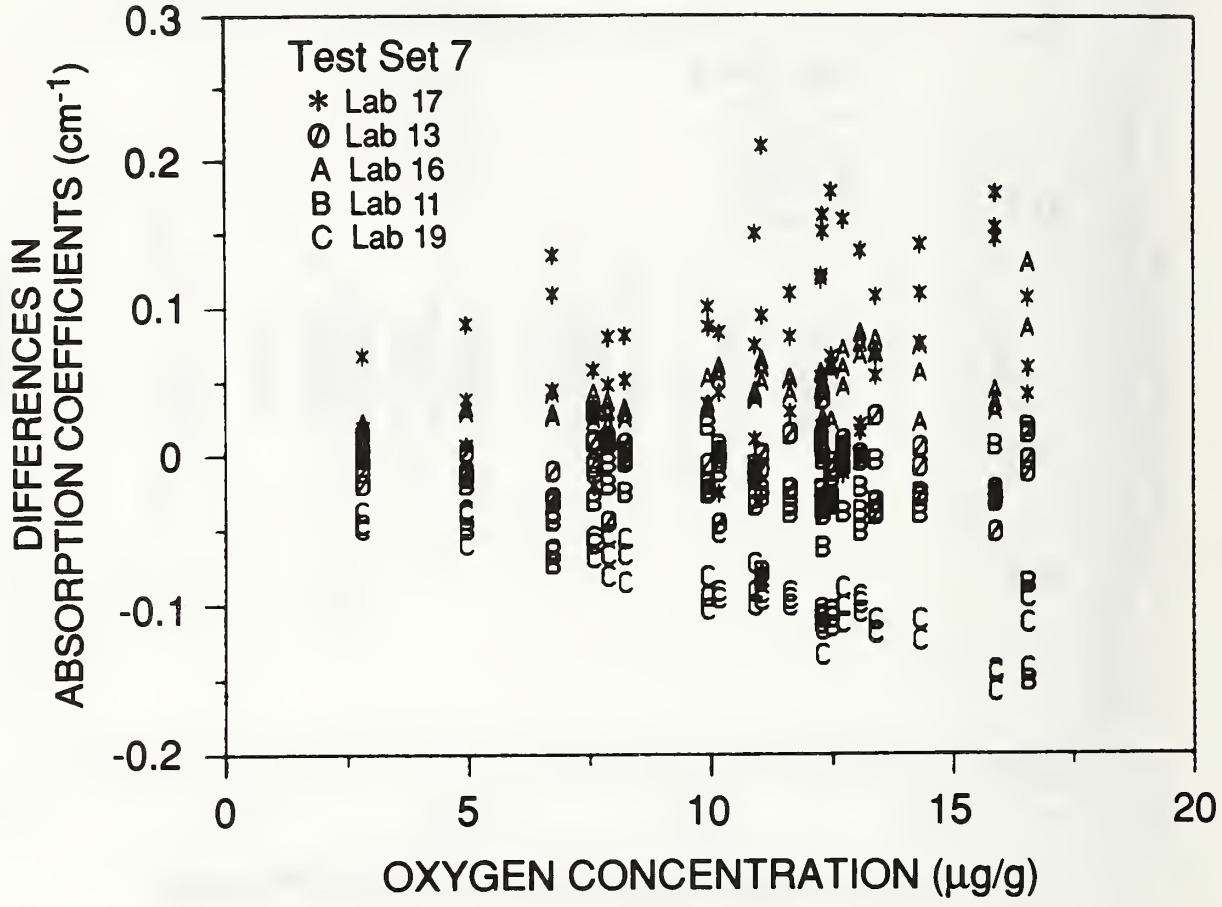

Figure 4-1g. For test set 7, differences of each laboratory's triplicate measurements from the mean of IR laboratories vs. oxygen concentration showing systematic errors among IR laboratories.

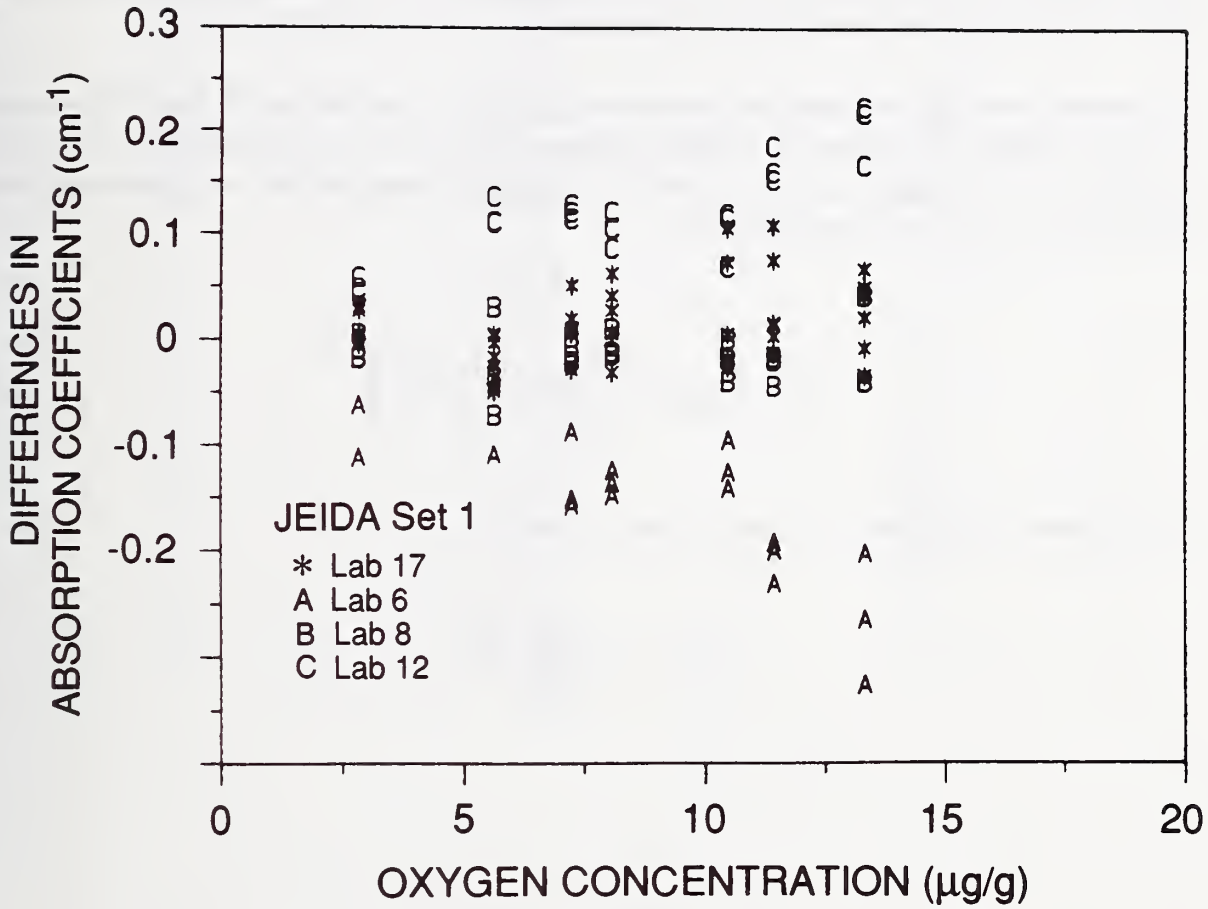

Figure 4-1h. For JEIDA set 1, differences of each laboratory's triplicate measurements from the mean of IR laboratories vs. oxygen concentration showing systematic errors among IR laboratories. Note that the y-axis scale has been changed, compared to the previous plots.

$$s_j = \left(\frac{\nu_{1j} s_{1j}^2 + \ldots + \nu_{nj} s_{nj}^2}{n_{1j} + \ldots + \nu_{nj}} \right)^{1/2} \qquad (4-2)$$

with degrees of freedom $\nu_j = \nu_{1j} + \ldots + \nu_{nj}$ where the s_{ij} represent the within standard deviations for the n specimens and the ν_{ij} represent the corresponding degrees of freedom. Pooled standard deviations for each laboratory are shown in table 4-2.

The second level of measurement precision is related to the ability of the IR laboratories to agree among themselves in making measurements on the same artifacts. For the i^{th} specimen from a *single test set*, a total standard deviation for the m laboratories which measured the test set is estimated by

$$s_i = \left(\frac{1}{m-1} \sum_{j=1}^{m} (X_{ij.} - X_{i..})^2 \right)^{1/2} \qquad (4-3)$$

with degrees of freedom $\nu_i = (m-1)$ and where

$$X_{i..} = \frac{1}{m} \sum_{j=1}^{m} X_{ij.} \; .$$

Table 4-2. Pooled standard deviations reflecting within-laboratory precision in absorption units

Lab No.	Within Std Dev	Degrees of Freedom
1	0.03265	52
2	0.02552	54
3	0.01313	12
4	0.01824	54
5	0.02736	26
6	0.02942	54
8	0.03642	54
9	0.02761	54
10	0.02352	54
11	0.02225	184
12	0.03144	52
13	0.01809	188
15	0.01552	54
16	0.01518	188
17	0.03446	176
18	0.02802	48
19	0.01293	184
31	0.01749	9

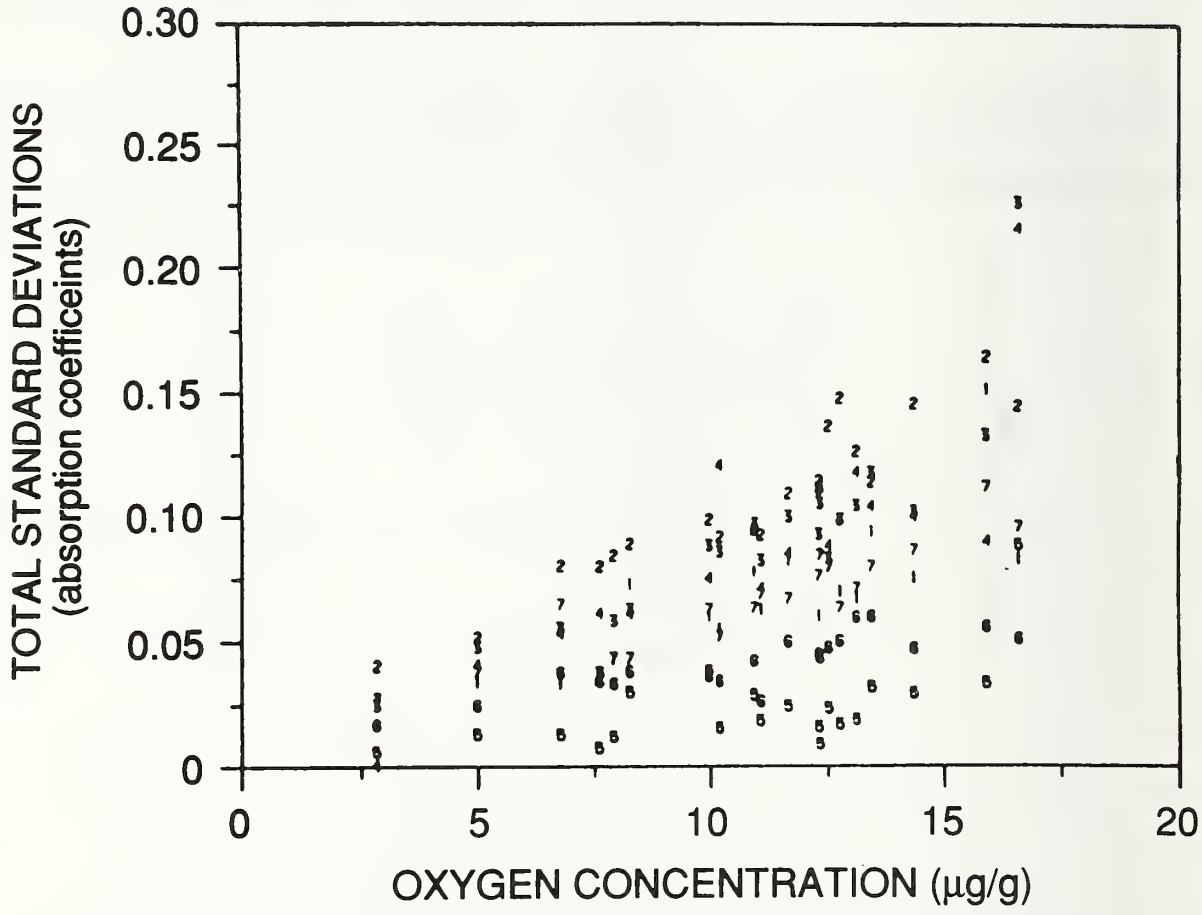

Figure 4-2. Total standard deviations in absorption units coded by test set vs. oxygen concentration showing instrumental variability and dispersion among IR laboratories as a function of oxygen concentration.

Table 4-3. Total standard deviations reflecting within-laboratory and between-laboratory variability

Ingot No.	Total Standard Deviation		Degrees of Freedom
	Absorption Units	Percentage (net absorption)	ν
2101	0.0376	2.6	21
2102	0.0543	2.9	21
2103	0.0559	2.4	21
2104	0.0678	2.4	21
2105	0.0712	2.2	21
2106	0.0823	2.4	21
2107	0.0881	2.3	20
2108	0.1081	2.5	20
2109	0.1451	3.0	17
1101	0.0619	2.1	19
1102	0.0523	2.3	19
1201	0.0905	2.4	19
1202	0.0944	2.4	19
1203	0.0866	2.4	19
1204	0.0787	2.3	20
501	0.0858	2.4	20
401	0.0669	2.2	19
301	0.0760	2.4	20
201	0.0470	2.2	20
101	0.0255	3.1	20

Figure 4-2 is a plot of total standard deviations by test set plotted versus oxygen concentration showing the relationship to oxygen concentration. Table 4-3 lists total standard deviations, pooled over the seven test sets from each ingot, in absorption units and as percentages of net absorption showing these standard deviations as a constant percentage of measurement units.

4.9 HOMOGENEITY OF OXYGEN WITHIN AN INGOT

Test set 1 and test set 7 were measured by the coordinating laboratories. Thus, differences in net absorption coefficients between two specimens from a single ingot, one assigned to test set 1 and the other assigned to test set 7, give an estimate of ingot inhomogeneity that is free of laboratory bias. The differences averaged over four of the coordinating laboratories are shown in table 4-4 as a percentage of net absorption. The table shows ingot inhomogeneities varying between 0.1% and 3.7%.

Ingot homogeneity for test sets 2, 3, 4, 5, and 6 is critical because these sets are used to relate infrared absorption coefficients to total oxygen concentration. Each coordinating laboratory provided IR measurements on one of these test sets in addition to measurements on test sets 1 and 7. Refer to table 4-1 for the scheme of test sets as measured by each laboratory.

Table 4-5 shows the differences between net absorption coefficients for test set 1 and another test set measured by the same coordinating laboratory. Differences which are significant at the 95% probability level are shown with a superscripted a. The t statistics [4-1] for testing significance were constructed as

$$t = \frac{\text{Differences in average absorption coefficients for two test sets}}{\sqrt{2/3}\ \text{Within standard deviation for } j^{th} \text{ laboratory}} . \qquad (4-4a)$$

There are significant differences among specimens from the same ingot for about 20% of the specimens. The differences are largest for ingot 2109 which has the highest oxygen concentration. The table shows that laboratories with good precision can detect inhomogeneities within ingots. However, these differences may not be significant relative to the precision of the absolute laboratories.

Percentage differences from the average IR absorption coefficient over test sets 2, 3, 4, 5, and 6 are shown in figure 4-3 where the numbers in the figure refer to test set. The plot shows that the range of absorption coefficients for specimens from the same ingot is usually less than 5% except for the ingot with the largest oxygen content where the range is about 7%. Whether or not differences of this magnitude will impact the study and the estimation of a conversion coefficient is not clear at this point; this question is examined in section 4.12.

Table 4-4. Average differences between test set 1 and test set 7 as measured by four[a] coordinating laboratories

Units in percentages of net absorption coefficients

Ingots	% Diff	Ingots	% Diff
2101	0.7	1102	0.3
2102	1.9	1201	0.4
2103	1.8	1202	0.3
2104	3.7	1203	0.8
2105	0.5	1204	1.1
2106	0.2	101	0.3
2107	0.4	201	0.8
2108	0.0	301	1.4
2109	1.4	401	0.5
1101	0.3	501	0.1

[a]Laboratory 17 was excluded because of poor precision relative to the other coordinating laboratories. See table 4-2.

Table 4-5. Differences between test set 1 and another test set as observed by each coordinating IR laboratory

		Net Absorption Units				
	IR Lab:	17	11	19	13	16
Ingot	Test Set:	1–2	1–3	1–4	1–5	1–6
2101		0.032	0.012	–0.004	–0.007	0.002
2102		0.032	0.024	0.012	0.049[a]	0.012
2103		0.092[a]	–0.004	–0.009	0.042[a]	0.043[a]
2104		0.031	0.006	0.010	0.096[a]	0.105[a]
2105		0.035	–0.002	0.014	0.004	0.002
2106		0.044	–0.009	0.000	0.032[a]	0.010
2107		0.024	0.010	0.006	0.001	0.022
2108		0.149[a]	0.002	–0.007	0.010	0.038[a]
2109		0.011	–0.141[a]	0.130[a]	–0.089[a]	–0.182[a]
1101		0.005	–0.029	0.022[a]	0.019	0.001
1102		0.003	–0.014	–0.007	–0.008	–0.010
1201		0.019	0.002	0.008	0.027	–0.013
1202		0.013	–0.039[a]	0.010	0.018	–0.014
1203		0.063[a]	–0.028	–0.022[a]	0.015	–0.014
1204		–0.024	0.003	0.000	0.032[a]	–0.017
101		0.017	–0.015	–0.015	0.000	0.002
201		–0.002	–0.014	0.004	0.035[a]	0.013
301		0.070[a]	0.023	–0.013	0.076[a]	0.024
401		0.039	–0.026	0.000	–0.004	–0.011
501		–0.022	–0.025	0.002	0.020	0.003

[a]Indicates a significant difference at the 95% probability level.

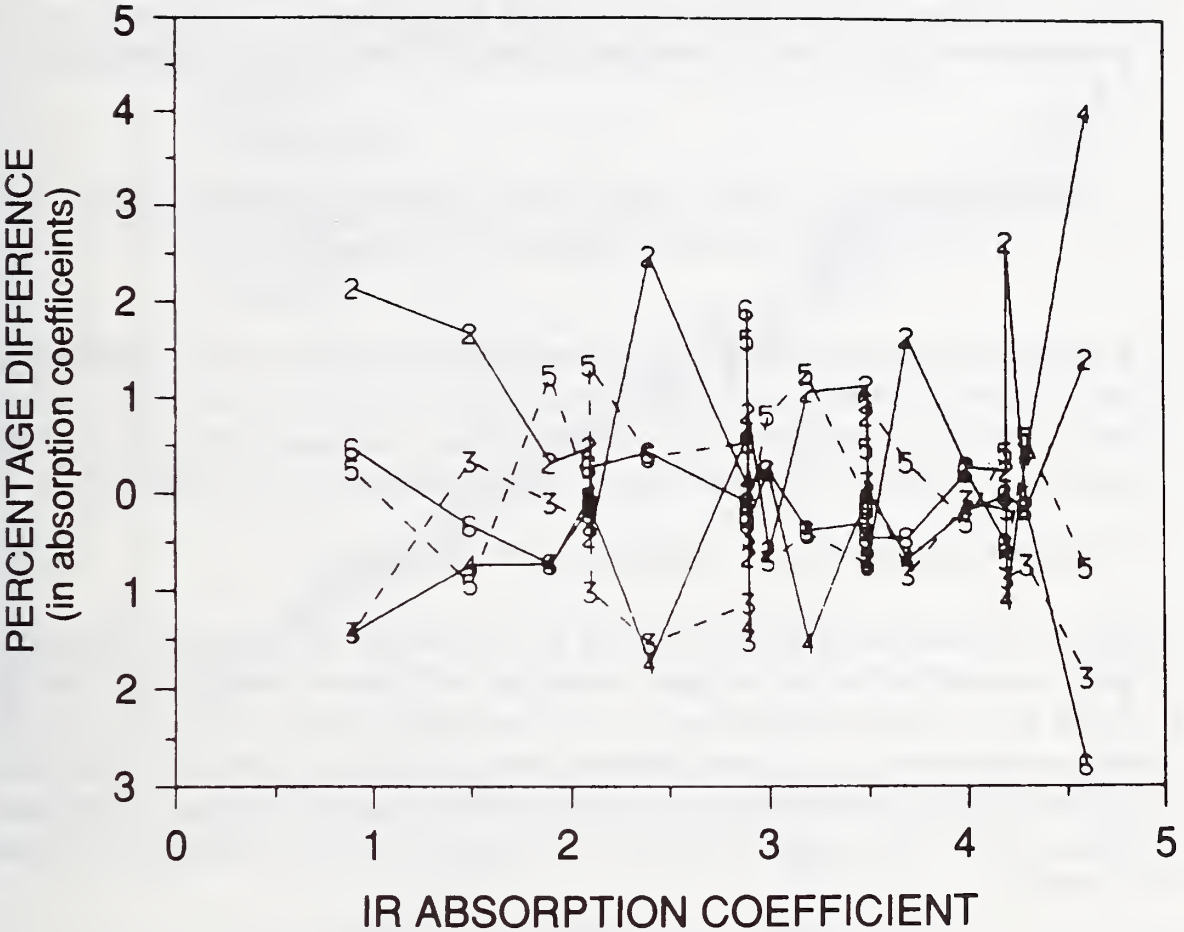

Figure 4-3. Percentage differences from the average IR absorption coefficient for test sets 2, 3, 4, 5, and 6 vs. net absorption coefficient showing inhomogeneity among specimens within an ingot.

4.10 CHANGES IN OXYGEN CONCENTRATION WITHIN A SPECIMEN

Coordinating laboratories were required to make measurements on the test set that circulated within their respective countries or regions, both before and after circulation to the auxiliary laboratories. The differences between the average absorption coefficients from "before" and "after" measurements can be tested for significance. The statistic for testing for a change in a single artifact as measured by the j^{th} laboratory is constructed as

$$t = \frac{\text{Differences in average "before" and "after" coefficients for one specimen}}{\sqrt{2/3}\ \text{Standard deviation for } j^{th} \text{ laboratory}} . \quad (4-4b)$$

Of the 80* specimens which saw both before and after measurements, seven show a significant change at the 95% probability level, hardly more than is expected to occur at random. Thus, it is concluded that the artifacts were unchanged with respect to oxygen concentration during the time that they circulated among the IR laboratories.

4.11 IDENTIFICATION OF OUTLIERS IN THE CPAA DATA

Outliers in the absolute data are identified by a procedure that compares the ranking of oxygen concentration for the 20 ingots according to IR determinations with the ranking according to the absolute determinations. The technique relies on the consistency among infrared measurements and is most effective where the absolute data have high precision and where oxygen concentrations are spread evenly across the regime. It is helpful for identifying fairly large outliers, especially where there are obvious anomalies which are not easily resolved.

Figures 4-4a to 4-4d are plots of the IR measurements by individual IR laboratories on a single test set versus absolute measurements by a single CPAA laboratory on the same test set. Thus, figure 4-4a shows a plot of IR measurements on test set 2, as measured by the five coordinating laboratories, plotted versus the corresponding CPAA measurements by laboratory 21. A few of the data points appear to be misplaced relative to the others.

To clarify the situation, figure 4-5a shows IR measurements for each specimen in test set 2 connected by lines.† The individual points represent measurements by individual laboratories plotted against the linearity of the IR instrument in that laboratory. The plots

---

* Laboratory 17 reported "before" but not "after" measurements.

† For convenience, this figure has been broken up into three parts, the first covering the range 0 to 2.5 cm^{-1}, the second covering the range 2.5 to 4 cm^{-1}, and the third, the range from 4 to 5 cm^{-1}.

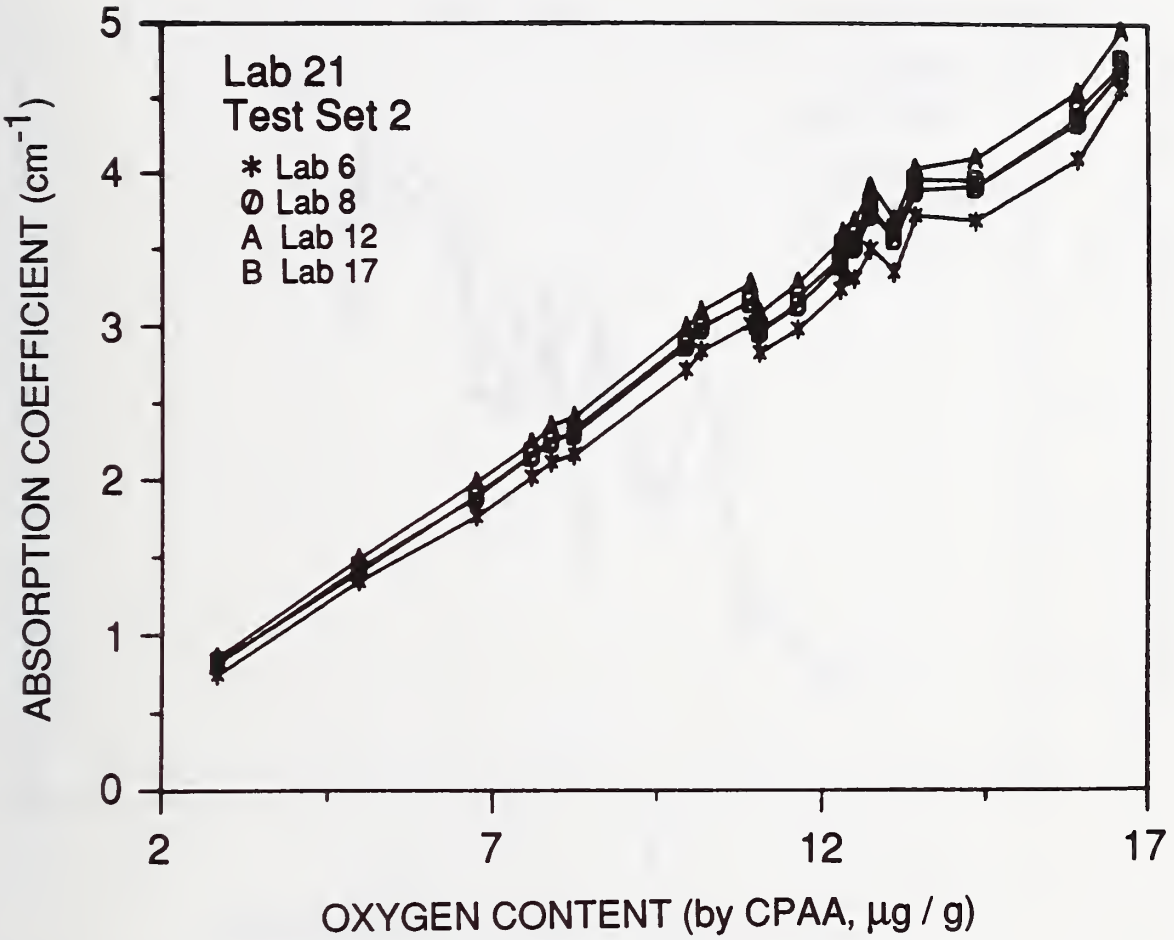

Figure 4-4a. For Lab 21, test set 2, IR absorption coefficients plotted vs. CPAA measurements on the same test squares.

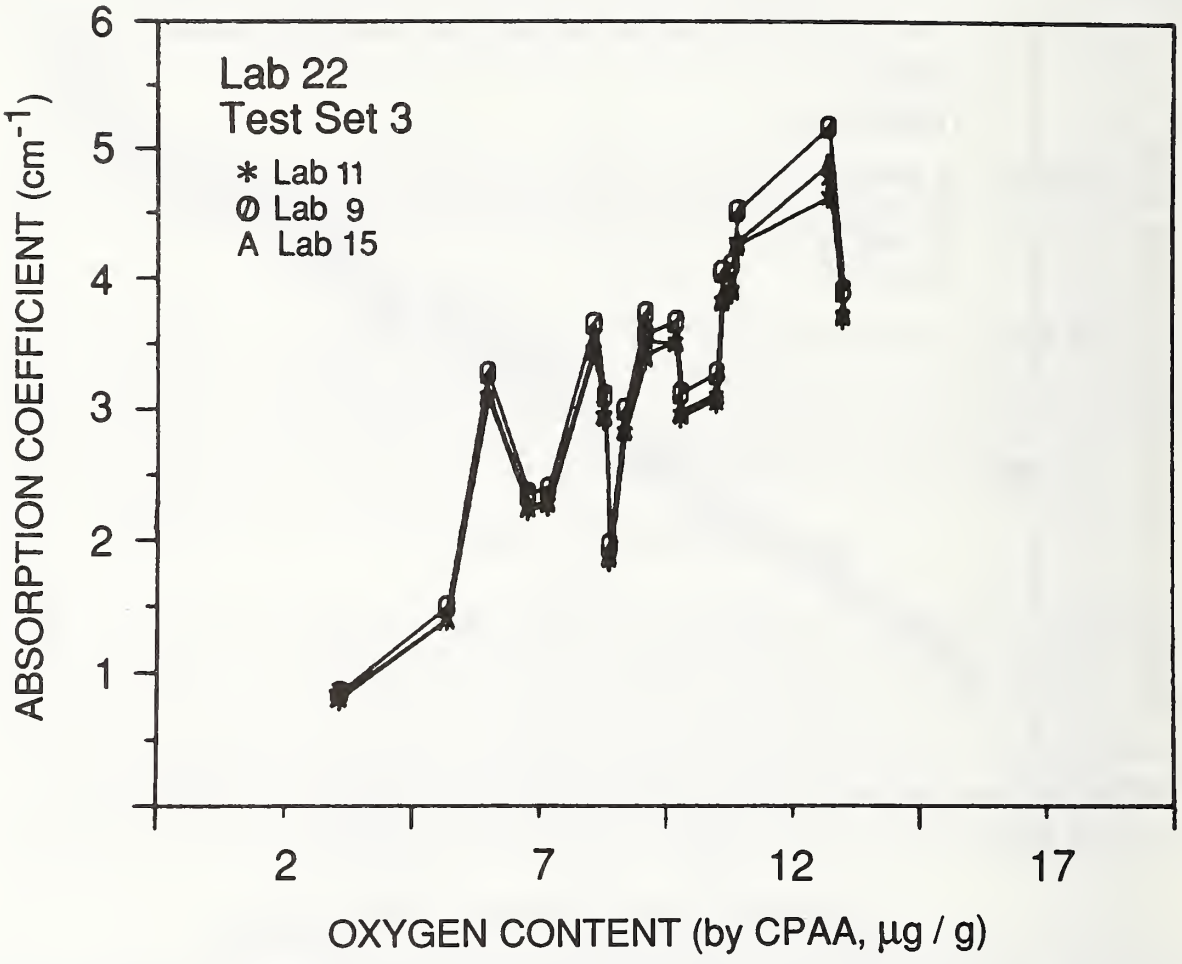

Figure 4-4b. For Lab 22, test set 3, IR absorption coefficients plotted vs. CPAA measurements on the same test squares.

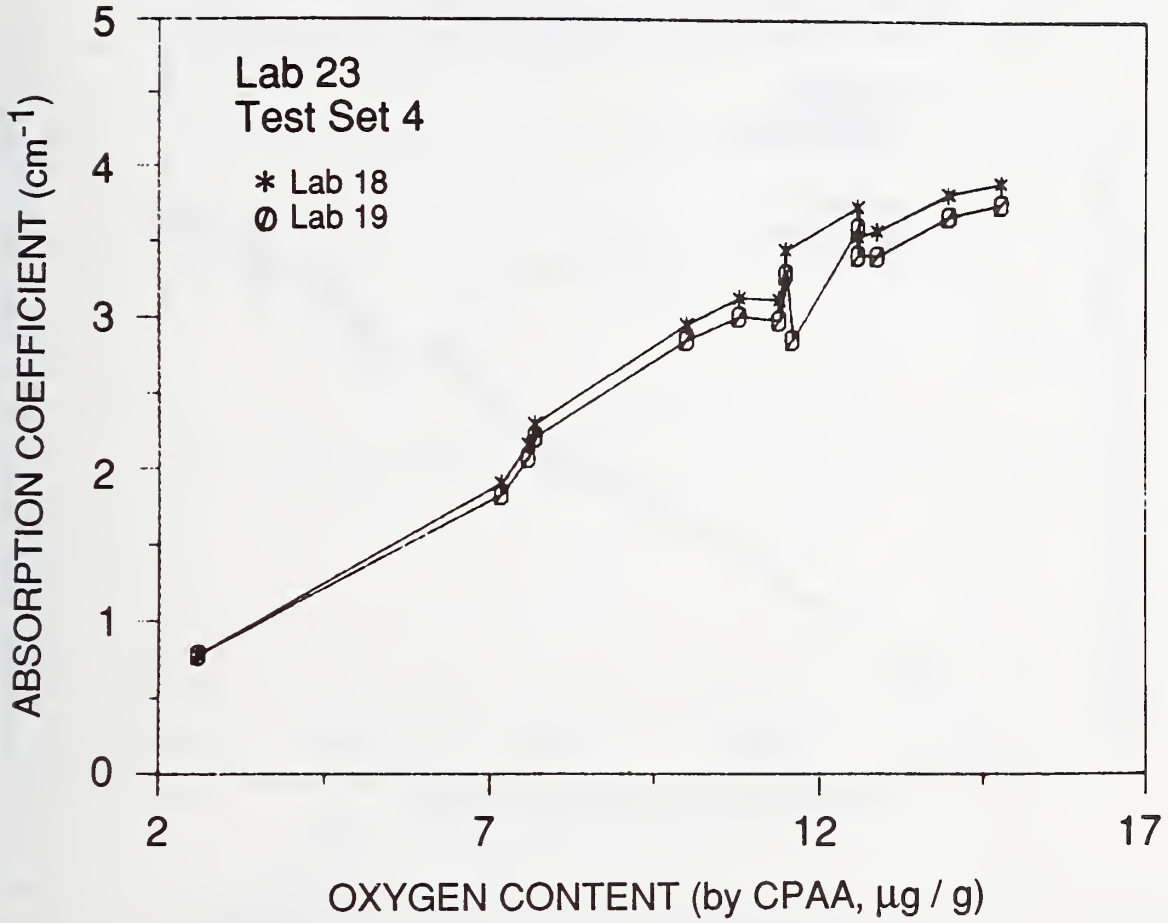

Figure 4-4c. For Lab 23, test set 4, IR absorption coefficients plotted vs. CPAA measurements on the same test squares.

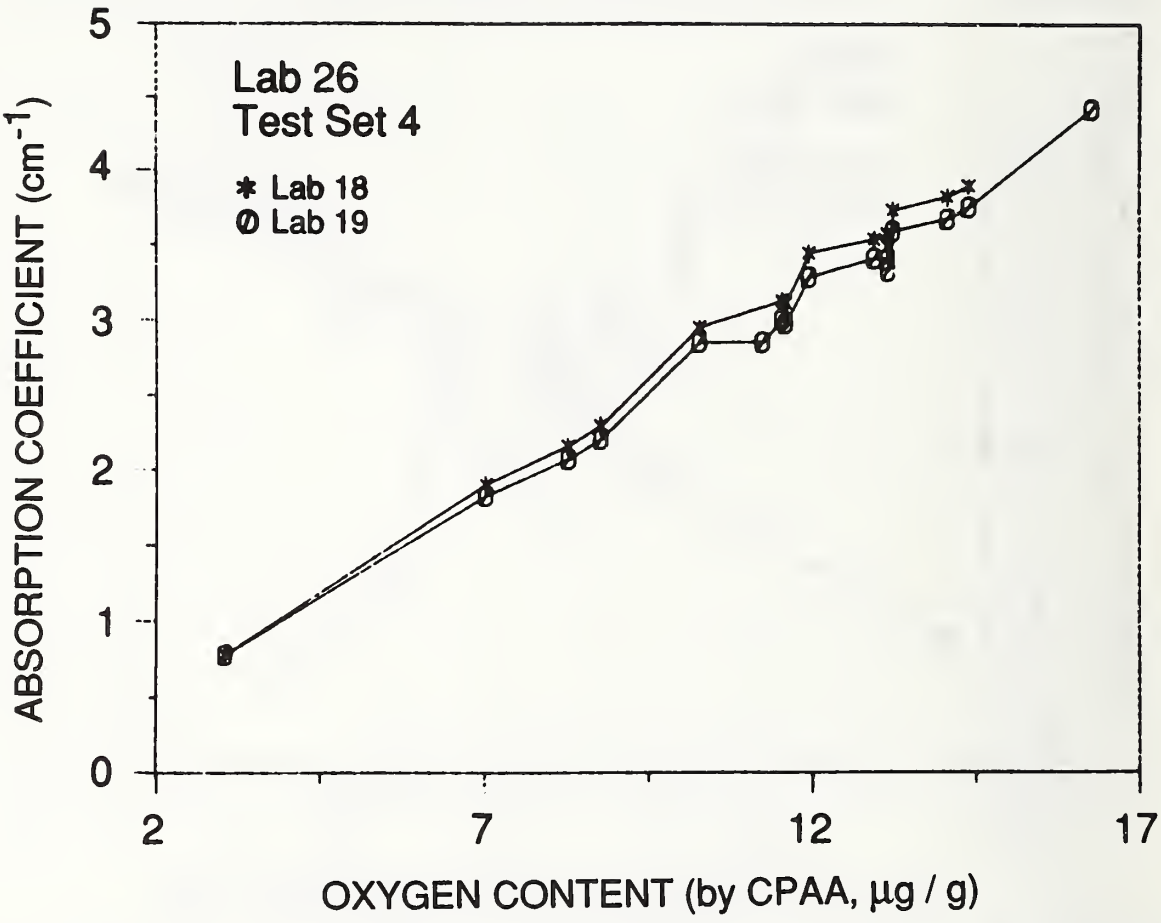

Figure 4-4d. For Lab 26, test set 4, IR absorption coefficients plotted vs. CPAA measurements on the same test squares.

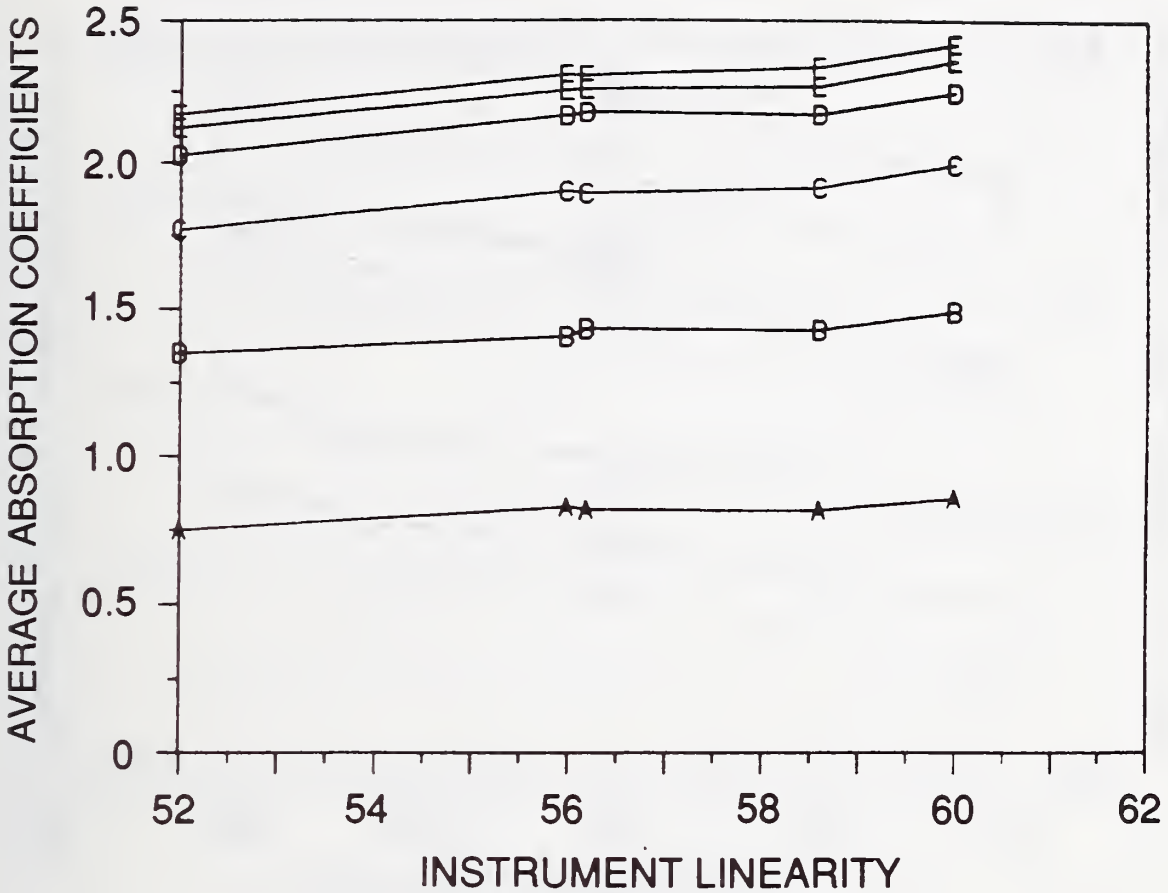

Figure 4-5a (pages 49-51). IR absorption coefficients for each test square in test set 2, delineated and ranked alphabetically by CPAA according to laboratory 21, the convention being that the symbol A refers to the specimen with the lowest oxygen concentration and the symbol T, the specimen with the highest oxygen concentration. Lines I and and J and O and P, out of alphabetical order indicating an improper oxygen measurement by the CPAA laboratory, are flagged as outliers.

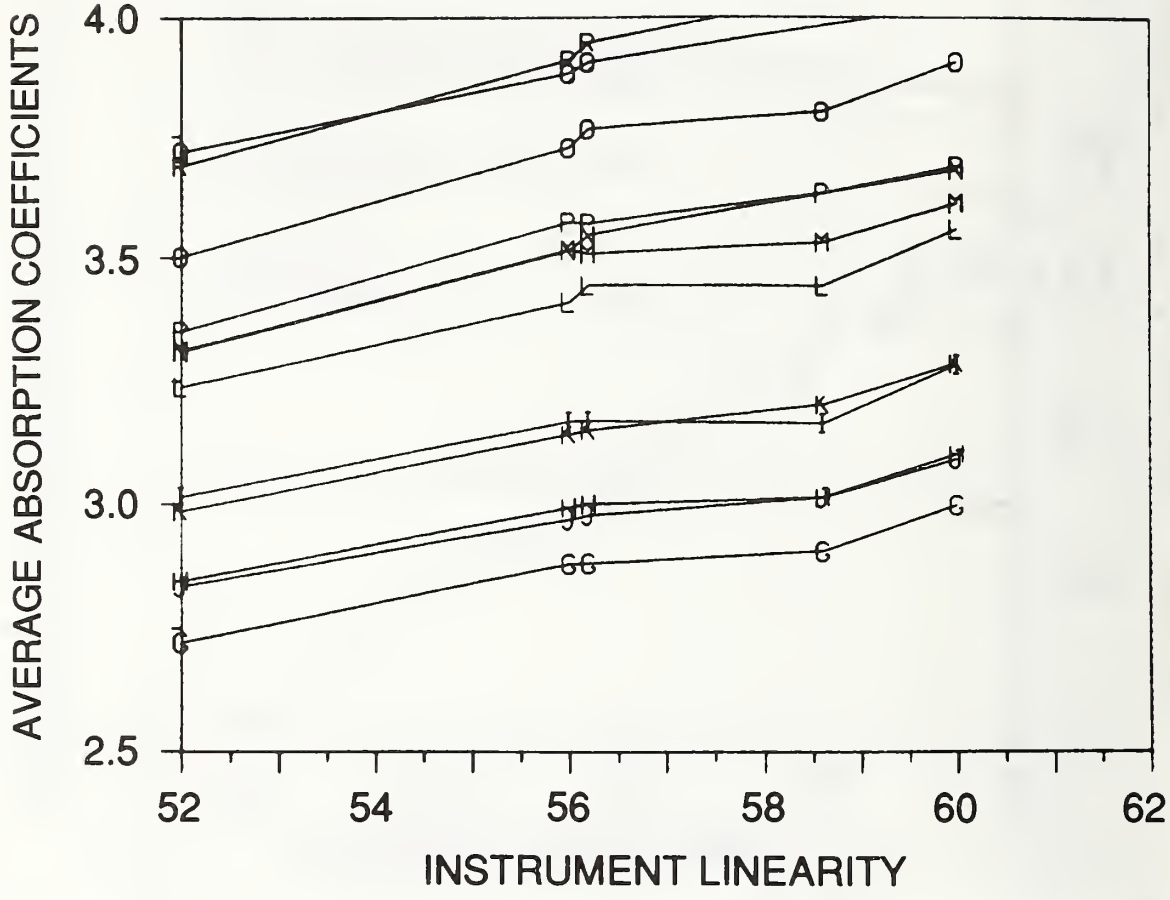
AVERAGE ABSORPTION COEFFICIENTS
4.0
3.5
3.0
2.5
52
54
56
58
60
62
INSTRUMENT LINEARITY

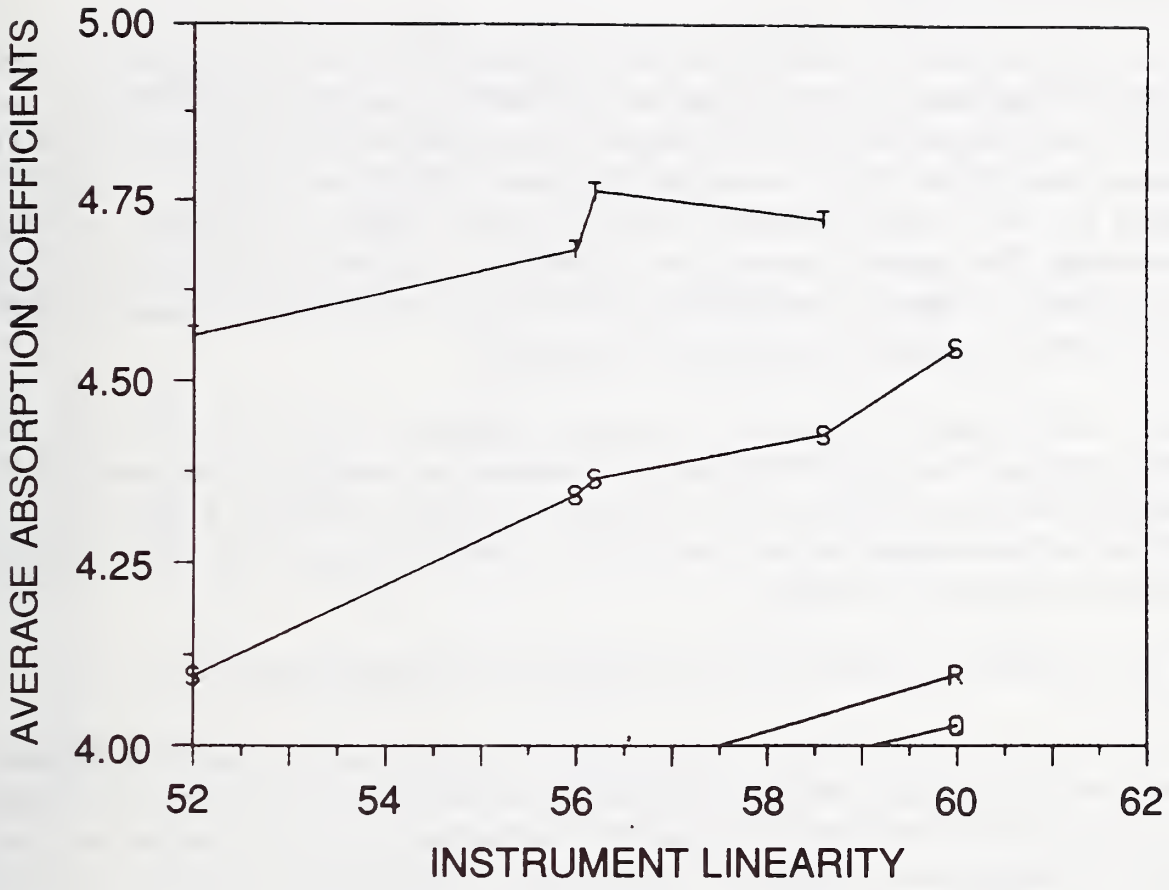
AVERAGE ABSORPTION COEFFICIENTS
5.00
4.75
4.50
4.25
4.00
52
54
56
58
60
62
INSTRUMENT LINEARITY
T
S
R
O

corresponding to the 20 specimens are ranked sequentially by CPAA oxygen concentration according to laboratory 21, the convention being that the symbol A refers to the specimen with lowest oxygen concentration, and the symbol T refers to the specimen with highest oxygen concentration.

Because of the internal consistency of the IR laboratories in determining absorption coefficients, the rankings provide a mechanism for identifying outliers in the CPAA data. A line that is out of sequential order with respect to the alphabet indicates an improper oxygen measurement by the CPAA laboratory. Specimens #120102 and #50102, identified in the graph by lines P and O, appear to have been interchanged; both specimens are flagged as outliers. The rankings for specimens #210502 and #40102, identified by lines J and I, respectively, are likewise unsatisfactory; these two specimens are also flagged as outliers. All outliers were omitted from further consideration.

In a similar analysis in figure 4-5b, absorption coefficients for test set 4 as seen by two IR laboratories are ranked by CPAA oxygen concentrations according to laboratory 26. This analysis indicates possible problems among the specimens identified by lines H, I, J, and K; the problems are not resolvable and are not considered egregious enough to warrant the data being flagged as outlying.

4.12. DIAGNOSTIC TESTS FOR ABSOLUTE DETERMINATIONS

In this section, absolute laboratories are evaluated individually by regarding IR measurement as the dependent variable and absolute measurement as the independent variable in a linear model. See figure 4-4 where IR measurements on a single test set are plotted versus absolute measurements on the same test set. This approach is taken, even though absolute measurements may be less precise than IR measurements, so that the aptness of the linear model can be tested relative to the dispersion among IR laboratories.

The model

$$X_{ij.} = \alpha + \beta Z_i + \xi_{ij.} \qquad \begin{matrix} i = 1, \ldots, n \\ j = 1, \ldots, m \end{matrix} \qquad (4-5)$$

with slope β and intercept α describes a linear relationship between the two types of measurements where the quantity Z_i represents the average absolute measurement on the i^{th} specimen; the term $X_{ij.}$ represents the IR measurement on the i^{th} specimen by the j^{th} IR laboratory; and the $\xi_{ij.}$ represent random error terms which are assumed to be independent and come from a distribution with mean zero and standard deviation σ_i. The standard deviations σ_i represent the total standard deviations that describe the dispersion among IR laboratories, and the index i indicates dependence on oxygen concentration.

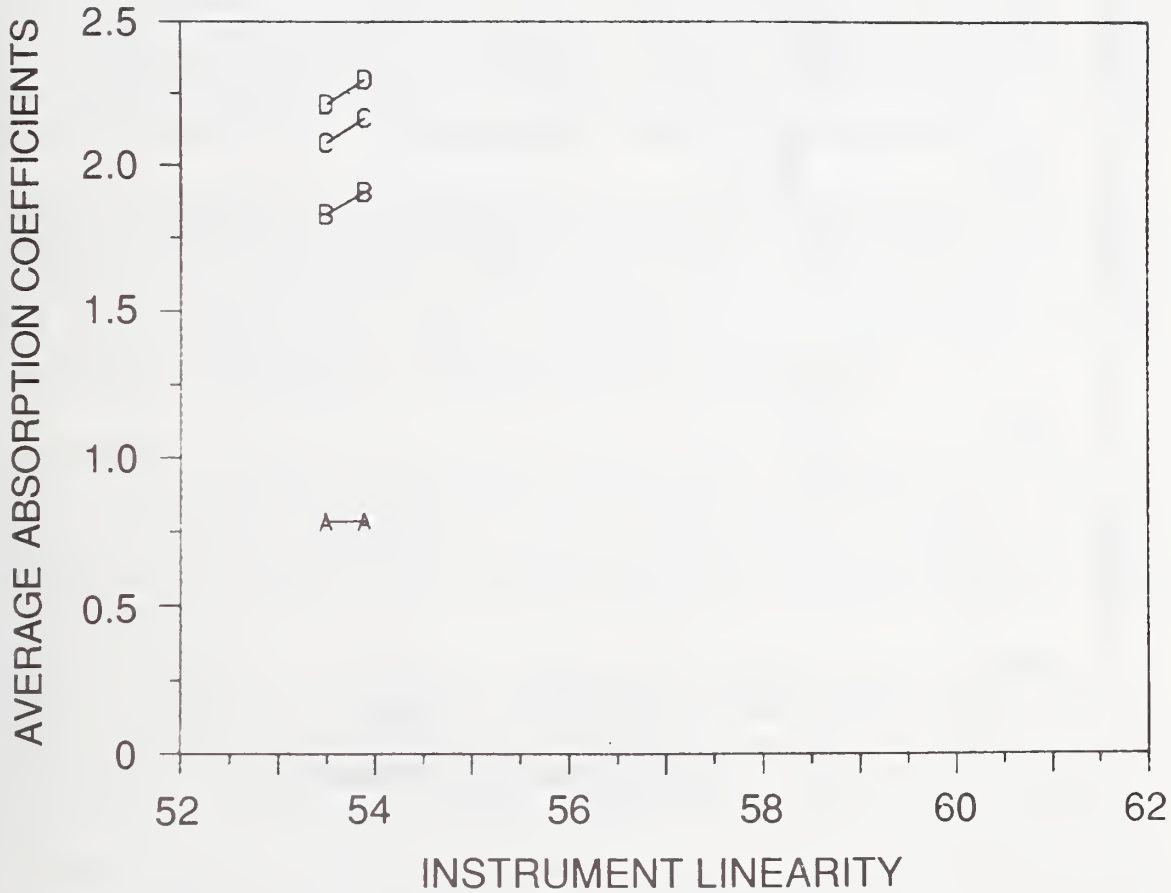

Figure 4-5b. IR absorption coefficients for each test square in test set 4, delineated and ranked alphabetically by CPAA according to laboratory 26, showing consistency of CPAA values.

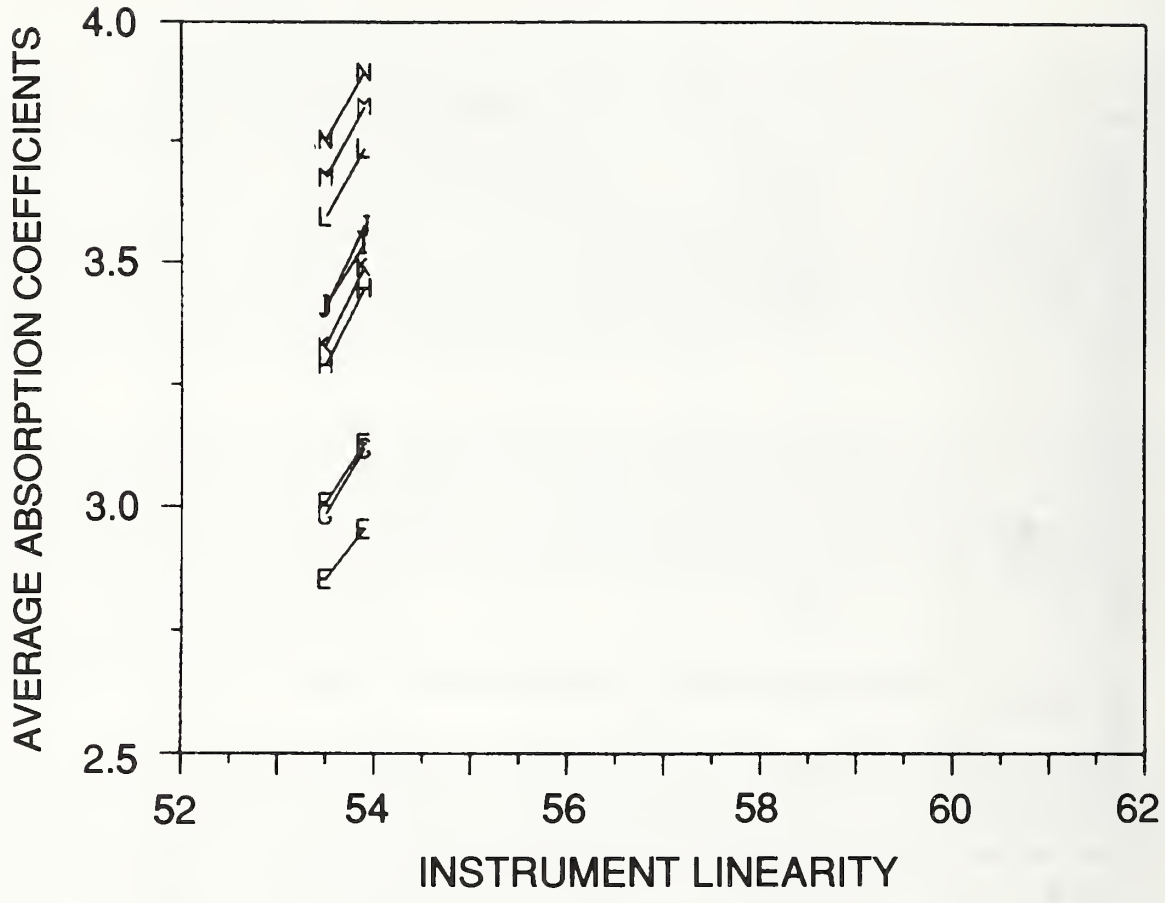
AVERAGE ABSORPTION COEFFICIENTS
4.0
3.5
3.0
2.5
52
54
56
58
60
62
INSTRUMENT LINEARITY

Results of a diagnostic test for the absolute measurements are shown in table 4-6. The F statistics [4-3] in the table test the goodness of fit where large values of F indicate lack of fit of the experimental data to the linear model.*

The F statistic compares the dispersion of IR data about the fitted line with the dispersion among IR laboratories. If the comparison is unfavorable, a large F statistic results. Such a finding can be caused by: i) an improper model; ii) an erroneous measurement by the absolute laboratory; or iii) inhomogeneity within an ingot. Homogeneity is not an issue for cases (1), (2), (3), and (4) where the CPAA measurements made at each coordinating laboratory are paired with the IR measurements made on the same specimens.

The F statistics for laboratories 21 and 26 on test sets 2 and 4, respectively, are satisfactory, indicating that the results for these laboratories are consistent with a model that is linear in the IR data. It is noted that four specimens, identified as outliers (see the section on outliers for CPAA data) for laboratory 21, are excluded from the analysis. The F statistic is not satisfactory for this laboratory if these specimens are included.

For these two laboratories, the cases are included where the IR measurements for all test sets are regressed against the absolute measurements (cases (1a) and (4a)). The lack of fit for these cases is indicative of inhomogeneity among test squares and should be compared with the concordancy achieved for IR measurements made on the same specimens as the absolute measurements.

The F statistic for laboratory 23 is marginal; the F statistic for laboratory 22 is unsatisfactory. Plots of studentized residuals† from the least-squares analyses versus IR absorption coefficients are shown in figure 4-6. Residual plots provide amplification of the information contained in the F statistic and should be used in conjunction with the F statistic in assessing goodness of fit. Ideally, the residuals should be distributed randomly about zero with no obvious patterns or extreme values. Nonrandom patterns and clumping of residuals are indicative of measurement anomalies.

---

* Because the precision of IR measurements is nonconstant across oxygen concentrations, a weighted least-squares fit [4-2] is appropriate for making this test. This procedure assigns weights to the IR measurements which are inversely proportional to the square of the standard deviations σ_i where estimates for σ_i are given by the total standard deviations in table 4-3.

† The residuals are standardized so that they are distributed approximately according to Student's t distribution [4-4]; values should fall in the interval (−3, +3).

Table 4-6. Results of fitting IR data[a] as a linear function of absolute data showing F statistics for testing lack of fit

Case	Absolute Lab	Abs Method	Abs Test Set	IR Test Set	DF of Fit	F Statistic
(1)	21	CPAA	2	2	74	1.9
(1a)	21	CPAA	2	2,3,4,5 & 6	293	15.9[b]
(2)	22	CPAA	3	3	73	155.3[b]
(3)	23	CPAA	4	4	25	5.9[b]
(4)	26	CPAA	4	4	28	1.6
(4a)	26	CPAA	4	2,3,4,5 & 6	312	26.0[b]
(5)	25	PAA	10-mm slugs	2,3,4,5 & 6	294	32.6[b]
(5a)	25	PAA	10-mm slugs	2,3,4,5 & 6	257[c]	12.8[b]
(6)	24	PAA	10-mm slugs	2,3,4,5 & 6	218	412.5[b]
(6a)	24	PAA	10-mm slugs	2,3,4,5 & 6	201[d]	285.9[b]
(7)	28	IGFA	10-mm slugs	2,3,4,5 & 6	294	216.3[b]
(7a)	28	IGFA	10-mm slugs	2,3,4,5 & 6	277[c]	164.6[b]

[a]IR data with fewer than triplicate measurements excluded from the analysis.
[b]Indicates lack of fit at the 99% probability level.
[c]Ingots #2105 and #2102 excluded from the analysis.
[d]Ingot #1102 excluded from the analysis.

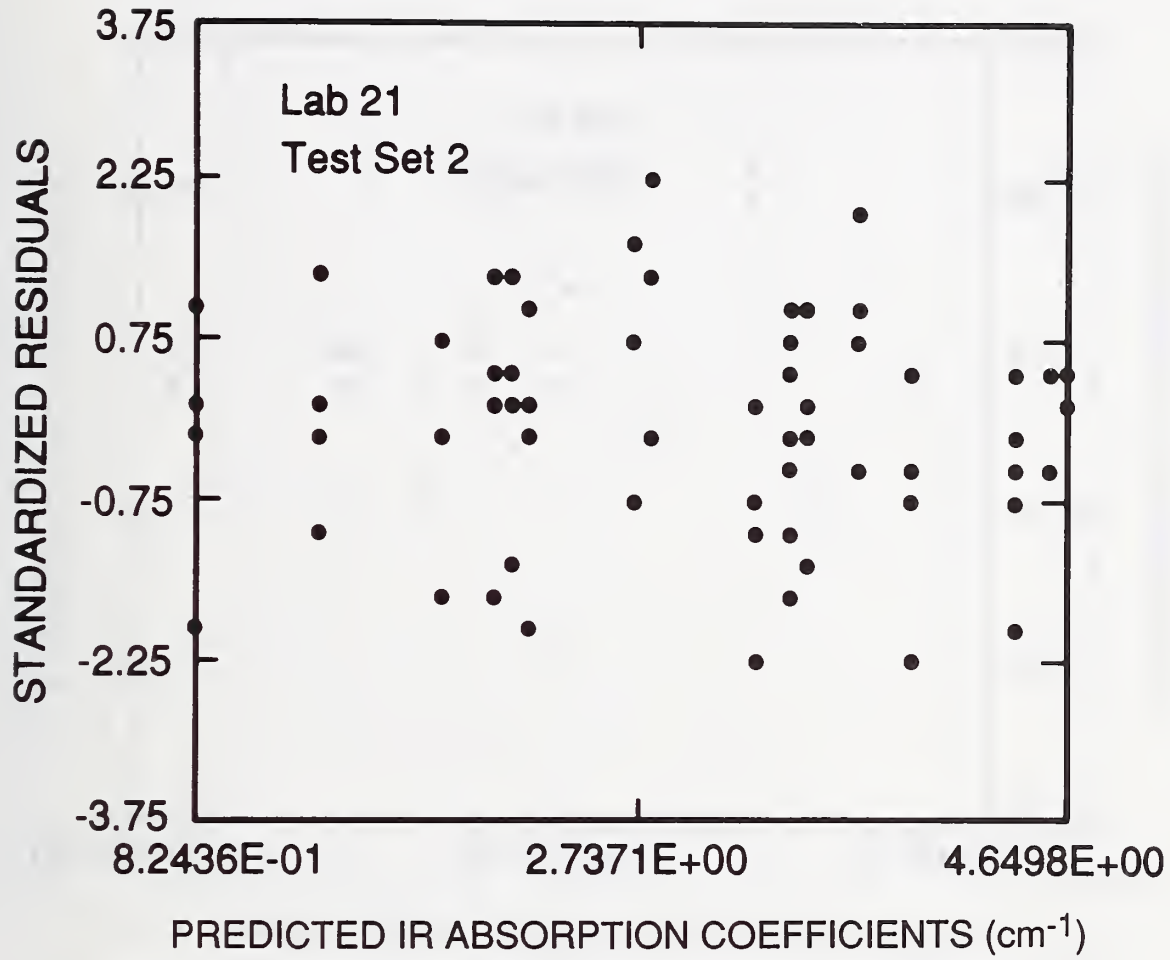

Figure 4-6a. For Lab 21 (CPAA), test set 2, standardized residuals from linear fit to test set data vs. predicted IR absorption coefficients.

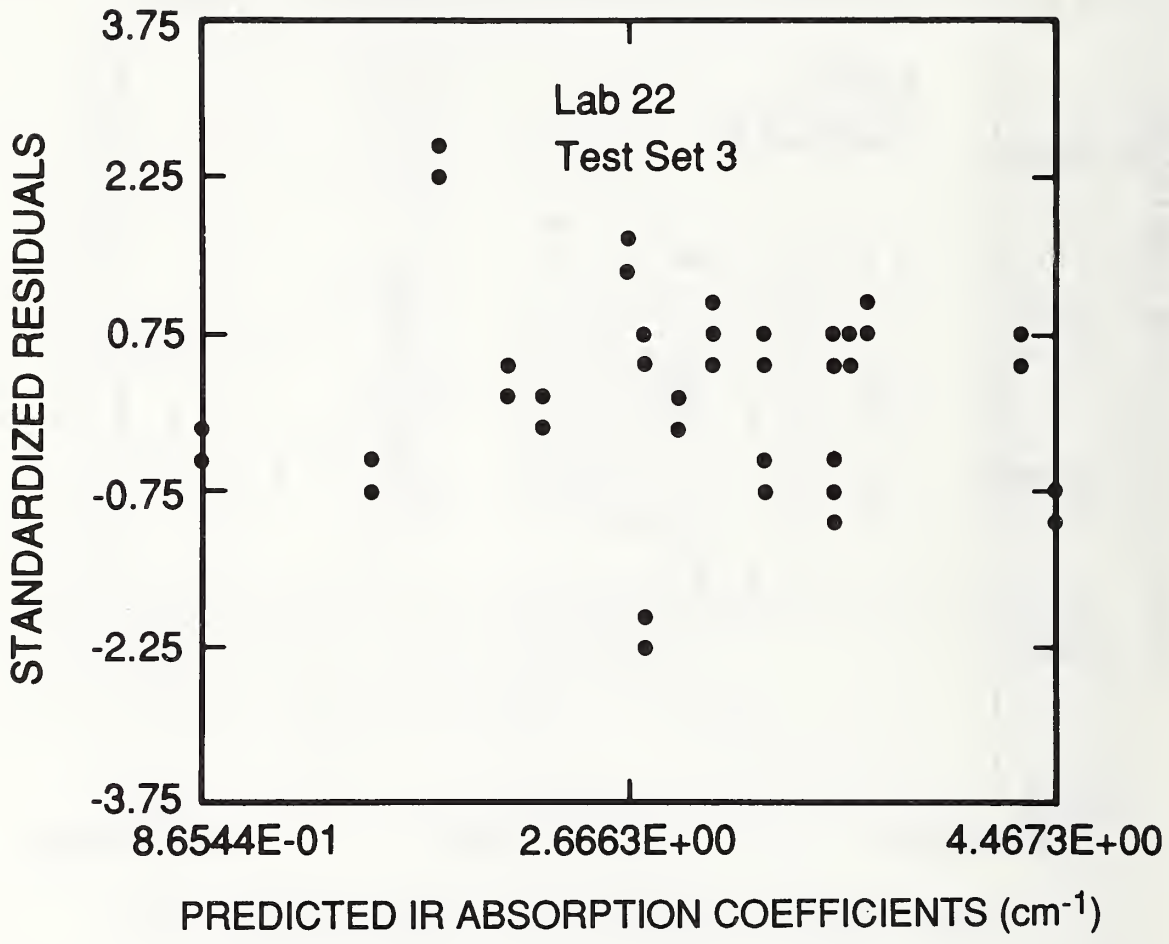

Figure 4-6b. For Lab 22 (CPAA), test set 3, standardized residuals from linear fit to test set data vs. predicted IR absorption coefficients.

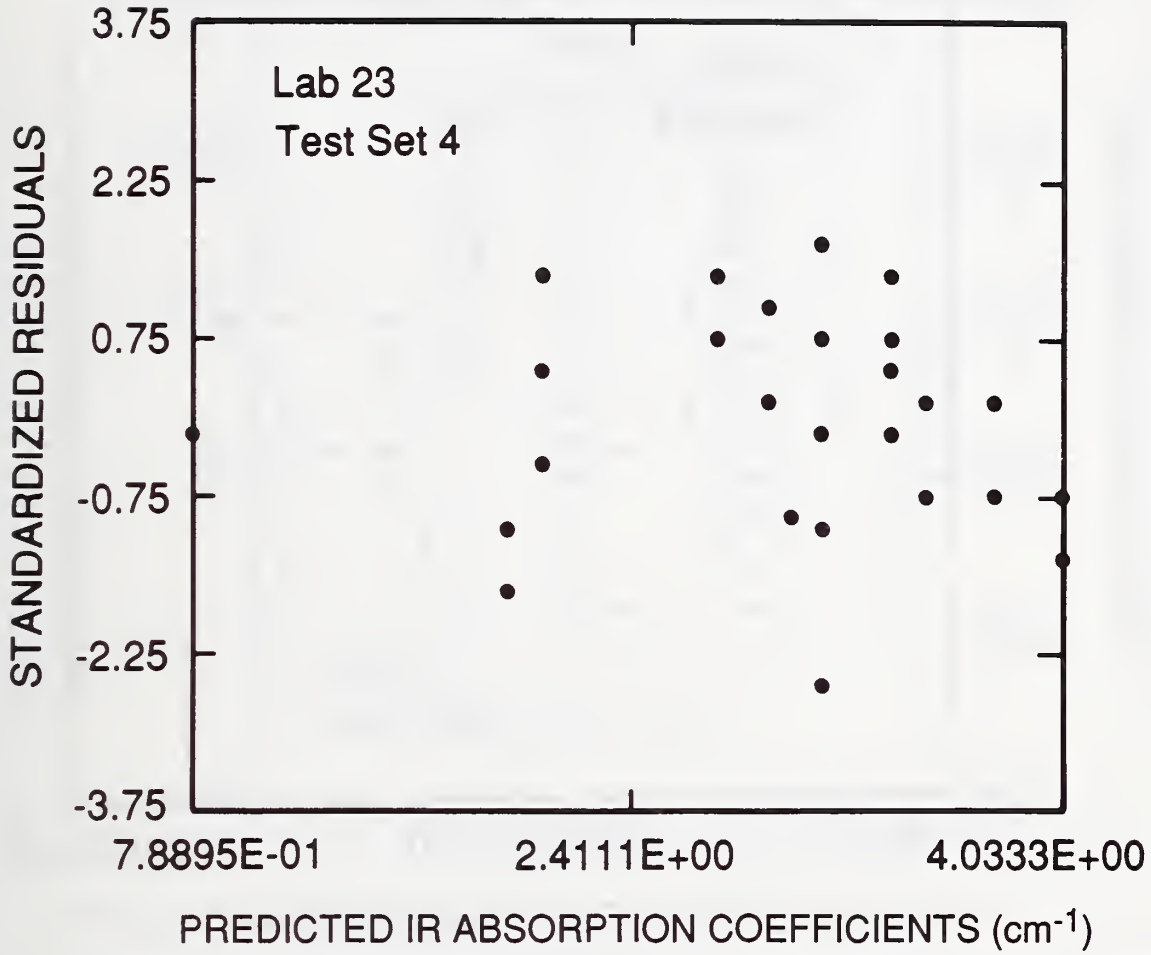

Figure 4-6c. For Lab 23 (CPAA), test set 4, standardized residuals from linear fit to test set data vs. predicted IR absorption coefficients.

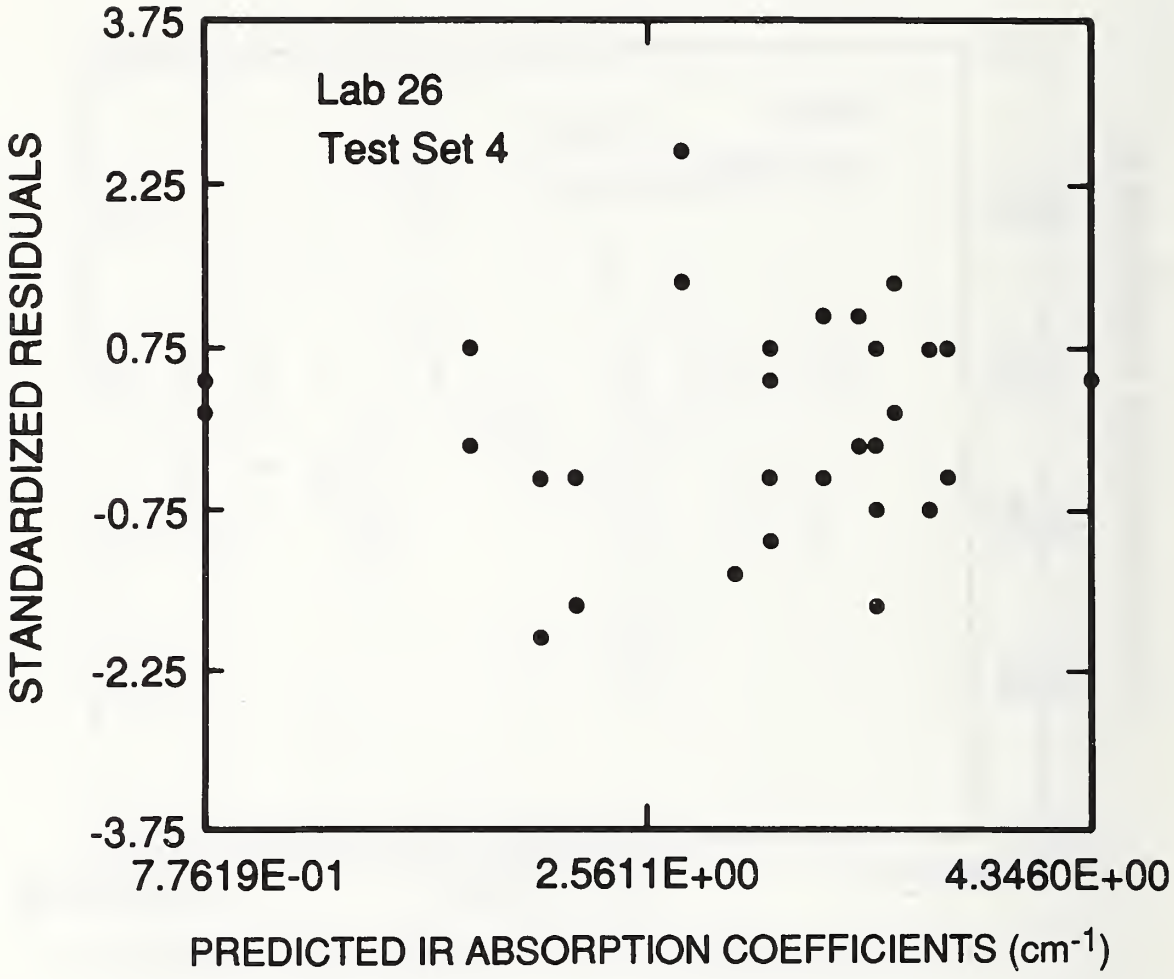

Figure 4-6d. For Lab 26 (CPAA), test set 4, standardized residuals from linear fit to test set data vs. predicted IR absorption coefficients.

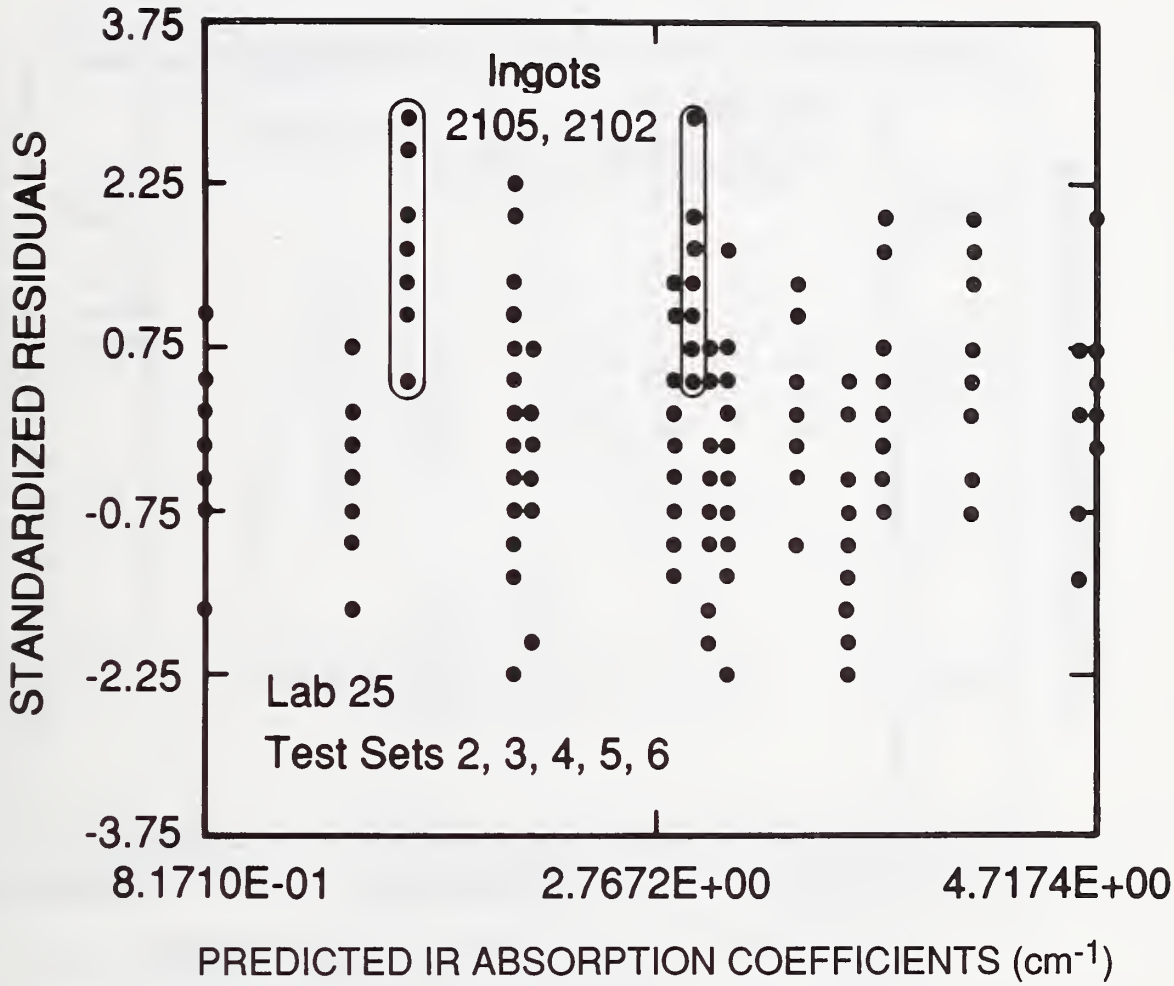

Figure 4-6e. For Lab 25 (PAA), test sets 2, 3, 4, 5, and 6, standardized residuals from linear fit to test set data vs. predicted IR absorption coefficients.

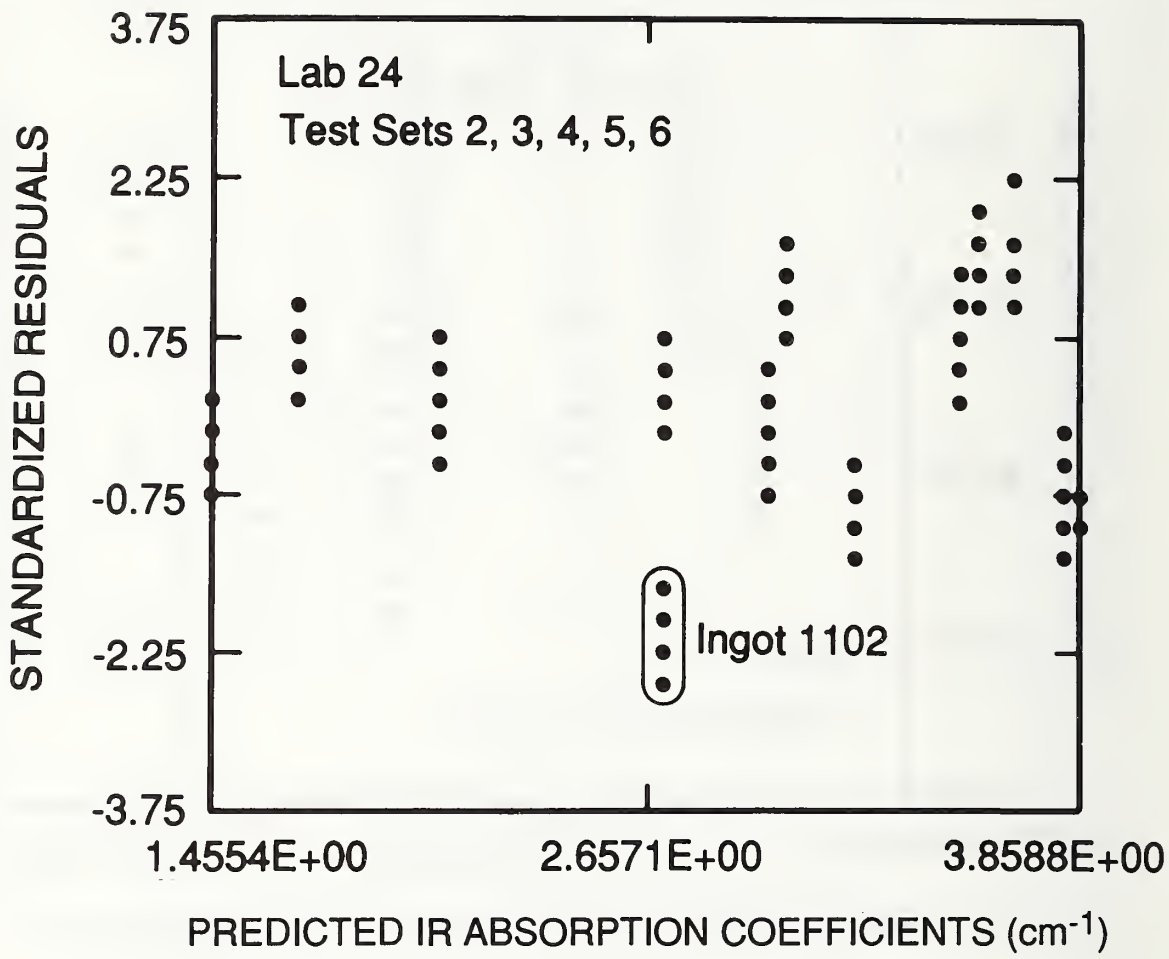

Figure 4-6f. For Lab 24 (PAA), test sets 2, 3, 4, 5, and 6, standardized residuals from linear fit to test set data vs. predicted IR absorption coefficients.

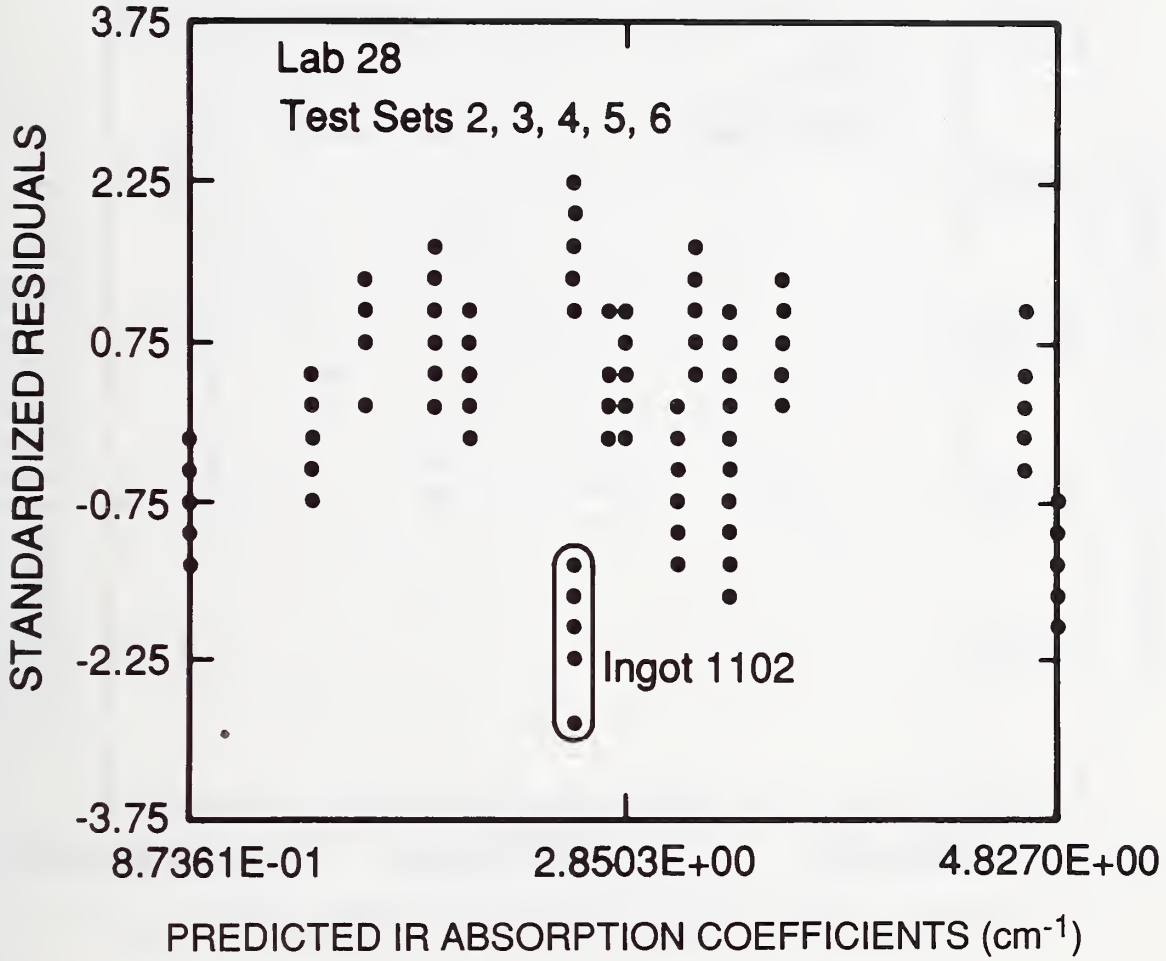

Figure 4-6g. For Lab 28 (IGFA), test sets 2, 3, 4, 5, and 6, standardized residuals from linear fit to test set data vs. predicted IR absorption coefficients.

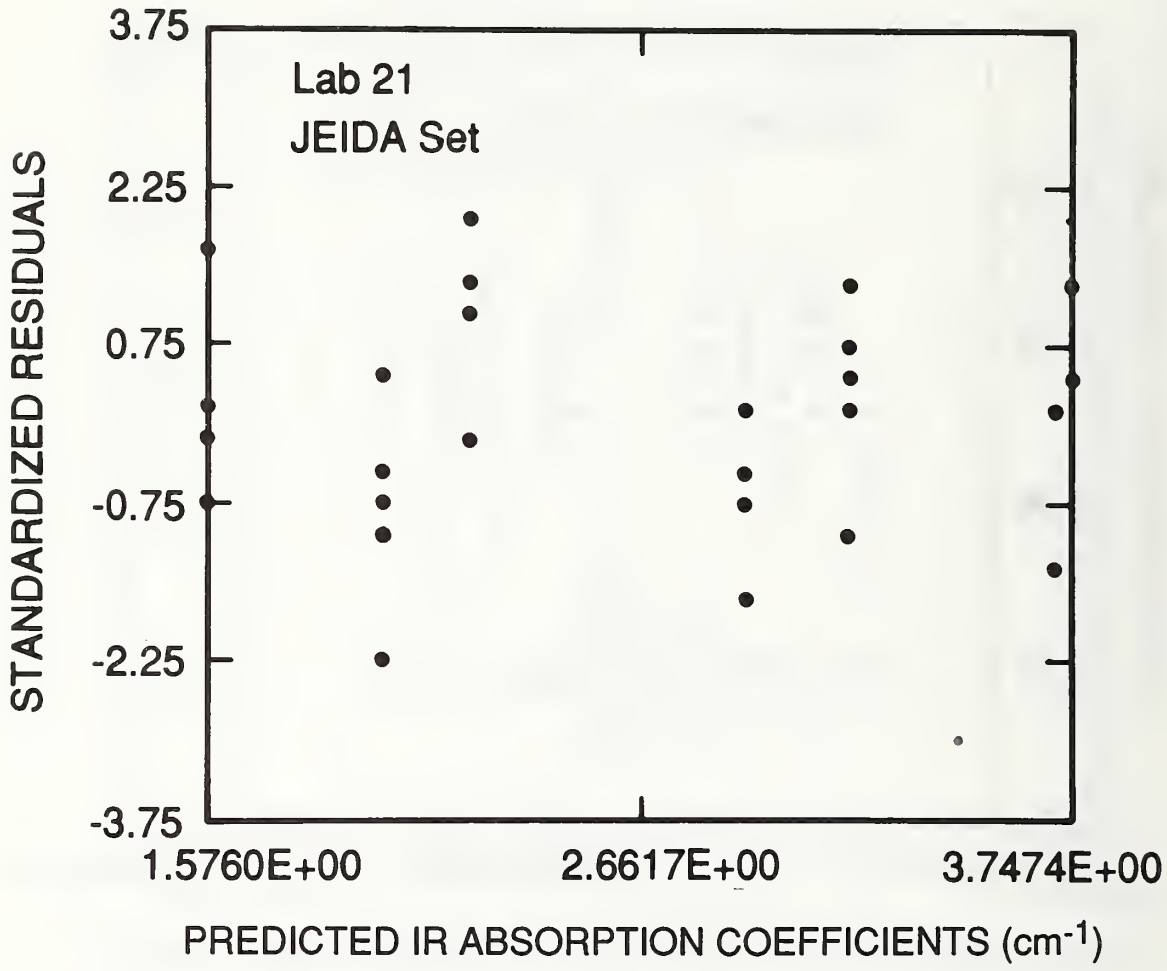

Figure 4-7a. For Lab 21, standardized residuals from linear fit to JEIDA data plotted vs. predicted IR absorption coefficient.

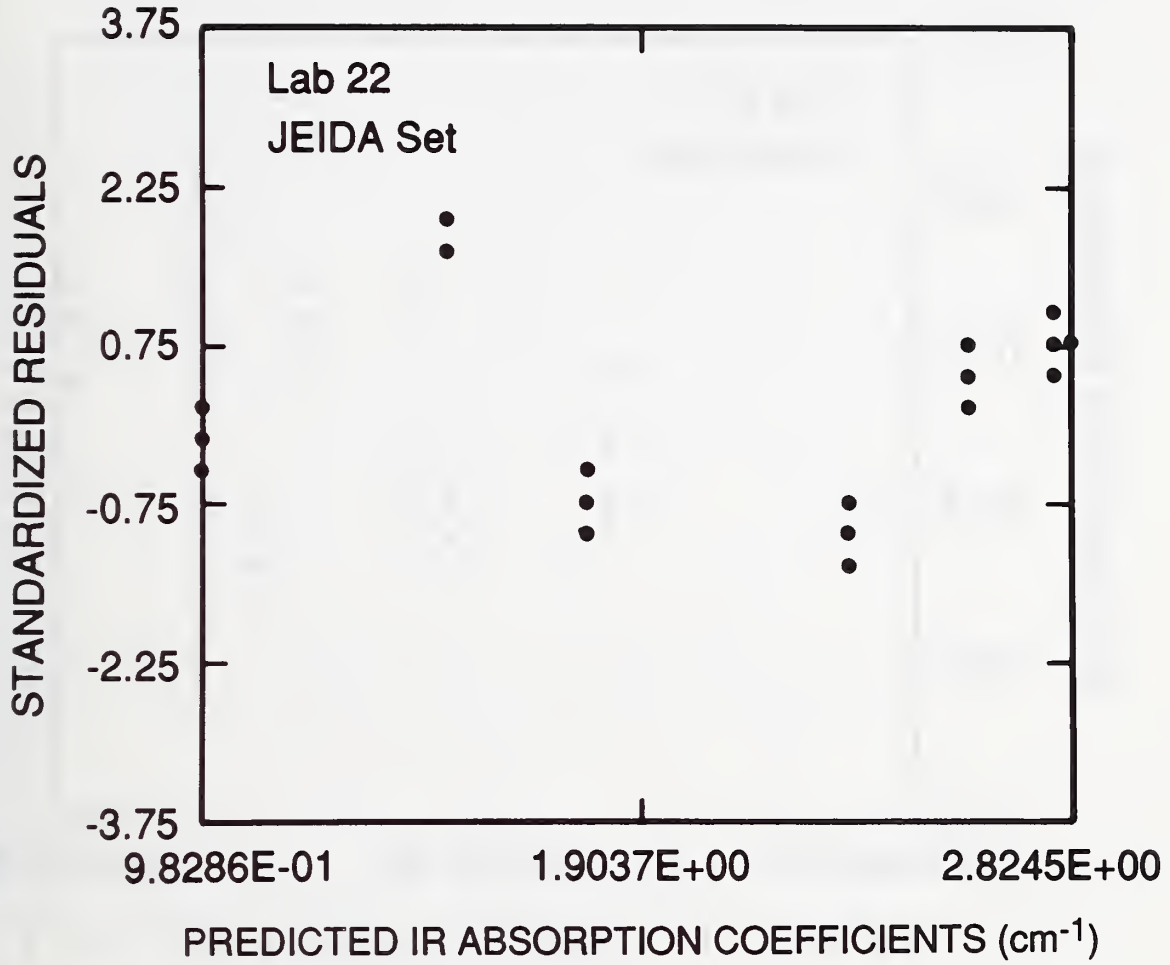

Figure 4-7b. For Lab 22, standardized residuals from linear fit to JEIDA data plotted vs. predicted IR absorption coefficient.

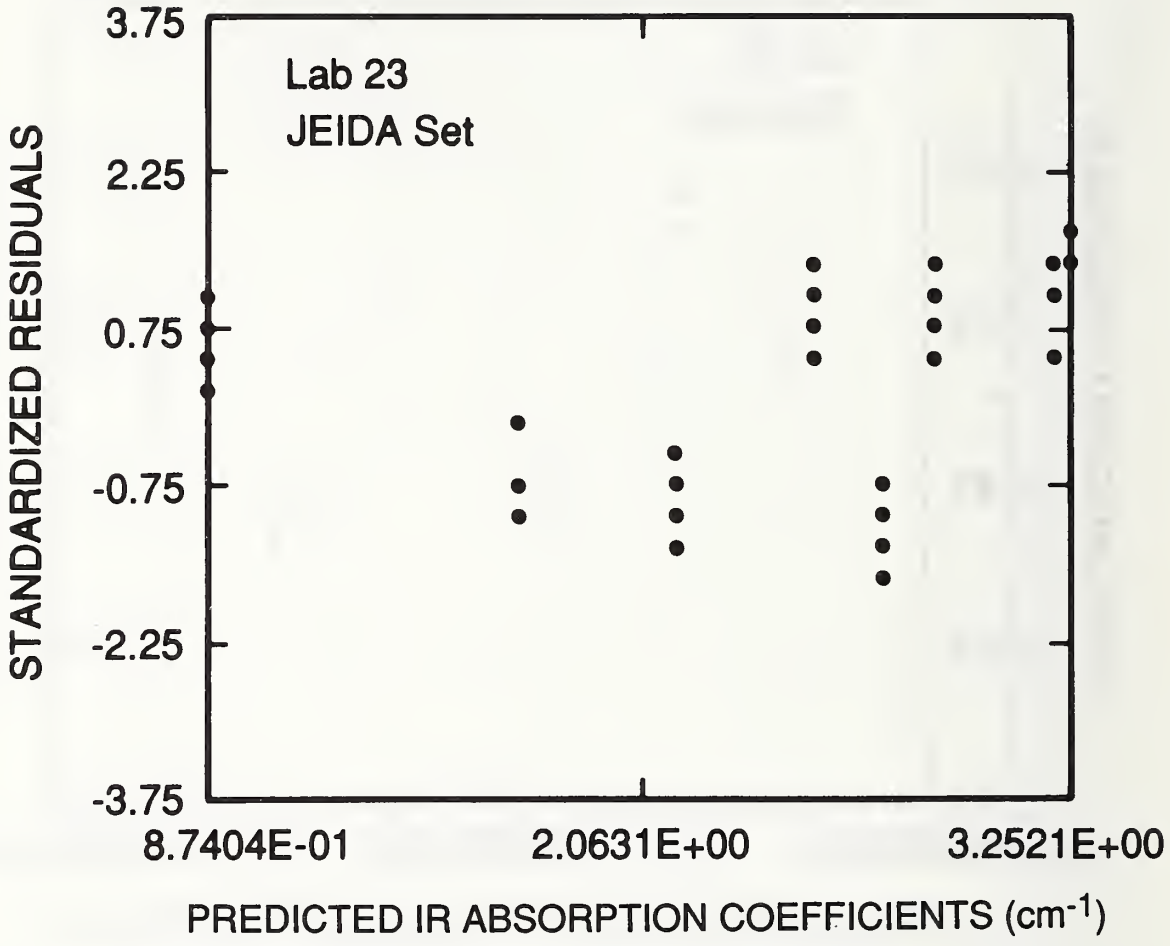

Figure 4-7c. For Lab 23, standardized residuals from linear fit to JEIDA data plotted vs. predicted IR absorption coefficient.

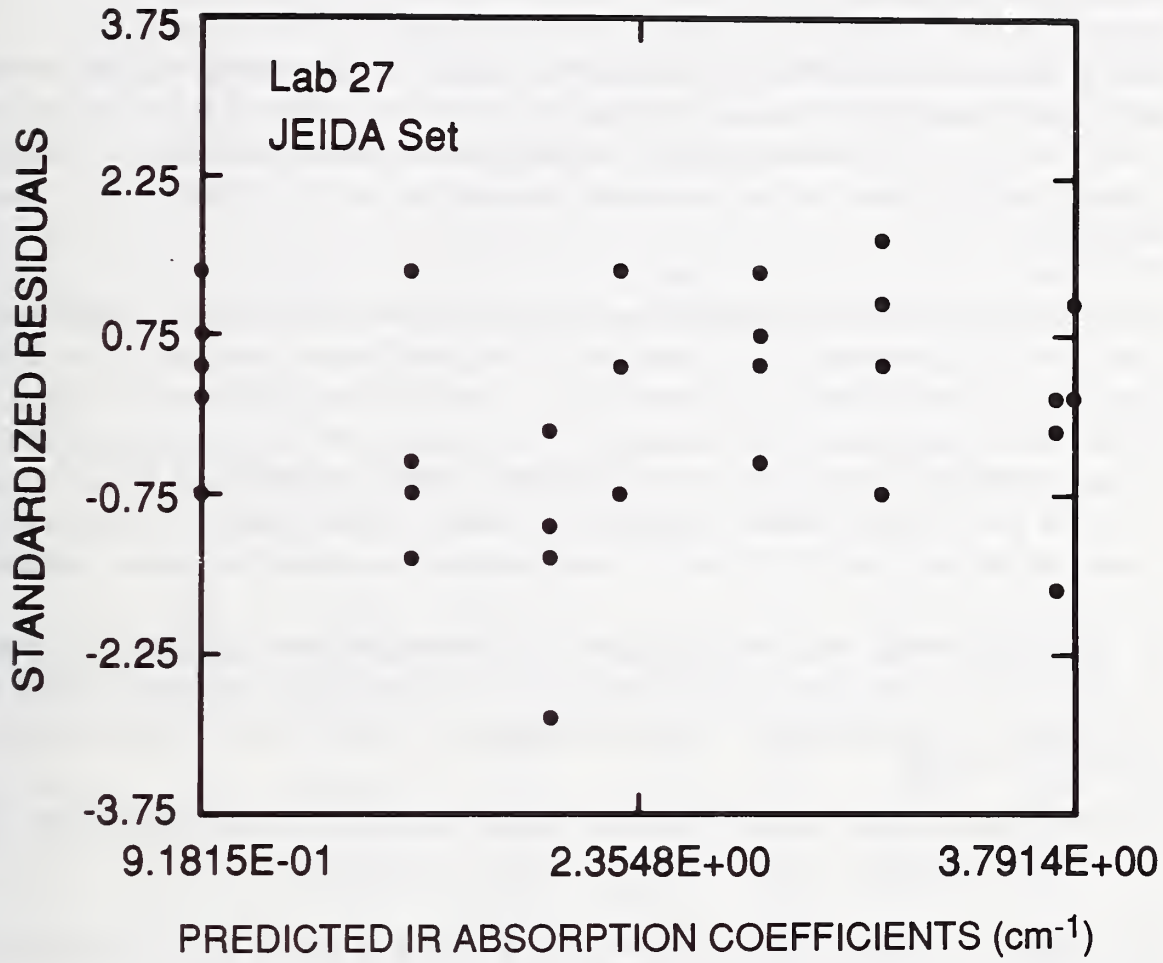

Figure 4-7d. For Lab 27, standardized residuals from linear fit to JEIDA data plotted vs. predicted IR absorption coefficient.

The residual plots for laboratories 21, 23, and 26 (figs. 4-6a, 4-6c, and 4-6d) are satisfactory. The residual plot for laboratory 22 (fig. 4-6b) is unsatisfactory. It is characterized by such clumping of residuals for each specimen that individual residuals are not always visible in the plot. This behavior implies agreement among IR laboratories and erratic responses by the absolute laboratory.

The F statistic for laboratory 25 is somewhat large, but the residual plot (fig. 4-6e) does not indicate erratic or nonlinear behavior for the absolute method but rather anomalous results for ingots #2102 and #2105. Recomputation omitting the data on these ingots reduced the F statistic to the same order of magnitude as the F statistics for cases (1a) and (4a).

The F statistics for laboratory 24 (case 6) and laboratory 28 (case 7) indicate egregious lack of fit. For laboratory 24, the residual plot (fig. 4-6f) shows an erratic pattern which is presumably caused either by the composition of the individual slugs from the ingots or by measurement problems in the laboratory. For laboratory 28, the residual plot (fig. 4-6g) indicates that the IR data are not a linear function of the absolute data over all concentrations. In fact, the plot indicates quadratic behavior, meaning that the IR measurements cannot be related to absolute oxygen concentrations via a simple conversion coefficient.

In order to eliminate the possibility that a few slugs are affected by ingot inhomogeneity, a recomputation was done for laboratories 24 and 28 omitting the data on ingot #1102 which appear to be anomalous. The recomputations reduced the F statistics, but not to an acceptable level.

4.13 ESTIMATION OF A CONVERSION COEFFICIENT FOR EACH ABSOLUTE LABORATORY

The linear statistical model of the last section does not account for the fact that both the absolute measurements and the infrared measurements are subject to random error. Fuller [4-5] proposes the following model where both types of measurements are subject to random error; namely,

$$Z_i = A + C\,(X_i + \xi_i) + \epsilon_i \qquad i = 1,\ \ldots,\ n \qquad (4-6)$$

where Z_i represents the average measurement by an absolute laboratory on the i^{th} specimen; ϵ_i represents an associated random error term; X_i represents the average IR value over all laboratories measuring the i^{th} specimen; and ξ_i represents the associated random error term. The terms ϵ_i are assumed to be independent and come from a distribution with standard deviation σ. All random error terms are assumed to be mutually independent.

Given the model defined in eq (4-6), Fuller has shown that the ordinary least-squares estimate of the slope C is biased towards zero. The bias, in this case, is approximately -0.005μg/g and is not significant for this study.

Therefore, we simplify the model by deleting the error terms ξ_i so that

$$Z_i = A + CX_i + \epsilon_i \qquad i = 1, \ldots, n. \tag{4-7}$$

Furthermore, based on multiple measurements by some absolute laboratories, it is assumed that the random error terms ϵ_i have standard deviations inversely proportional to oxygen concentration. The data from the study were analyzed by a weighted least-square technique that allows for the dependence of precision on oxygen concentration and for multiple measurements by absolute laboratories. Results are shown in table 4-7.

Where the intercept term A is effectively zero, the slope C can be used as a factor for converting from IR absorption coefficient to total oxygen concentration. The t statistics in table 4-7 indicate whether or not a laboratory is producing a calibration curve with zero intercept.

Table 4-7: Results of fitting absolute data as a function of IR data showing estimates of the intercept term A and slope C

Case	Abs Lab	Abs Test Set	IR Test Set	Intercept $\hat{A}$	t Statistics	Slope $\hat{C}$	Std Dev of $\hat{C}$	Residual Std Dev	DF ν
(1)	21	2	2	−0.037	−0.27	3.569	0.052	0.222	14
(1a)	21	2	2,3,4,5,6	−0.022	−0.15	3.583	0.054	0.234	14
(2)	22	3	3	2.391	3.32[a]	2.243	0.253	0.779	17
(2a)	22	3	2,3,4,5,6	2.378	3.29[a]	2.277	0.258	0.787	17
(3)	23	4	4	−0.151	−0.23	3.584	0.231	0.641	12
(3a)	23	4	2,3,4,5,6	−0.161	−0.25	3.528	0.226	0.633	12
(4)	26	4	4	0.239	1.50	3.678	0.057	0.270	14
(4a)	26	4	2,3,4,5,6	0.370	1.86	3.552	0.071	0.341	15
(5)	25[b]	10-mm slug	2,3,4,5,6	−0.009	−0.08	3.252	0.045	0.124	12
(6)	24[c]	10-mm slug	2,3,4,5,6	−0.268	−0.26	3.040	0.354	0.697	9
(7)	28[c]	10-mm slug	2,3,4,5,6	−1.302	−2.95[a]	3.505	0.169	0.472	13

[a]Indicates that the intercept is significantly different from zero at the 95% probability level.
[b]Ingots #2102 and #2105 excluded from this analysis.
[c]Ingot #1102 excluded from these analyses.

4.14 ESTIMATION OF A FINAL CONVERSION COEFFICIENT

There are two issues which must be resolved before a final conversion coefficient can be estimated from this study. First of all, there is a question as to whether a better estimate for the conversion coefficient is attained by averaging the IR data over test sets 2, 3, 4, 5, and 6, or by considering only IR data from the same test set as the absolute data. Table 4-7 lists results for both alternatives for the CPAA laboratories.

Where homogeneity is in question, we prefer measurements on the same physical artifacts. This course of action is not wholly satisfying for this study because we do not have absolute measurements on test set 5 and test set 6. Thus, the IR measurements on test sets 5 and 6 can only be tied to oxygen concentrations via the measurements on the 10-mm slugs. For this reason, IR measurements are averaged over all test sets, and the resulting bias is taken as a component of uncertainty in the final conversion coefficient.

The second fundamental question of how data from the absolute laboratories are combined to construct a final conversion coefficient is resolved by fitting all data from equivalent laboratories to the linear model (4-7) and taking the resulting slope as the best unbiased estimate of the conversion coefficient. This approach assumes that measurements by all laboratories are consistent and without bias, meaning that a zero intercept and a single slope characterize the relationship between IR measurements and absolute measurements. Data from laboratories 22 and 28 are excluded because of nonzero intercepts (table 4-7) and lack of fit (table 4-6). Data from laboratory 24 are excluded because of lack of fit (table 4-6).

We check the assumption of a zero intercept by a weighted fit to model (4-7) for data from laboratories 21, 23, 25, and 26. The t statistic for $\hat{A}$ in table 4-8 shows that the intercept term is not significantly different from zero. Therefore, a conversion coefficient is used to relate IR measurement to oxygen concentration. The conversion coefficient C is estimated from the model restricted to have zero intercept. Results are shown in table 4-8.

The plot of standardized residuals in figure 4-8 shows a slight offset for laboratory 25 and excellent agreement for the other three laboratories. The small value of the F statistic for testing the goodness of fit indicates that the restricted linear model is appropriate relative to the dispersion among absolute measurements by the four absolute laboratories.

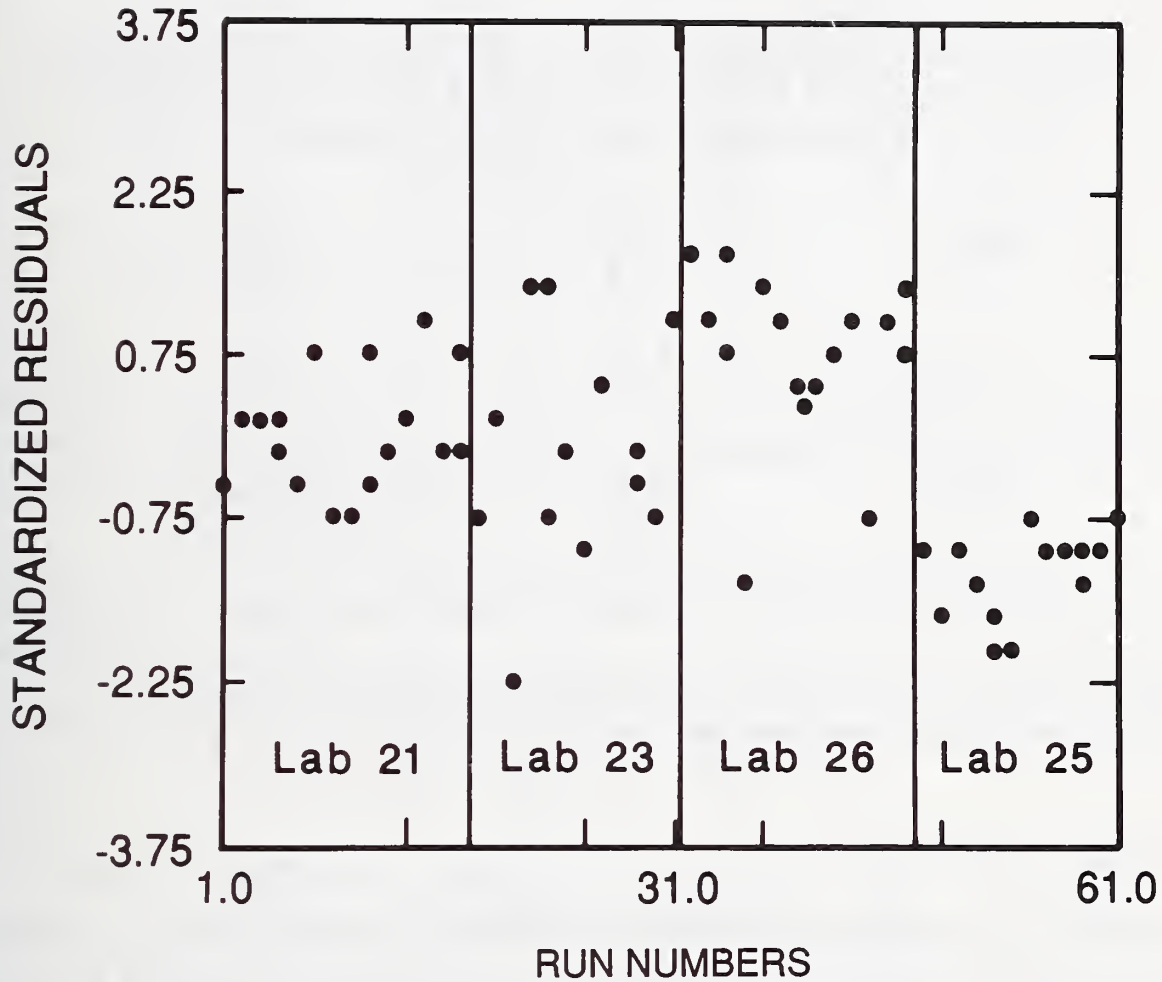

Figure 4-8. Standardized residuals from linear fits to data from absolute laboratories 21, 23, 26, and 25 plotted against run numbers.

A final conversion coefficient based on data from these four laboratories is 3.575 parts per million (weight) (ppmw) per cm^{-1}. The uncertainty associated with this value is discussed in the last section.

Table 4-8. Results of fitting absolute data from laboratories 21, 23, 25, and 26 as a linear function of IR data[a] on test sets 2, 3, 4, 5, and 6 showing estimates of the intercept A and conversion coefficient C

Intercept $\hat{A}$	Std Dev of $\hat{A}$	t Statistic for $\hat{A}$
0.070	0.079	0.88
Slope[b] $\hat{C}$	**Std Dev of $\hat{C}$**	**F Statistic for Lack of Fit**
3.575	0.023	0.67

[a]IR data with fewer than triplicate measurements excluded from the analysis.
[b]Model reduced to have zero intercept.

4.15 JEIDA SPECIMENS

In addition to the test squares that were specifically prepared for this study, 21 specimens, grouped into three test sets which had been used in an earlier Japanese study [4-6] were made available for the current international study. The analysis is restricted to data on JEIDA set 1 which was measured by four absolute laboratories. A limitation on this portion of the data base is that the IR measurements on the JEIDA specimens were made by four laboratories within a single national region. Therefore, the JEIDA data are used to corroborate the results from the test sets.

Total standard deviations across IR laboratories as defined by eq (4-3) are shown in table 4-9 for each specimen.

Table 4-9. Total standard deviations reflecting dispersion within and among IR laboratories

Specimen ID	Total standard deviation		Degrees of freedom
	Absorption units	Percent	
J – 2	0.0402	4	4
J – 6	0.0870	4	4
J – 8	0.1680	4	4
J – 16	0.0809	3	4
J – 17	0.1376	4	4
J – 23	0.0712	4	4
J – 25	0.0910	5	4

We apply the same diagnostic techniques to the measurements by the four CPAA laboratories on the JEIDA samples as were applied to the measurements on the test sets. Results for model (4-5) are shown in table 4-10.

Homogeneity is not an issue in this analysis because all absolute laboratories measured the same specimens. Studentized residuals from the fits are plotted versus predicted oxygen concentration in figure 4-7.

Table 4-10. Results of fitting IR data as a linear function of absolute data showing F statistics for testing lack of fit

Case	Absolute Lab	Abs Test Set	IR Test Set	DF of Fit	F Statistic
(1)	21	JEIDA	JEIDA	33	5.6[a]
(2)	22	JEIDA	JEIDA	28	173.5[a]
(3)	23	JEIDA	JEIDA	33	53.6[a]
(4)	27	JEIDA	JEIDA	33	3.9

[a] Indicates lack of fit at the 99% probability level.

Estimates of the conversion coefficient C, according to the model in eq (4-7), are shown in table 4-11 for the JEIDA specimens. Weighted least-squares analyses account for independent measurements of oxygen concentration by some absolute laboratories and for precision of absolute measurements as a function of oxygen concentration. Because the total standard deviations in table 4-9 are based on very few degrees of freedom, standard deviations for equivalent specimens from table 4-3 are used in the calculations.

Table 4-11. Results of fitting absolute data as a linear function of IR data showing estimates of the intercept A and slope C

Case	Abs Lab	Abs Test Set	IR Test Set	Intercept $\hat{A}$	Slope $\hat{C}$	Std Dev of $\hat{C}$	Residual Std Dev	DF
(1)	21	JEIDA	JEIDA	−0.372	3.696	0.147	0.489	5
(2)	22	JEIDA	JEIDA	−0.622	4.251	1.219	1.727	4
(3)	23	JEIDA	JEIDA	−0.244	3.358	0.428	0.734	5
(4)	27	JEIDA	JEIDA	−0.037	3.553	0.094	0.269	5

4.16 COMPARISON BETWEEN RESULTS FOR TEST SETS AND JEIDA SPECIMENS

Absolute laboratories 21, 22, and 23 measured both the JEIDA specimens and a test set. The differences between conversion coefficients calculated from the data on the test sets and those calculated from the data on the JEIDA specimens are shown in table 4-12. Differences in slopes for the two sets of artifacts are not significant relative to laboratory precision. This is true even for laboratory 22 which shows such divergent results. Laboratory 27, which measured only the JEIDA specimens, is compared with laboratory 26, which measured only test set 4.

Table 4-12: Differences between conversion coefficients computed from test sets data and JEIDA data

Absolute Lab	Diff in Slopes Test Set − JEIDA	Std Dev Diff	t-Statistic t
21	−0.127	0.081	0.8
22	−2.008	1.245	1.6
23	0.226	0.486	0.5
26 − 27	0.125	0.110	1.1

4.17 CONVERSION COEFFICIENT AND ASSOCIATED UNCERTAINTY

The conversion coefficient C for converting from IR measurement to total oxygen concentration is 3.575 ppmw per cm^{-1} with a total uncertainty of ± 0.10 ppmw per cm^{-1}. (This translates to 6.28 parts per million (atomic) (ppma) per cm^{-1} with a total uncertainty of ± 0.18 ppma/cm^{-1}.)

The random component of the uncertainty is taken to be two times the standard deviation associated with the estimate of C or 0.046 μg/g. The systematic component of the uncertainty is estimated to be 0.057 μg/g. The total uncertainty is the linear sum of the random and systematic components.

The systematic component accounts for any error in the conversion coefficient that we may have incurred by averaging the IR data over all test sets. This component accounts for the effect of inhomogeneities which occur at random within an ingot as well as any offset for a regional group of IR laboratories relative to the other IR laboratories. A bound for this error is difficult to calculate from the data of this experiment. We can, however, estimate the average effect from the data of laboratories 21, 23, and 26 (table 4-7). For each laboratory, we calculate the difference between a conversion coefficient based on IR and absolute measurements on the same specimens and a conversion coefficient based on IR measurements averaged over all test sets. The average difference over the three laboratories of 0.057 μg/g is our best estimate of systematic error.

4.18 CONCLUSION

Data from each absolute laboratory have been examined in detail to determine if the laboratory is producing measurements consistent with IR measurements. Absolute measurements should be a linear function of IR measurements for the range of oxygen concentrations in the study (0 to 10 μg/g). Diagnostic tests for zero intercept (table 4-7) and goodness of fit to the linear model (table 4-6) confirm that measurement problems or inhomogeneities invalidate the results for three absolute laboratories (22, 24, 28). The final conversion coefficient is based on data from four absolute laboratories that measured the specimens that were fabricated especially for this study (21, 23, 25, 26). Data from absolute laboratories that measured only the JEIDA specimens are in agreement with the final result.

The study has shown that IR laboratories are internally consistent in measuring interstitial oxygen and that systematic differences among laboratories can be as large as 0.6 absorption units at the highest oxygen concentrations. Because the final conversion coefficient is based on an average of IR laboratories, an IR laboratory that is systematically biased from the average by ± 0.3 absorption units could have a bias as large as ± 2 μg/g (or ± 3 ppma) in its determination of oxygen concentration using the recommended conversion coefficient.

REFERENCES

[4-1] Hogg, R. V., and Craig, A. T., *Introduction to Mathematical Statistics* (The Macmillan Co., New York, 1965).

[4-2] Draper, N. R., and Smith, H., *Applied Regression Analysis*, Second Edition (John Wiley & Sons, Inc., New York, 1981), p. 111.

[4-3] *Ibid.*, p. 33.

[4-4] *Ibid.*, p. 144.

[4-5] Fuller, W. A., *Measurement Error Models* (John Wiley & Sons, Inc., New York, 1987), p. 13.

[4-6] Iizuka, T., Takasu, S., Tajima, M., Arai, T., Nozaki, T., Inoue, N., and Watanabe, M., *J. Electrochem. Soc.* **132**, 1707 (1985).

5. STATISTICAL ANALYSIS OF THE DATA

by
John Mandel
National Measurement Laboratory

5.1 SCOPE

The analysis described in this report deals with the comparisons of the results obtained by "absolute" methods of measurement, i.e., by laboratories 21, 22, 23, and 26 for CPAA, 24 and 25 for PAA, and 28 for IGFA, with those obtained by the infrared (IR) method. For the latter, only sets 2 to 6 were included.

5.2 DATA

The full data for the infrared laboratories are listed in Appendix A, and for the absolute laboratories in Appendix B of this Special Publication. Tables 5-1 through 5-7 contain the data used for this analysis as the results from the absolute laboratories listed against the average IR absorption coefficient for each ingot. Figures 5-1a through 5-7a are plots of the oxygen content as determined by each of the absolute laboratories versus the infrared absorption coefficient. Figures 5-1b through 5-7b are bar plots showing the standardized residual errors ("H-Values") for each specimen.

5.3 METHODS OF ANALYSIS AND RESULTS

Each of the absolute laboratories for which replicate measurements of the absolute method exist was analyzed by the same statistical technique. This was a straight-line fit in which allowance was made for two sources of variability: replication error and additional lack-of-fit. The straight line is assumed to go through the origin. The mathematical model is

$$y_{ij} = \beta x_i + \delta_i + \epsilon_{ij} \ ,$$

where:

x_i = IR measurement for ingot i.

y_{ij} = absolute measurement for ingot i, replicate j.

δ_i = "lack-of-fit" error for point i, this point consisting of the abscissa x_i and an ordinate y_i, equal to the average of the replicates y_{ij}, for ingot i.

Table 5-1a. Absolute Laboratory 21 vs. IR (average of sets 2 to 6)

IR (cm^{-1})	Oxygen Content ($\mu g/g$)		
0.806	2.83	2.85	
1.429	4.62	5.35	5.01
1.882	6.89	6.66	
2.140	7.56	7.67	
2.256	7.94	7.90	
2.279	8.42	8.12	
2.814	10.04	9.70	10.17
2.957	10.34	10.05	
2.961	11.09	11.07	
3.108	11.63	11.69	
3.124	10.87	11.01	
3.403	12.40	12.22	
3.466	11.94	12.17	12.92
3.530	12.63	12.41	
3.543	12.98	13.27	
3.724	12.95	12.56	
3.836	13.07	13.69	13.56
3.902	14.54	14.19	
4.280	15.59	16.24	
4.770	16.62	16.59	

Fitted equation is: Y = 3.575881 *X.
Standard error of B = 0.0220.
Within standard deviation = 0.0793322 *X(I).
Between standard deviation = 8.216614E–02 *X(I).

Table 5-1b

X	Y	$\hat{Y}$	Resid.	Weight
0.8060	2.8400	2.8822	−0.0422	1.56E+02
1.4290	4.9933	5.1099	−0.1166	5.53E+01
1.8820	6.7750	6.7298	0.0452	2.85E+01
2.1400	7.6150	7.6524	−0.0374	2.21E+01
2.2560	7.9200	8.0672	−0.1472	1.99E+01
2.2790	8.2700	8.1494	0.1206	1.95E+01
2.8140	9.9700	10.0625	−0.0925	1.43E+01
2.9570	10.1950	10.5739	−0.3789	1.16E+01
2.9610	11.0800	10.5882	0.4918	1.15E+01
3.1080	11.6600	11.1138	0.5462	1.05E+01
3.1240	10.9400	11.1711	−0.2311	1.04E+01
3.4030	12.3100	12.1687	−0.1413	8.72E+00
3.4660	12.3433	12.3940	−0.0507	9.41E+00
3.5300	12.5200	12.6229	−0.1029	8.11E+00
3.5430	13.1250	12.6693	0.4557	8.05E+00
3.7240	12.7550	13.3166	−0.5616	7.29E+00
3.8360	13.4400	13.7171	−0.2771	7.68E+00
3.9020	14.3650	13.9531	0.4119	6.64E+00
4.2800	15.9150	15.3048	0.6102	5.52E+00
4.7700	16.6050	17.0570	−0.4520	4.44E+00

Table 5-2a. Absolute Laboratory 22 vs. IR (average of sets 2 to 6)

IR (cm^{-1})	Oxygen Content ($\mu g/g$)
0.8060	3.60
1.4290	5.70
1.8820	8.90
2.2560	7.30
2.2790	7.70
2.8140	9.20
2.9570	10.30
2.9610	8.80
3.1080	11.00
3.1240	6.50
3.4030	9.60
3.4660	8.60
3.5300	10.20
3.5430	9.60
3.7240	13.50
3.8360	11.10
3.9020	11.30
4.2800	11.40
4.7700	13.20

Fitted equation is: Y = 3.20475 *X.
Standard error of B = 0.1568.
Standard deviation of fit = 0.6834658 *X(I).

Table 5-2b

X	Y	$\hat{Y}$	Resid.	Weight
0.8060	3.6000	2.5830	1.0170	3.30E+00
1.4290	5.7000	4.5796	1.1204	1.05E+00
1.8820	8.9000	6.0313	2.8687	6.04E–01
2.2560	7.3000	7.2299	0.0701	4.21E–01
2.2790	7.7000	7.3036	0.3964	4.12E–01
2.8140	9.2000	9.0182	0.1818	2.70E–01
2.9570	10.3000	9.4764	0.8236	2.45E–01
2.9610	8.8000	9.4893	–0.6893	2.44E–01
3.1080	11.0000	9.9604	1.0396	2.22E–01
3.1240	6.5000	10.0116	–3.5116	2.19E–01
3.4020	9.6000	10.9058	–1.3058	1.85E–01
3.4660	8.6000	11.1077	–2.5077	1.78E–01
3.5300	10.2000	11.3128	–1.1128	1.72E–01
3.5430	9.6000	11.3544	–1.7544	1.71E–01
3.7240	13.5000	11.9345	1.5655	1.54E–01
3.8360	11.1000	12.2934	–1.1934	1.45E–01
3.9020	11.3000	12.5049	–1.2049	1.41E–01
4.2800	11.4000	13.7163	–2.3163	1.17E–01
4.7700	13.2000	15.2867	–2.0867	9.41E–02

Table 5-3a. Absolute Laboratory 23 vs. IR (average of sets 2 to 6)

IR (cm^{-1})	Oxygen Content ($\mu g/g$)	
0.8060	2.60	
1.8820	7.20	
2.1400	7.60	
2.2790	7.70	
2.9570	11.70	
2.9610	10.00	
3.1080	10.80	
3.1240	11.50	11.20
3.4030	11.70	11.30
3.5300	13.30	11.90
3.5430	12.90	
3.7240	12.60	
3.8360	14.00	
3.9020	15.00	14.70

Fitted equation is: Y = 3.562814 *X.
Standard error of B = 0.0548.
Within standard deviation = 0.1214559 *X(I).
Between standard deviation = 0.1721403 *X(I).

Table 5-3b

X	Y	$\hat{Y}$	Resid.	Weight
0.8060	2.6000	2.8716	−0.2716	3.47E+01
1.8820	7.2000	6.7052	0.4948	6.36E+00
2.1400	7.6000	7.6244	−0.0244	4.92E+00
2.2790	7.7000	8.1197	−0.4197	4.34E+00
2.9570	11.7000	10.5352	1.1648	2.58E+00
2.9610	10.0000	10.5495	−0.5495	2.57E+00
3.1080	10.8000	11.0732	−0.2732	2.33E+00
3.1240	11.3500	11.1302	0.2198	2.77E+00
3.4030	11.5000	12.1243	−0.6243	2.33E+00
3.5300	12.6000	12.5767	0.0233	2.17E+00
3.5430	12.9000	12.6231	0.2769	1.79E+00
3.7240	12.6000	13.2679	−0.6679	1.62E+00
3.8360	14.0000	13.6670	0.3330	1.53E+00
3.9020	14.8500	13.9021	0.9479	1.77E+00

Table 5-4a. Absolute Laboratory 24 vs. IR (average of sets 2 to 6)

IR (cm^{-1})	Oxygen Content ($\mu g/g$)
1.4290	3.70
1.8820	4.60
2.1400	6.10
2.2560	8.50
2.8140	8.40
2.9570	9.50
2.9610	10.30
3.4660	9.70
3.5430	12.60
3.8360	11.50
4.2800	11.70
4.7700	12.00

Fitted equation is: Y = 2.994181 *X.
Standard error of B = 0.1297.
Standard deviation of fit = 0.4493328 *X(I).

Table 5-4b

X	Y	$\hat{Y}$	Resid.	Weight
1.4290	3.7000	4.2787	−0.5787	2.43E+00
1.8820	4.6000	5.6351	−1.0350	1.40E+00
2.1400	6.1000	6.4075	−0.3075	1.08E+00
2.2560	8.5000	6.7549	1.7451	9.73E−01
2.8140	8.4000	8.4256	−0.0256	6.25E−01
2.9570	9.5000	8.8538	0.6462	5.66E−01
2.9610	10.3000	8.8658	1.4342	5.65E−01
3.4660	9.7000	10.3778	−0.6778	4.12E−01
3.5430	12.6000	10.6084	1.9916	3.95E−01
3.8360	11.5000	11.4857	0.0143	3.37E−01
4.2800	11.7000	12.8151	−1.1151	2.70E−01
4.7700	12.0000	14.2822	−2.2822	2.18E−01

Table 5-5a. Absolute Laboratory 25 vs. IR (average of sets 2 to 6)

IR (cm^{-1})	Oxygen Content ($\mu g/g$)							
0.8060	2.2000	2.5900	2.8100	2.6000	2.6500	2.2000	2.7200	2.7200
1.4290	3.7800	4.7500	5.0800	4.8800	4.8500	4.7000	4.2800	4.7800
1.8820	5.7600	5.7200	5.1600	5.5300	4.9100	5.9500	5.7000	5.8600
2.1400	6.7000	6.8000	6.9500	7.6200	7.0400	6.7100	6.7300	7.9400
2.2560	7.6600	7.2800	7.7800	7.3400	7.0800	7.3500	7.1700	
2.2790	7.1500	6.6500	7.1600	6.7800	7.5000	7.0500	7.5600	7.1500
2.8140	8.8400	9.4900	9.3900	8.5300	9.3600	9.0200	9.8900	9.6600
2.9570	9.6200	9.4000	10.3600	10.5000	10.1000	9.7800		
2.9610	8.9700	9.7600	9.8000	10.1000	9.9400	9.8000	9.8500	10.3700
3.1080	9.0400	9.2900	10.7500	10.1700	9.7800	9.8000	10.9100	10.1900
3.1240	9.6300	10.3200	10.4500	9.3300	8.0900	8.1900	10.3900	9.5200
3.4660	11.2000	10.8200	10.6600	11.4100	11.3900	11.2700	10.9800	12.0600
3.5430	12.4700	12.6200	12.0800	11.2300	10.9400	11.6900	12.4200	11.7700
3.8360	12.4000	13.2200	12.3600	11.0800	10.9700	12.6400	12.8000	12.6600
4.2800	14.5000	14.3000	13.0000	13.6300	13.4100	13.1300	13.4800	13.7300
4.7700	14.9000	15.7600	13.8900	14.9800	16.4500	14.8000	16.5700	15.1400

Fitted equation is: Y = 3.218106 *X.
Standard error of B = 0.0272.
Within standard deviation = 0.1894086 *X(I).
Between standard deviation = 8.515099E–02 *X(I).

Table 5-5b

X	Y	$\hat{Y}$	Resid.	Weight
0.8060	2.5613	2.5938	−0.0325	1.31E+02
1.4290	4.6375	4.5987	0.0388	4.17E+01
1.8820	5.5738	6.0565	−0.4827	2.41E+01
2.1400	7.0612	6.8867	0.1745	1.86E+01
2.2560	7.3800	7.2600	0.1200	1.59E+01
2.2790	7.1250	7.3341	−0.2091	1.64E+01
2.8140	9.2725	9.0558	0.2167	1.08E+01
2.9570	9.9600	9.5159	0.4441	8.64E+00
2.9610	9.8237	9.5288	0.2949	9.72E+00
3.1080	9.9913	10.0019	−0.0106	8.82E+00
3.1240	9.4900	10.0534	−0.5634	8.73E+00
3.4660	11.2237	11.1540	0.0698	7.09E+00
3.5430	11.9025	11.4018	0.5007	6.79E+00
3.8360	12.2663	12.3447	−0.0784	5.79E+00
4.2800	13.6475	13.7735	−0.1260	4.65E+00
4.7700	15.3113	15.3504	−0.0391	3.75E+00

Table 5-6a. Absolute Laboratory 26 vs. IR (average of sets 2 to 6)

IR (cm^{-1})	Oxygen Content ($\mu g/g$)		
0.8060	3.2200	2.9200	
1.8820	6.6500	7.1700	7.2600
2.1400	8.4800	8.1200	
2.2560	8.7700	8.3100	8.3900
2.2790	8.7900	8.7300	8.8500
2.9570	11.2800	10.9000	11.2400
2.9610	10.7500	9.6400	10.4900
3.1080	12.3000	11.4700	10.8700
3.1240	11.5200	11.2200	12.0900
3.4030	13.2800	12.7700	11.5100
3.4660	13.6700	12.9500	12.9100
3.5300	12.9900	12.3800	13.3000
3.5430	13.4800	12.9500	13.0700
3.7240	13.8500	13.1600	13.3900
3.8360	14.4300	13.6300	14.2200
3.9020	14.5700	13.9200	14.2900
4.7700	16.2100	16.3800	

Fitted equation is: Y = 3.701534 *X.
Standard error of B = 0.0282.
Within standard deviation = 0.1316959 *X(I).
Between standard deviation = 8.562864E–02 *X(I).

Table 5-6b

X	Y	$\hat{Y}$	Resid.	Weight
0.8060	3.0700	2.9834	0.0866	9.62E+01
1.8820	7.0267	6.9663	0.0604	2.15E+01
2.1400	8.3000	7.9213	0.3787	1.36E+01
2.2560	8.4900	8.3507	0.1393	1.50E+01
2.2790	8.7900	8.4358	0.3542	1.47E+01
2.9570	11.1400	10.9454	0.1946	8.72E+00
2.9610	10.2933	10.9602	−0.6669	8.70E+00
3.1080	11.5467	11.5044	0.0423	7.89E+00
8.1240	11.6100	11.5636	0.0464	7.81E+00
3.4030	12.5200	12.5963	−0.0763	6.59E+00
3.4660	13.1767	12.8295	0.3471	6.35E+00
3.5300	12.8900	13.0664	−0.1764	6.12E+00
3.5430	13.1667	13.1145	0.0521	6.07E+00
3.7240	13.4667	13.7845	−0.3178	5.50E+00
3.8360	14.0933	14.1991	−0.1058	5.18E+00
3.9020	14.2600	14.4434	−0.1834	5.01E+00
4.7700	16.2950	17.6563	−1.3613	2.75E+00

Table 5-7a. Absolute Laboratory 28 vs. IR (average of sets 2 to 6)

IR (cm^{-1})	Oxygen Content ($\mu g/g$)
0.8060	1.8000
1.4290	3.8000
1.8820	4.8000
2.1400	5.8000
2.2560	8.1000
2.2790	6.5000
2.8140	8.6000
2.9570	9.8000
2.9610	8.9000
3.1080	8.2000
3.1240	10.8000
3.4660	10.6000
3.5430	10.2000
3.8360	11.6000
4.2800	15.9000
4.7700	15.4000

Fitted equation is: Y = 2.998246 *X.
Standard error of B = 0.1032.
Standard deviation of fit = 0.412666 *X(I).

Table 5-7b

X	Y	$\hat{Y}$	Resid.	Weight
0.8060	1.8000	2.4166	−0.6166	9.04E+00
1.4290	3.8000	4.2845	−0.4845	2.88E+00
1.8820	4.8000	5.6427	−0.8427	1.66E+00
2.1400	5.8000	6.4162	−0.6162	1.28E+00
2.2560	8.1000	6.7640	1.3360	1.15E+00
2.2790	6.5000	6.8330	−0.3330	1.13E+00
2.8140	8.6000	8.4371	0.1629	7.42E−01
2.9570	9.8000	8.8658	0.9342	6.72E−01
2.9610	8.9000	8.8778	0.0222	6.70E−01
3.1080	8.2000	9.3185	−1.1185	6.08E−01
3.1240	10.8000	9.3665	1.4335	6.02E−01
3.4660	10.6000	10.3919	0.2081	4.89E−01
3.5430	10.2000	10.6228	−0.4228	4.68E−01
3.8360	11.6000	11.5013	0.0987	3.99E−01
4.2800	15.9000	12.8325	3.0675	3.21E−01
4.7700	15.4000	14.3016	1.0984	2.58E−01

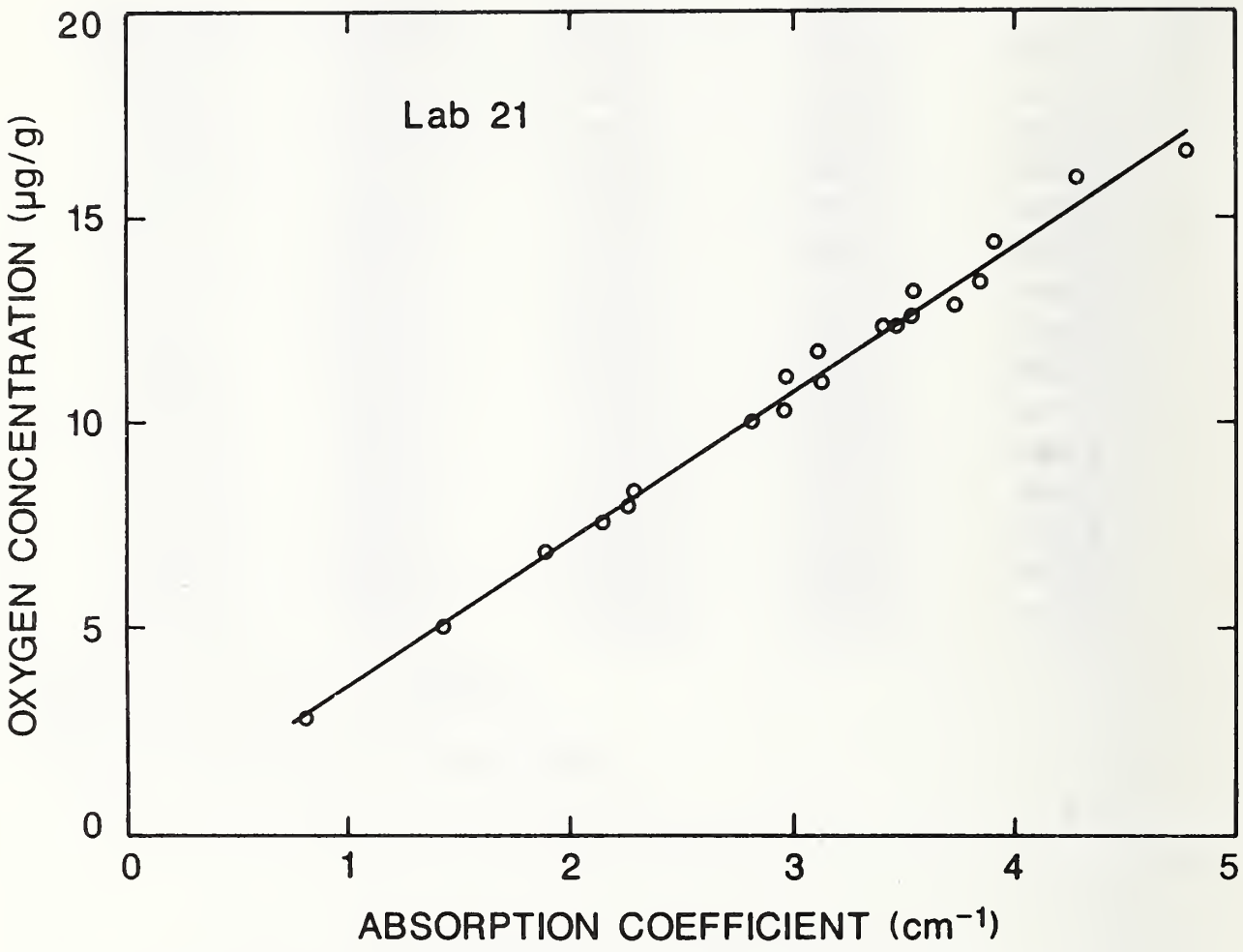

Figure 5-1a. For Lab 21, oxygen content vs. infrared absorption coefficient.

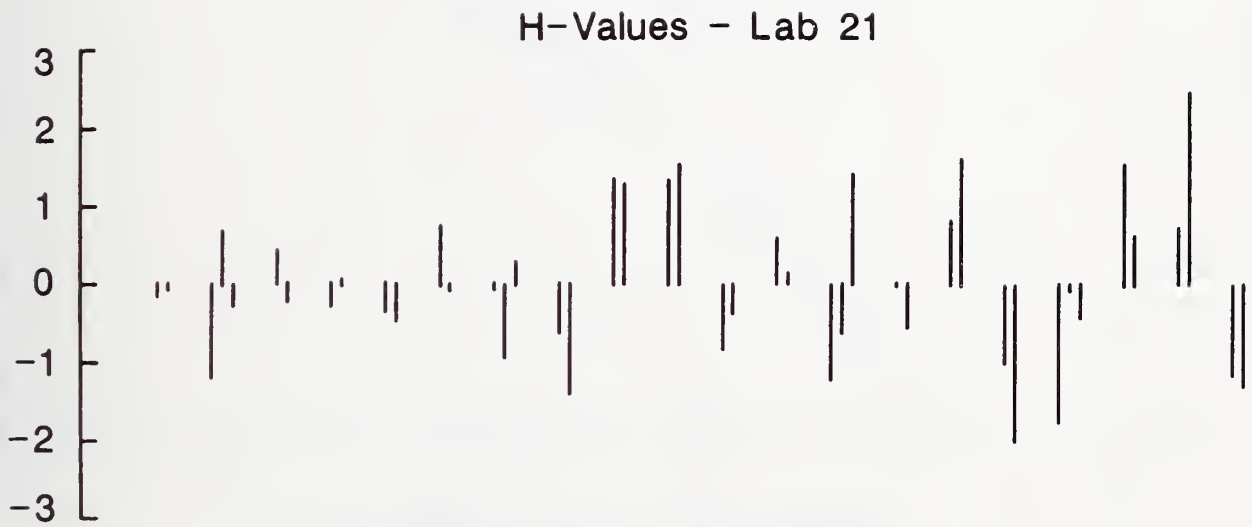

Figure 5-1b. For Lab 21, standardized residual errors ("H-Values") for each specimen.

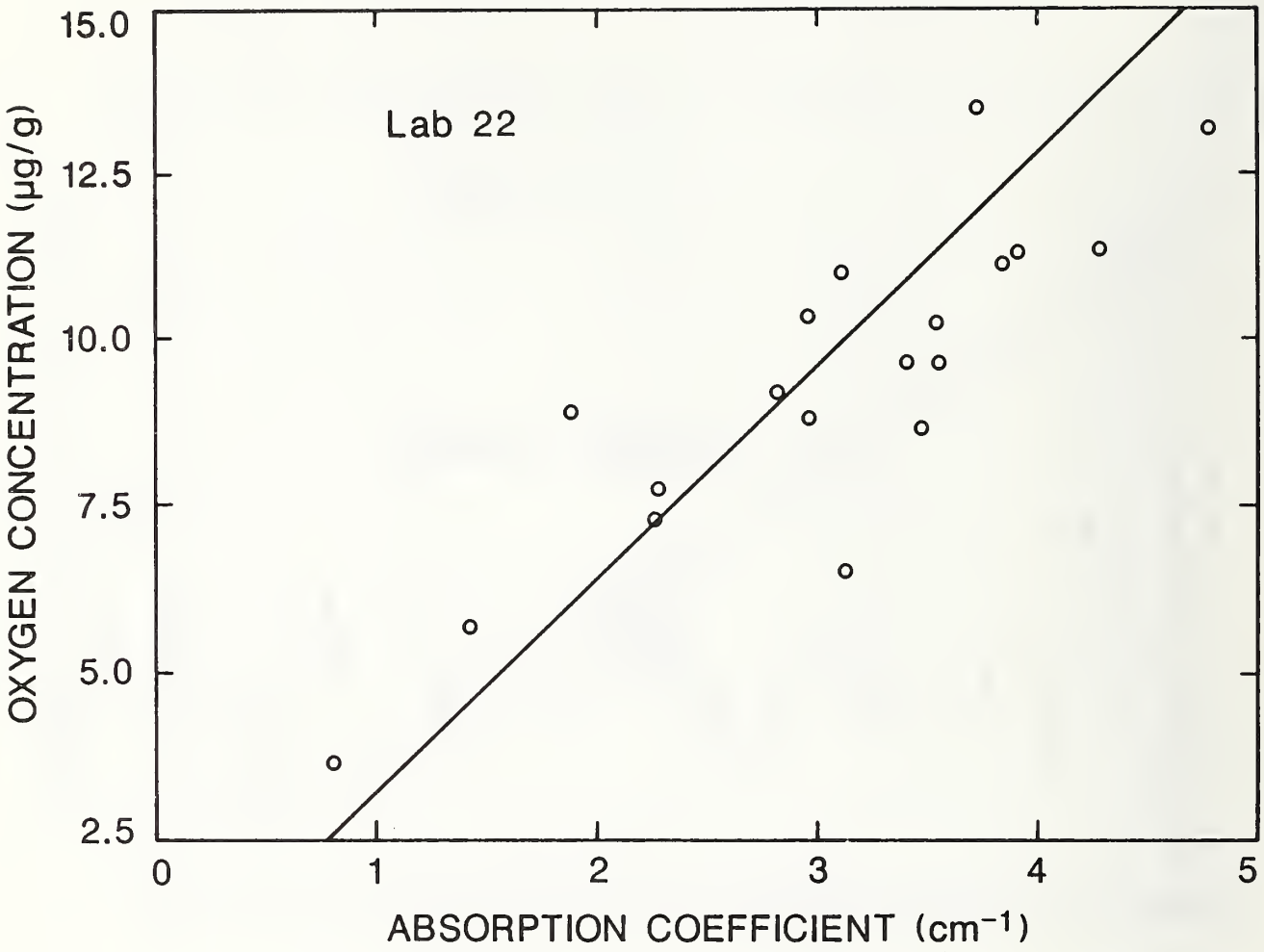

Figure 5-2a. For Lab 22, oxygen content vs. infrared absorption coefficient.

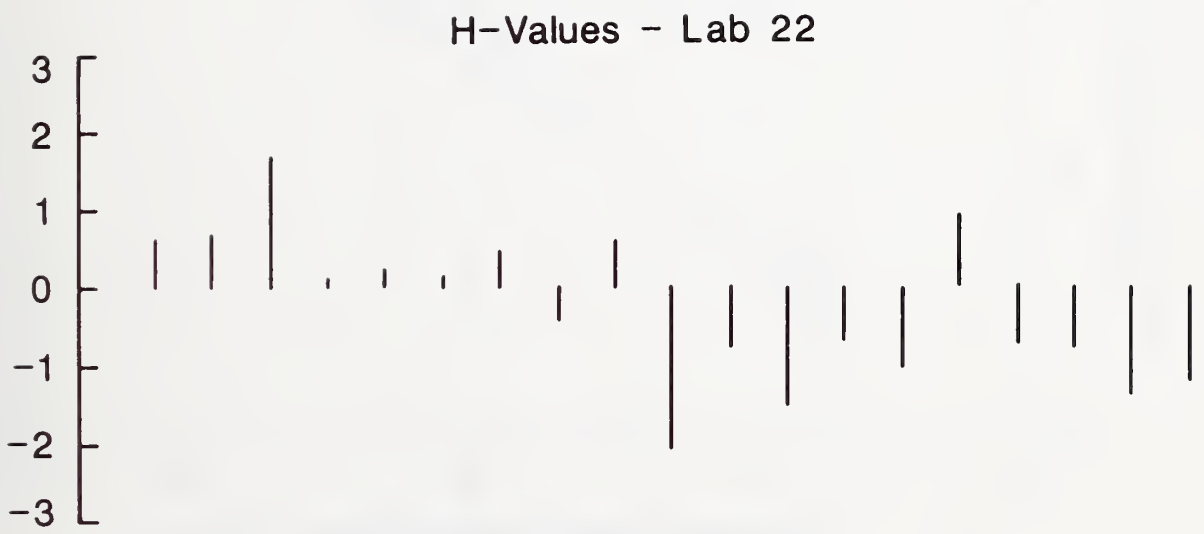

Figure 5-2b. For Lab 22, standardized residual errors ("H-Values") for each specimen.

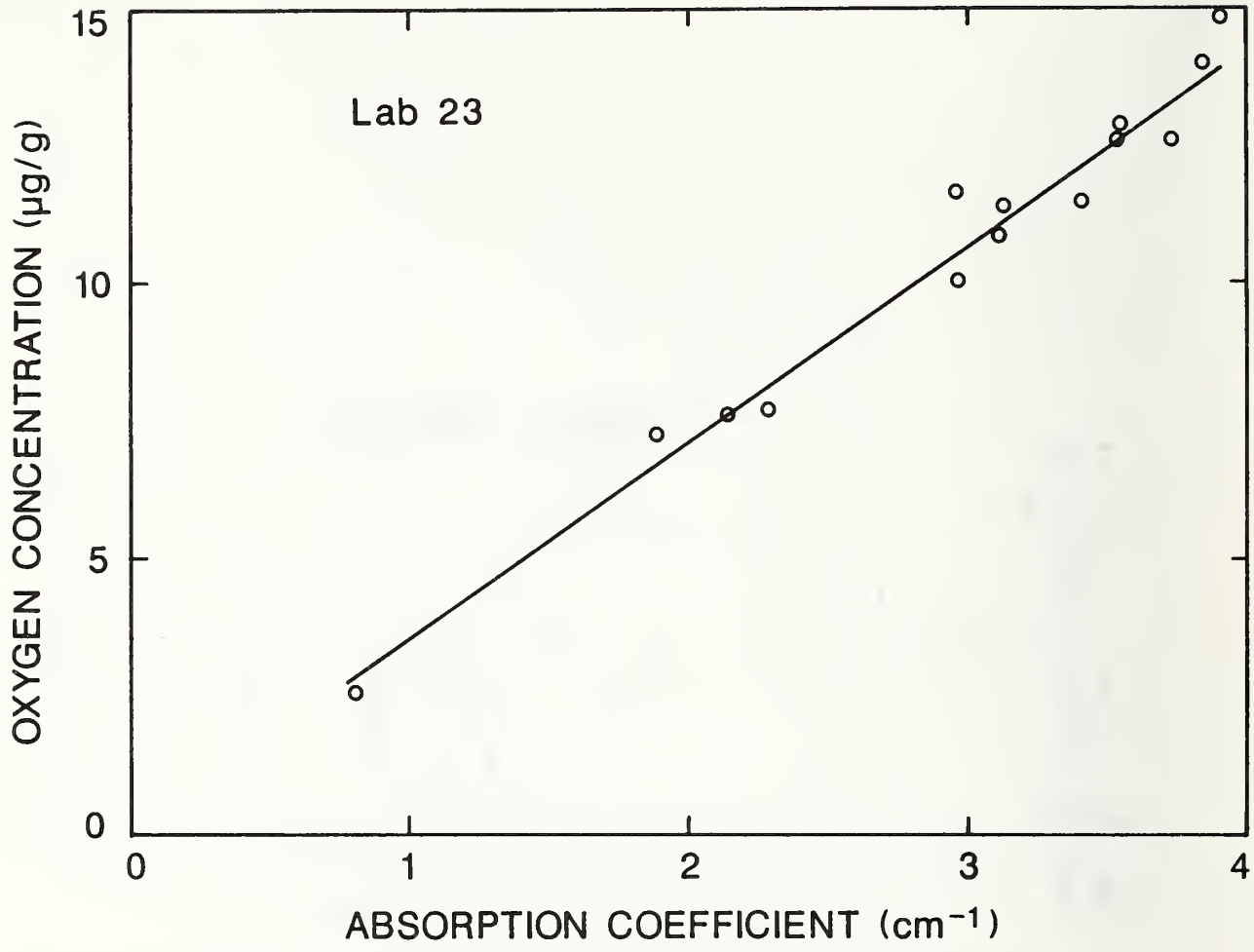

Figure 5-3a. For Lab 23, oxygen content vs. infrared absorption coefficient.

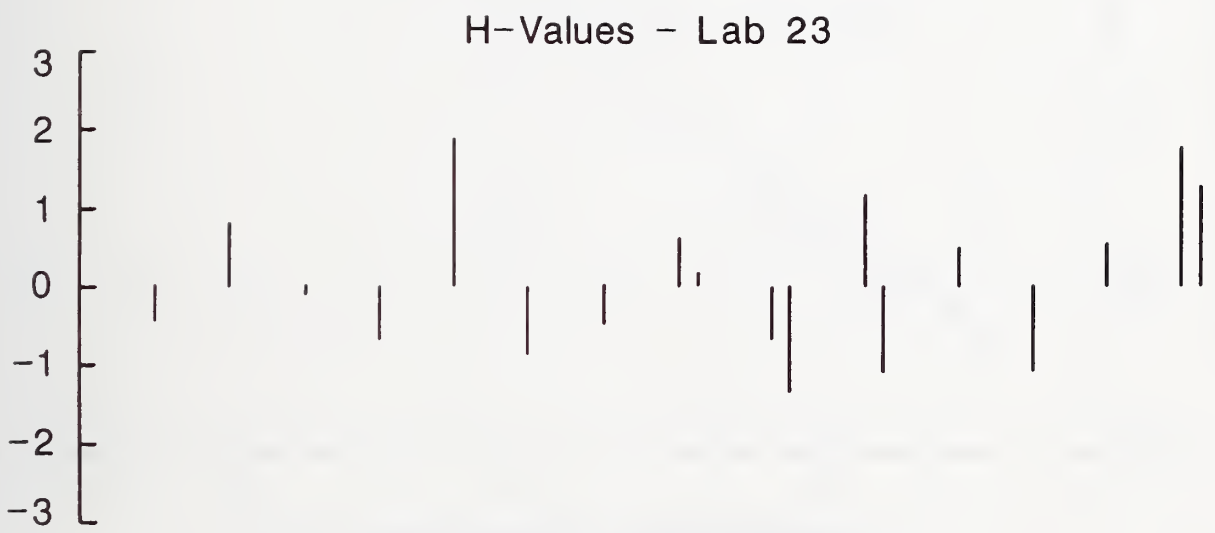

Figure 5-3b. For Lab 23, standardized residual errors ("H-Values") for each specimen.

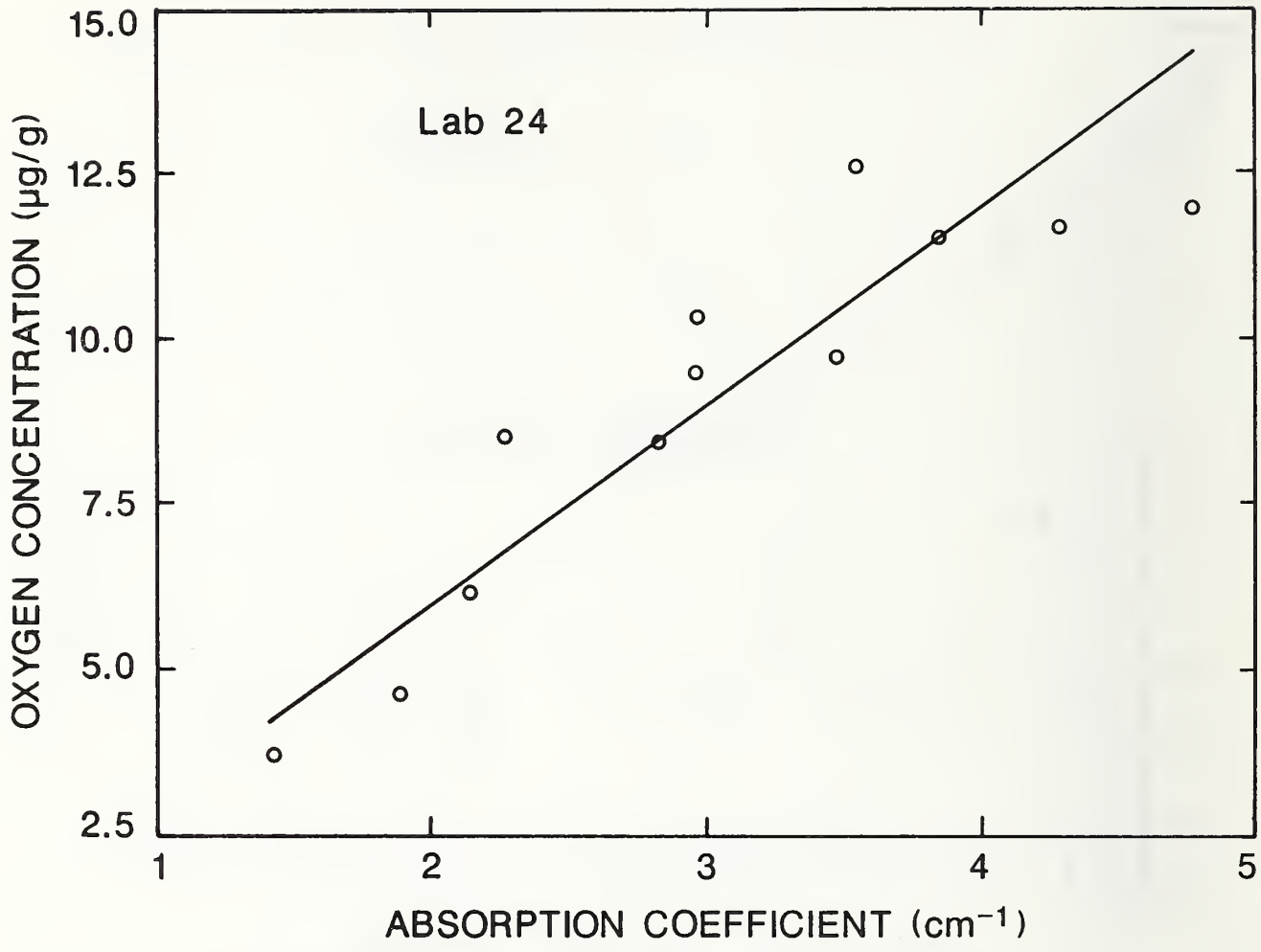

Figure 5-4a. For Lab 24, oxygen content vs. infrared absorption coefficient.

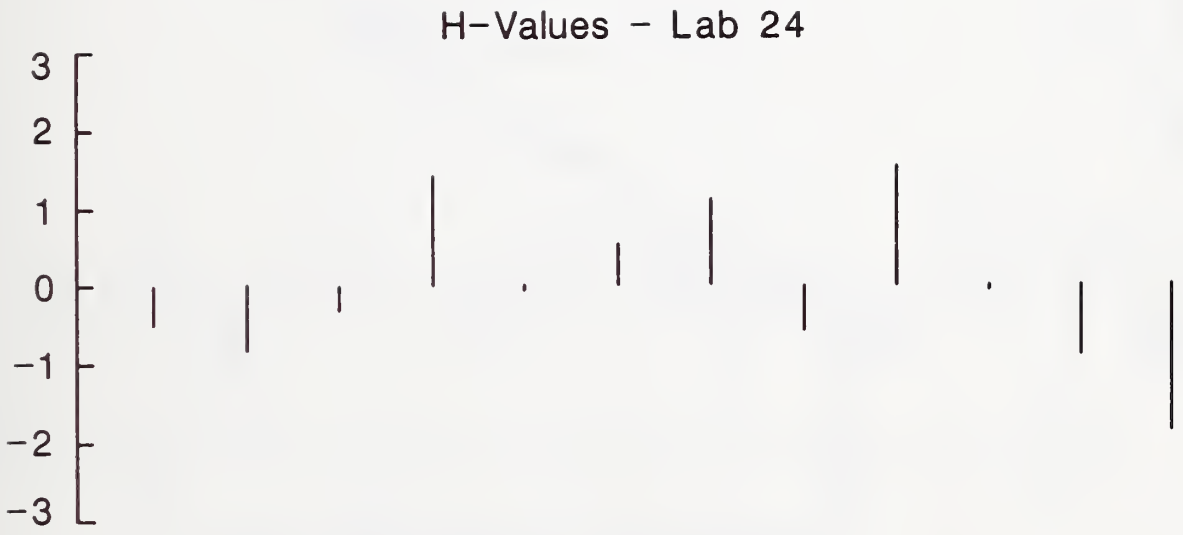

Figure 5-4b. For Lab 24, standardized residual errors ("H-Values") for each specimen.

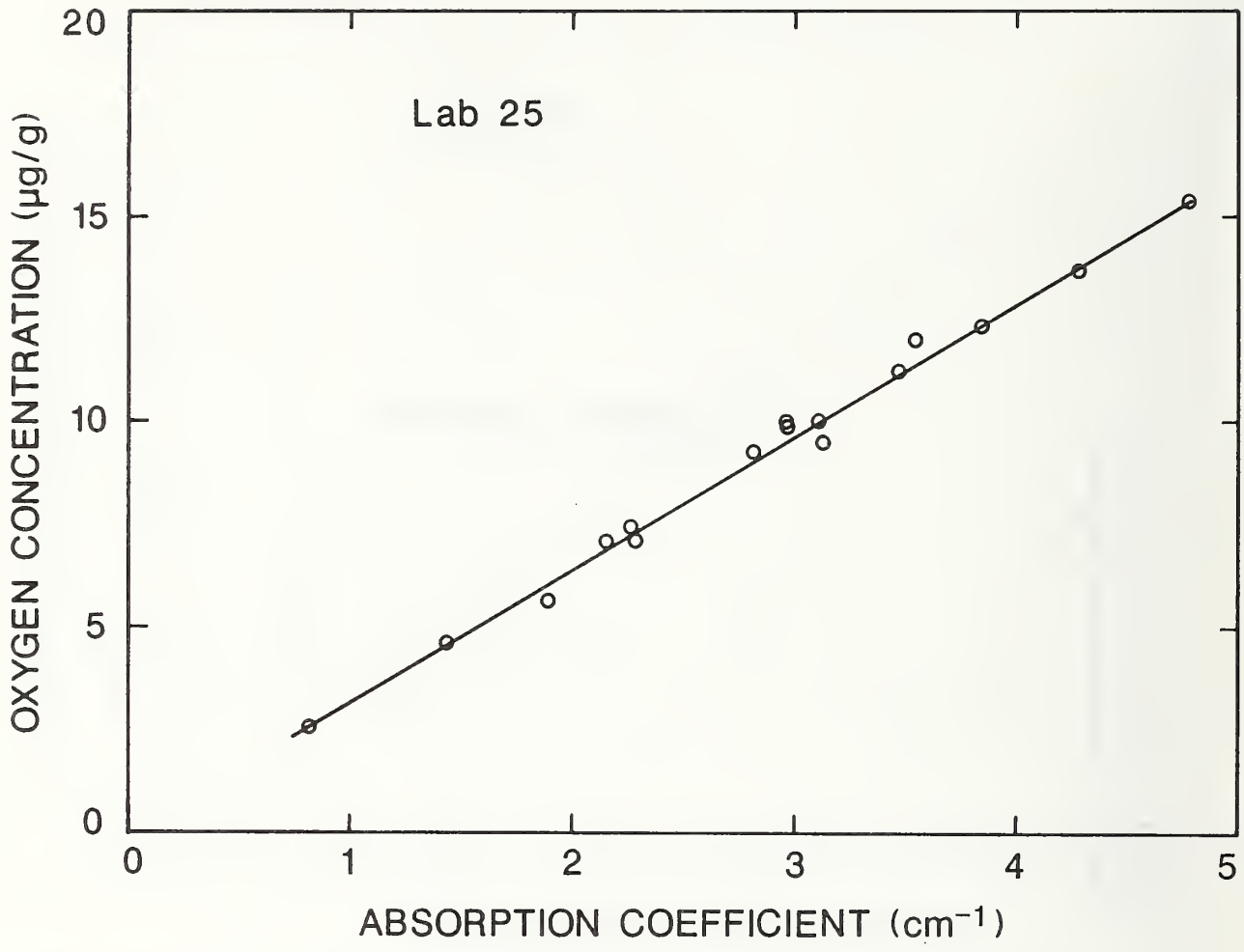

Figure 5-5a. For Lab 25, oxygen content vs. infrared absorption coefficient.

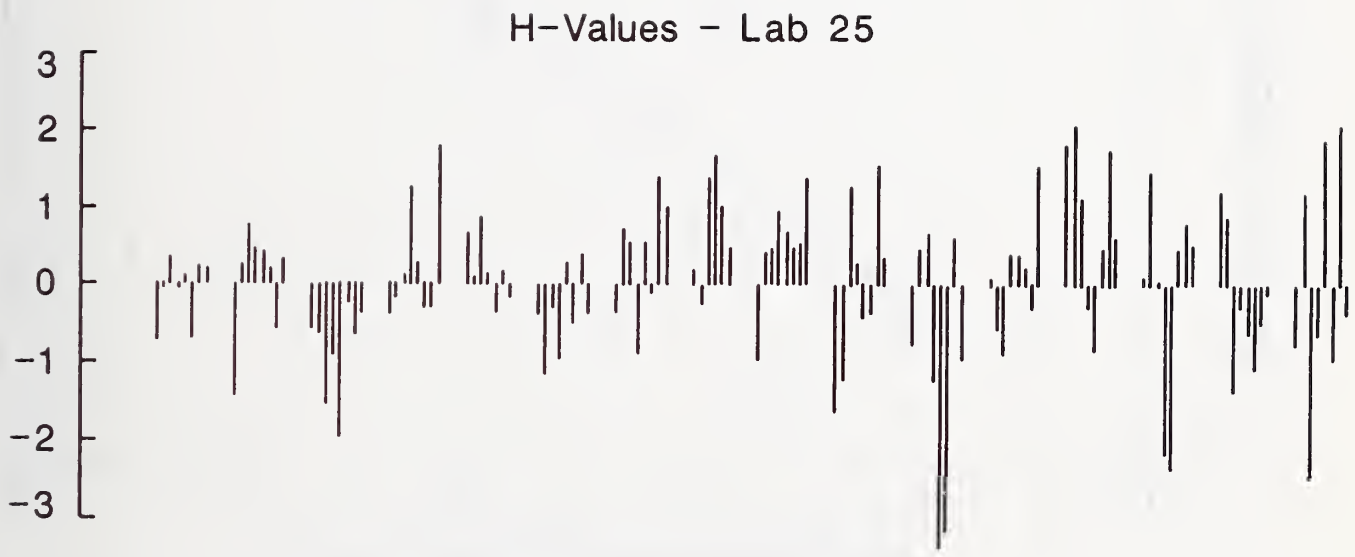

Figure 5-5b. For Lab 25, standardized residual errors ("H-Values") for each specimen.

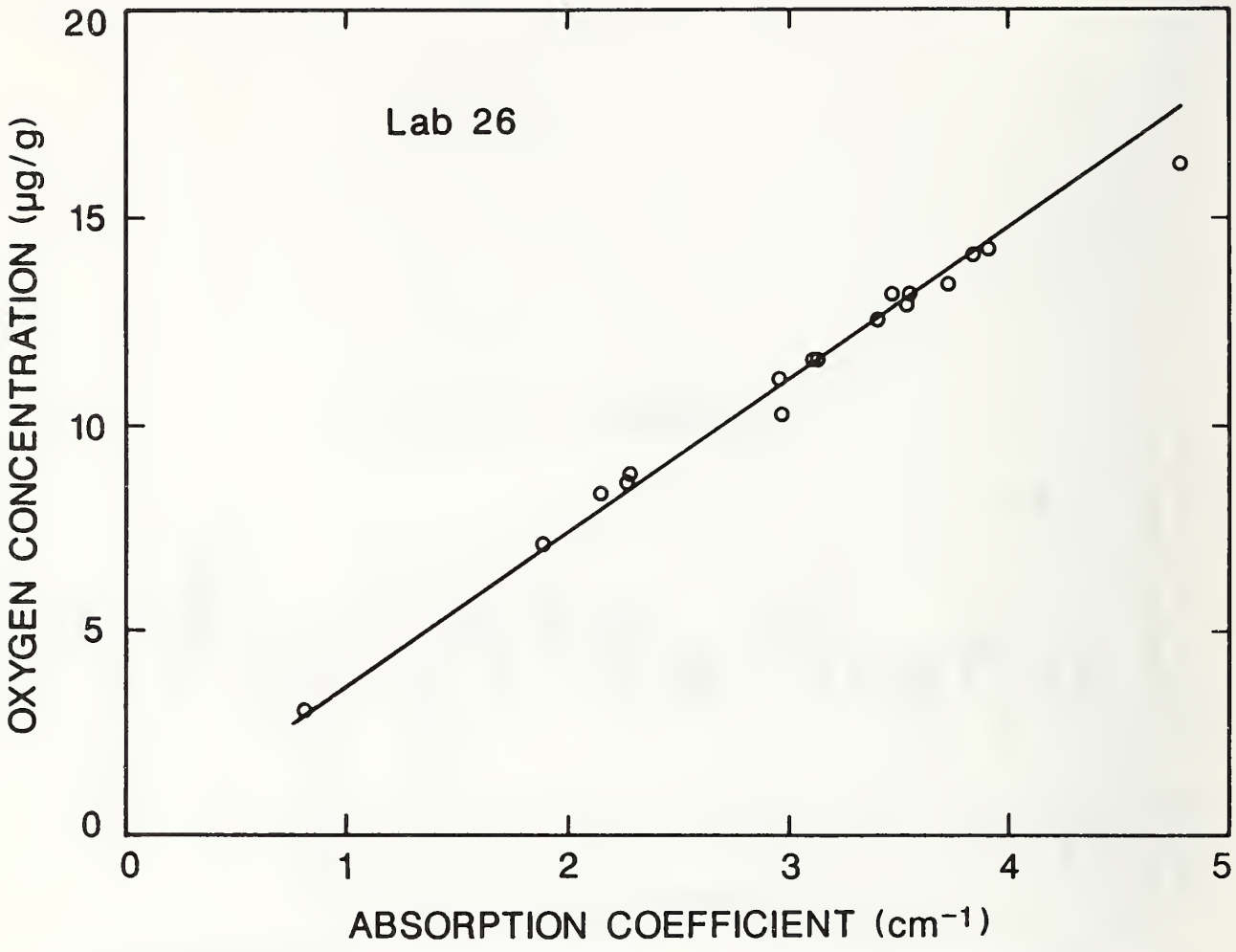

Figure 5-6a. For Lab 26, oxygen content vs. infrared absorption coefficient.

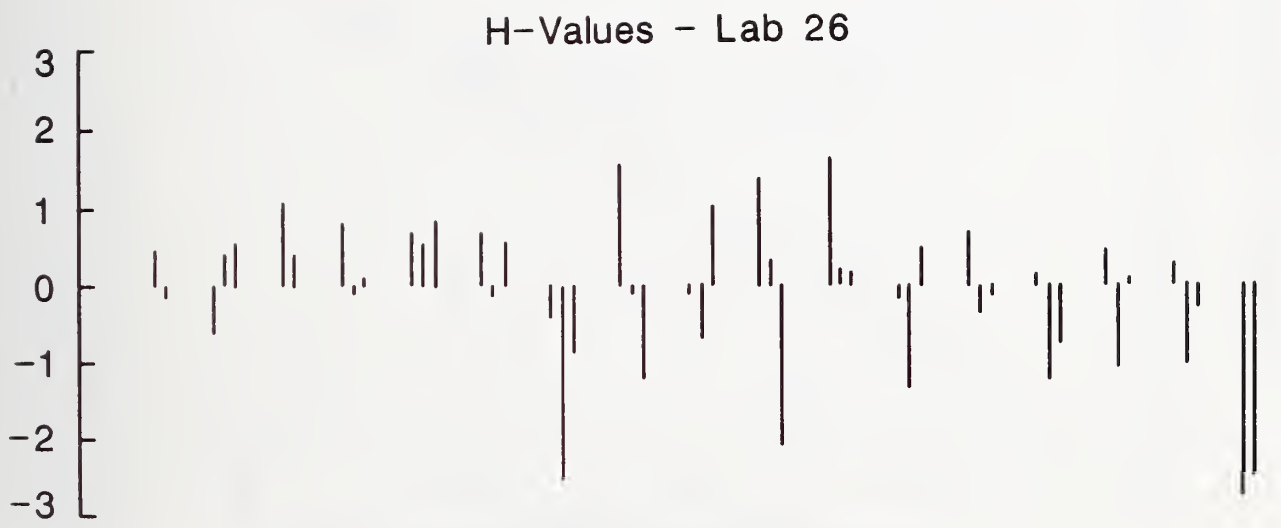

Figure 5-6b. For Lab 26, standardized residual errors ("H-Values") for each specimen.

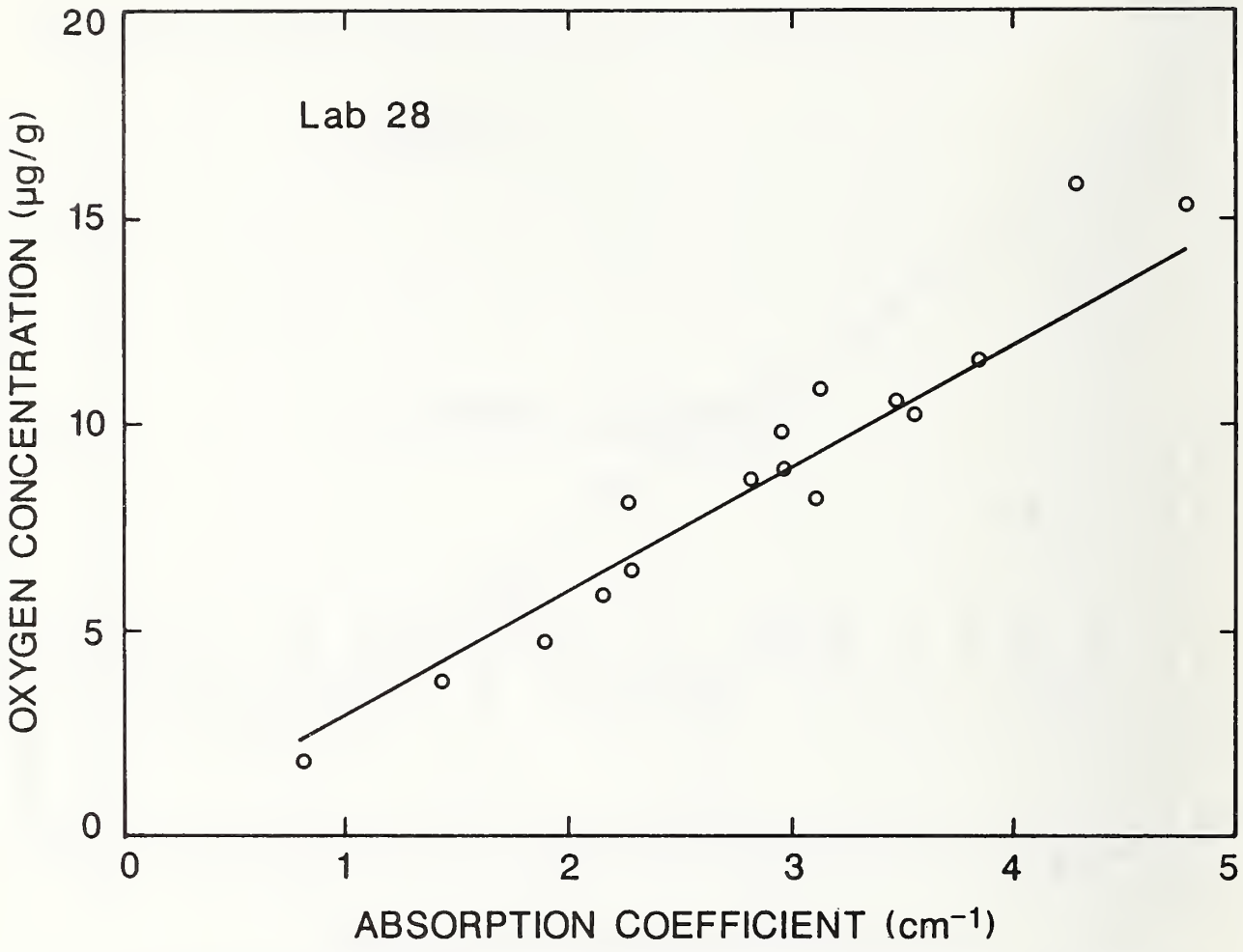

Figure 5-7a. For Lab 28, oxygen content vs. infrared absorption coefficient.

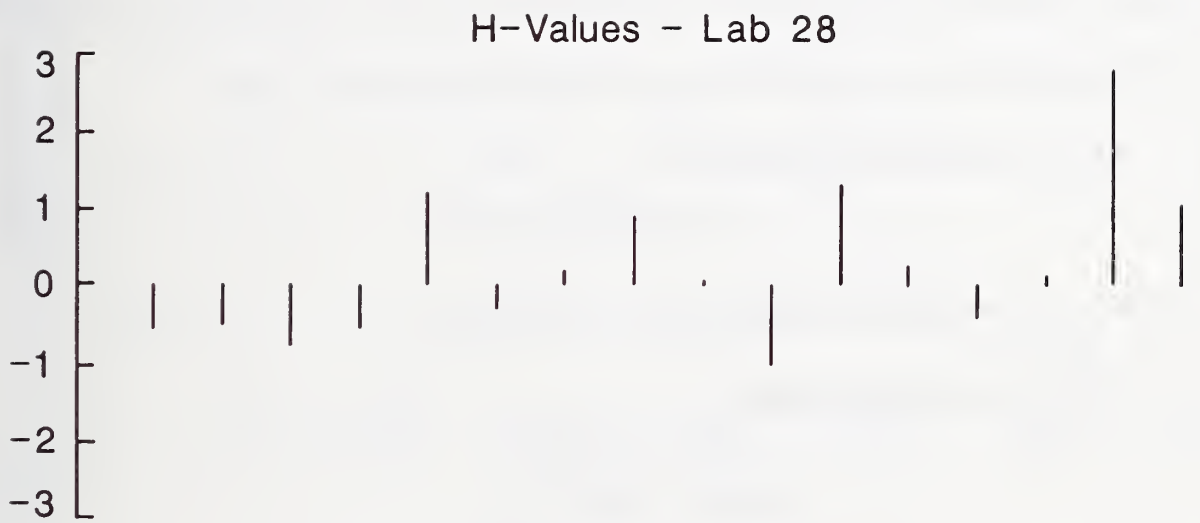

Figure 5-7b. For Lab 28, standardized residual errors ("H-Values") for each specimen.

ε_{ij} = replication error.

It is assumed that both δ_i and ε_{ij} are proportional to x_i. The hypothesis that the standard deviation of the replication error is proportional to X (the IR value) can be experimentally checked. In figure 5-8, the standard deviations calculated at each x_i are plotted against x_i, for the data from laboratory 25, and a straight line going through the origin has been fitted to these data, because the intercept is not statistically significant. The slope of the straight line is significantly different from zero. The data for the other laboratories are not as conclusive as for laboratory 25, but they do not contradict the assumption that the standard deviation of replication is proportional to x_i. This is shown in figure 5-9 where, again, a line going through the origin has been fitted to the combined data for all three laboratories.

Assuming that both δ_i and ε_{ij} are proportional to x_i, we can estimate the factors of proportionality from the analysis. The procedure is based on the following considerations.

Let $\bar{y}_i$ represent the average of all replicates y_{ij} at the point i. Then

(1) the variance of $\bar{y}_i$ is equal to

$$Var(\bar{y}_i) = \sigma_\delta^2 + \sigma_\varepsilon^2/n_i \ , \qquad (5-1)$$

where n_i is the number of replicates y_{ij} at the point i.

(2) By assumption, we have

$$\sigma_\delta^2 = c_1^2 x_i \qquad (5-2a)$$

$$\sigma_\varepsilon^2 = c_2^2 x_i \ . \qquad (5-2b)$$

An estimate for c_2 is readily obtained by regressing s_ε^2 (which can be observed at each x_i for which there are at least two measurements) on x_i. Thus the problem is to estimate c_1.

$$Var(\bar{y}_i) = x_i^2 \left[c_1^2 + \frac{c_2^2}{n_i} \right] \ , \qquad (5-3)$$

where c_2 has been determined.

The weight of $\bar{y}_i$ is equal to

$$W_i = \frac{1}{x_i^2 \left[c_1^2 + \frac{c_2^2}{n_i} \right]} \ . \qquad (5-4)$$

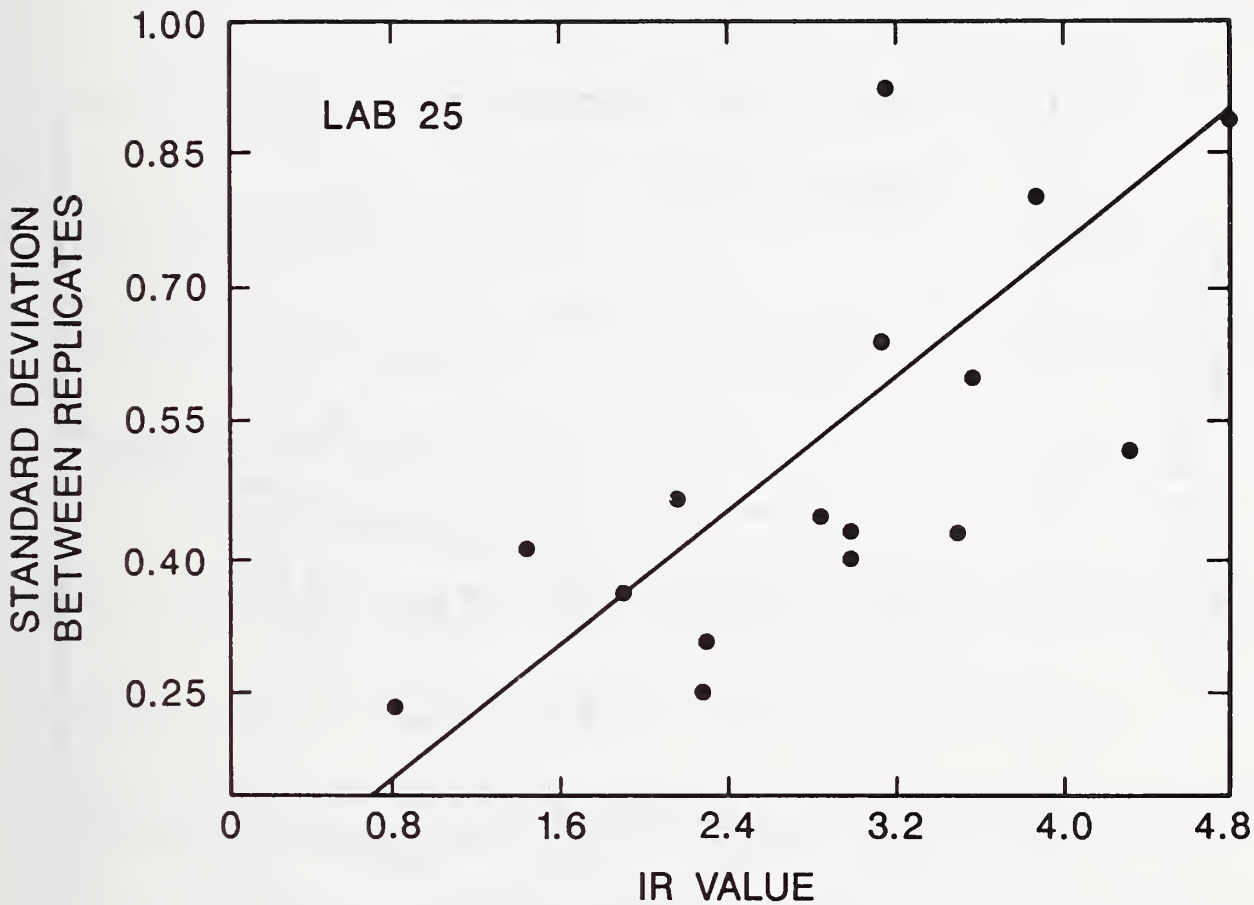

Figure 5-8. Standard deviation between replicates for laboratory 25.

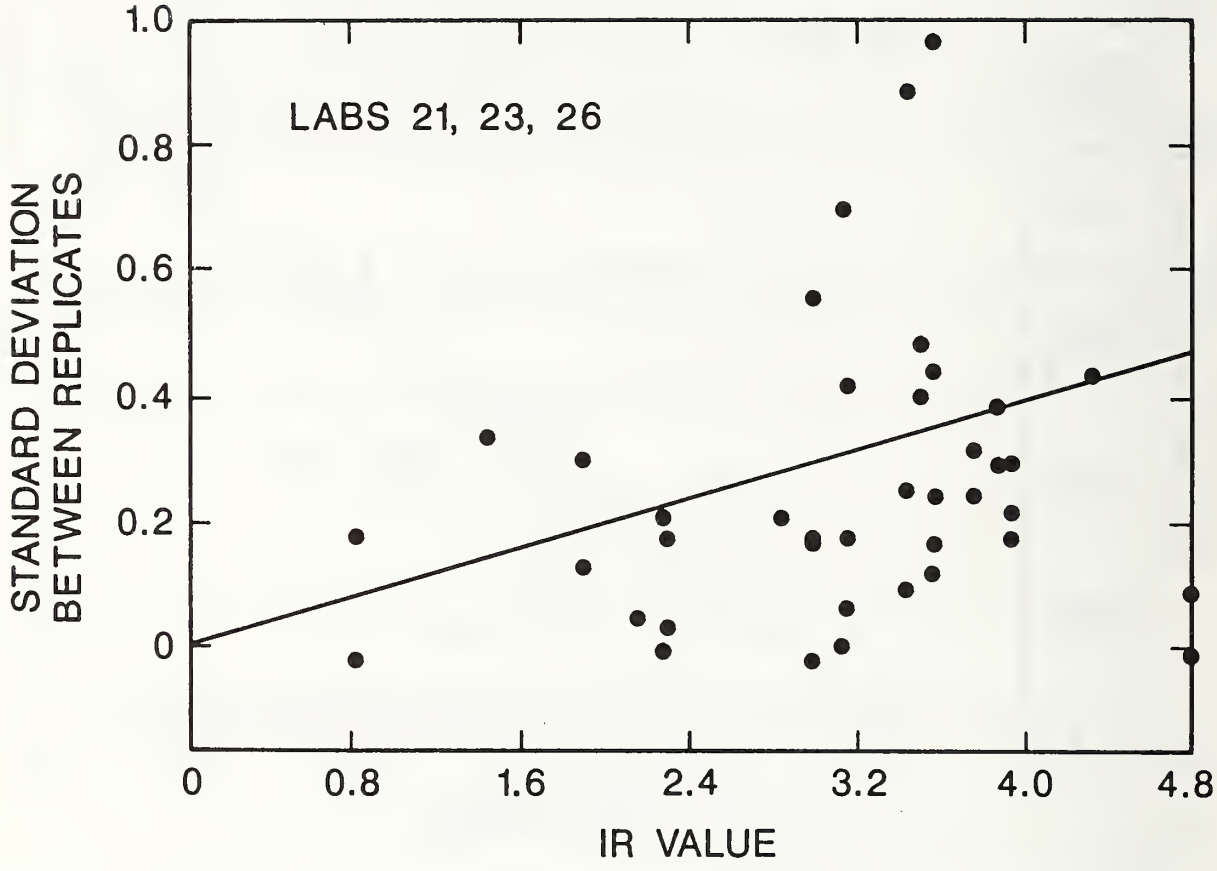

Figure 5-9. Standard deviation between replicates for laboratories 21, 23, and 26.

Since W_i is the exact weight,

$$\frac{\sum_i W_i(\bar{y}_i - \hat{y}_i)^2}{N-2} = 1 \ ,$$

or

$$\sum_i W_i(\bar{y}_i - \hat{y}_i)^2 - (N-2) = 0 \ , \qquad (5-5)$$

where $\hat{y}_i$ is the estimated value of $\bar{y}_i$.

The object is to solve eq (5-5) for c_1, with the value for W_i substituted from eq (5-4). This is done by an iterative process.*

The analysis resulted in the following:

(a) an estimate $\hat{\beta}$ for the slope β and

(b) a "weight" based, for each point, on the appropriate combination of the errors of δ and ϵ.

In addition, estimates were obtained for the standard error of $\hat{\beta}$.

Tables 5-2, 5-4, and 5-7 contained only single measurements by the absolute methods. For these tables, the standard deviation of replication could not be estimated.

To detect, and safeguard against, questionable measurements, two graphical procedures were used:

(1) a graph of the individual ϵ_{ij} estimates in a standardized scale,

(2) a graph of the fitted straight line, together with the plotted points $(x_i, \bar{y}_i)$.

The graphs of the first type revealed two questionable values, one for lab 23, and one for lab 26.

The graphs of the second type revealed large differences in lack-of-fit between different labs, but in no case was there any evidence of nonlinearity (curvature), thus justifying the

* Paule, R. C., and Mandel, J., Consensus Values and Weighting Factors, *J. Res. Natl. Bur. Stand.* **87**, 377 (1982).

linear fitting procedures.

For labs 23 and 26, the fit was repeated after replacing, in both cases, the questionable value by the average of the remaining replicates. The figures corresponding to these labs are, however, based on the original data.

5.4 RESULTS OF THE ANALYSIS

Table 5-8 lists the results of the analyses.

The slopes vary appreciably between labs, but the two most discrepant values (for labs 22 and 24) are based on data showing considerable scatter (see figs. 5-2a and 5-4a).

Laboratories 22 and 28 can be eliminated, since a separate analysis shows that there is evidence of nonzero intercept for both. Laboratory 24 had no replicate determinations. In addition, the fit for this laboratory is appreciably worse than for laboratories 21, 23, 25, and 26, as seen from the standard deviations listed. Laboratories 25 and 26 are not consistent with laboratories 21 and 23, nor are they consistent with each other: their slopes are definitely different. If, nevertheless, laboratories 21, 23, 25, and 26 are combined in a single set, the results are as follows (a single regression):

$$\text{slope} = 3.435\ \mu\text{g/g cm}^{-1}$$
$$\text{standard error of slope} = 0.031$$
$$c_1 = 0.188 \quad c_2 = 0.168$$

In conclusion, if laboratories 22, 24, and 28 are eliminated, the remaining four laboratories are still somewhat incompatible. Combining them, nevertheless, yields the above result. Converted to ppma/cm^{-1}, the conversion coefficient is 6.030, with an error, based upon two standard deviations, of 0.108.

Table 5-8. Results of the analyses

Laboratory	Value	Slope Standard Error	Multiplier for Standard Deviation[a] Fit	Replication
21	3.5759	0.0220	0.082	0.079
22	3.2048	0.1568	0.683	NR[b]
23	3.5628	0.0548	0.172	0.121
24	2.9942	0.1297	0.449	NR
25	3.2181	0.0272	0.085	0.189
26	3.7015	0.0282	0.086	0.132
28	2.9982	0.1032	0.413	NR

[a] Values of c_1 for c_2, respectively.

[b] No replicates were made.

6. ACKNOWLEDGMENTS

The editors wish to express their appreciation for the successful completion of this project to a great number of organizations and individuals. The silicon crystals used for this study were generously supplied by Japan Silicon, Komatsu Electronic Materials, Monsanto Electronic Materials, Osaka Titanium Corporation, Shin-Etsu Handotai, Siltec Silicon, Toshiba Ceramics, and Wacker Chemitronic. Union Carbide provided the sapphire squares used in the instrumental verification procedure.

We would like to thank the individual researchers at the IR laboratories: Dr. D. Andrews (General Electric Co., Ltd.), Mr. P. Ashby (Mullards, Ltd.), Dr. M. Domenici (Dynamit Nobel Silicon), Dr. K. Graff (Telefunken), Dr. N. Inoue (Nippon Telegraph & Telephone), Li Guang Ping (Tianjin Electronic Materials Research Institute), Lin Yu Ping (Zhejiang University), E. Ohashi (Komatsu Electronic Materials), Dr. B. Pajot (Ecole Normale Supérieure), Dr. L. Shive (Monsanto Electronic Materials), H. Suzuki (Hitachi), and Ye Yu Zong (Shanghai Second Smelting Plant).

We would also like to thank those responsible for making the very difficult absolute measurements of the oxygen content of the silicon specimens: Dr. K. Bethge (Institut für Kernphysik, Johann Wolfgang Goethe Universität, Frankfurt), Dr. E. Grallath (Max-Planck-Institut für Metallforschung, Dortmund), Dr. T. Nozaki (Institute of Physical and Chemical Research (RIKEN), Wako, Saitama), Dr. B. Schmitt (Bundesanstalt für Materialprüfung, Berlin), Dr. E. Schweikert (Center for Chemical Characterization and Analysis, Texas A & M University), Dr. J. Stoquert (Centre de Recherches Nucleaires, Strasbourg), Dr. K. Strijckmans (Institute for Nuclear Sciences, Rijksuniversiteit Gent), and Drs. D. Wood and J. Hislop (AERE Harwell, Oxfordshire).

The cooperation of Dr. H. Marchandise and the Community Bureau of Reference (BCR) was very important, as it enabled us to include results obtained at four additional highly skilled laboratories on this project.

APPENDIX A. INFRARED ABSORPTION DATA

Specimen ID	Lab ID	Noise Level	Linearity Parameter	Absorption Coefficient (cm^{-1}) 1	2	3
10101	11	0.30	54.3	0.79426	0.78753	0.77693
10101	13	0.10	53.8	0.79884	0.79668	0.80341
10101	16	0.10	55.0	0.81489	0.81794	0.82054
10101	17	0.70	58.6	0.80165	0.87771	0.84324
10101	19	0.10	53.5	0.76870	0.76422	0.77142
10102	6	1.00	52.0	0.75161	0.77353	0.72648
10102	8	0.10	56.0	0.83182	0.83765	0.82679
10102	12	0.10	60.0	0.85347	0.86596	0.86478
10102	17	0.20	56.2	0.83386	0.82501	0.81138
10102	17	0.70	58.6	0.79345	0.82517	0.84786
10103	9	0.30	57.0	0.85020	0.86185	0.86626
10103	11	0.30	53.8	0.82065	0.80801	0.81021
10103	11	0.30	54.3	0.81039	0.79203	0.80184
10103	15	0.20	52.5	0.83091	0.83095	0.82877
10104	18	0.10	53.9	0.81291	0.81291	0.72803
10104	19	0.10	53.5	0.78160	0.78687	0.78160
10105	4	0.10	61.4	0.78798	0.79350	0.79033
10105	5	0.20	57.0	0.78640	0.78871	*
10105	10	0.10	54.0	0.79817	0.80165	0.79925
10105	13	0.20	54.7	0.80731	0.79144	0.80165
10105	13	0.20	54.0	0.79411	0.80976	0.79843
10106	1	0.10	52.8	0.80967	0.79055	0.78429
10106	2	0.10	54.7	0.79244	0.78083	0.80758
10106	3	0.10	53.0	0.77877	*	*
10106	16	0.10	55.0	0.81518	0.82648	0.81963
10106	16	0.10	55.0	0.81726	0.82086	0.81060
10107	11	0.30	54.3	0.79911	0.80783	0.79671
10107	13	0.10	54.4	0.78757	0.81258	0.77876
10107	16	0.10	55.0	0.80692	0.81115	0.82023
10107	17	0.70	58.6	0.79758	0.81714	0.86572
10107	19	0.10	53.5	0.76016	0.75224	0.74876
20101	11	0.30	54.3	2.13201	2.12148	2.11088
20101	13	0.10	53.8	2.15474	2.14686	2.13951
20101	16	0.10	55.0	2.17514	2.17254	2.16592
20101	17	0.70	58.6	2.13015	2.15738	2.23449
20101	19	0.10	53.5	2.08669	2.06833	2.08981

20102	6	1.00	52.0	2.05042	2.02528	2.00244
20102	8	0.10	56.0	2.13852	2.20527	2.15269
20102	12	0.10	60.0	2.22755	2.25392	2.25735
20102	17	0.20	56.2	2.17904	2.16400	2.18645
20102	17	0.70	58.6	2.16066	2.18645	2.16391
20103	9	0.30	57.0	2.16263	2.23655	2.26892
20103	11	0.30	53.8	2.13711	2.17568	2.14170
20103	11	0.30	54.3	2.13575	2.14742	2.12416
20103	15	0.20	52.5	2.15924	2.16724	2.15348
20104	18	0.10	53.9	2.16342	2.17307	2.15741
20104	19	0.10	53.5	2.07411	2.07411	2.08479
20105	4	0.10	61.4	2.11033	2.07692	2.12611
20105	5	0.20	57.0	2.12300	2.12343	*
20105	10	0.10	54.0	2.10919	2.11840	2.10919
20105	13	0.20	54.7	2.08079	2.11840	2.13728
20105	13	0.20	54.0	2.11156	2.12757	2.11379
20106	1	0.10	52.8	2.10845	2.12847	2.12982
20106	2	0.10	54.7	2.14212	2.12759	2.15617
20106	3	0.10	53.0	2.07019	*	*
20106	16	0.10	55.0	2.16285	2.15822	2.15359
20106	16	0.10	55.0	2.14052	2.15031	2.14758
20107	11	0.30	54.3	2.08993	2.15004	2.11242
20107	13	0.10	54.4	2.11562	2.13084	2.12947
20107	16	0.10	55.0	2.16223	2.14433	2.15169
20107	17	0.70	58.6	2.10041	2.17801	2.14988
20107	19	0.10	53.5	2.06563	2.06104	2.05184
30101	11	0.30	54.3	3.07490	3.10083	3.06504
30101	13	0.10	53.8	3.16260	3.10583	3.12973
30101	16	0.10	55.0	3.13851	3.15289	3.13920
30101	17	0.70	58.6	3.12571	3.28810	3.24562
30101	19	0.10	53.5	3.01453	2.96598	3.00756
30102	6	1.00	52.0	2.99891	2.97951	2.97855
30102	8	0.10	56.0	3.10318	3.15683	3.16441
30102	12	0.10	60.0	3.24207	3.30780	3.30755
30102	17	0.20	56.2	3.14228	3.14437	3.16268
30102	17	0.70	58.6	3.22369	3.17221	3.20718
30103	9	0.30	57.0	3.30981	3.29790	3.24562
30103	11	0.30	53.8	3.09087	3.09087	3.09321
30103	11	0.30	54.3	3.08707	3.08879	2.99630
30103	15	0.20	52.5	3.12092	3.12906	3.13004
30104	18	0.10	53.9	3.08044	3.15604	3.15302

30104	19	0.10	53.5	3.00253	3.01175	3.01175
30105	4	0.10	61.4	3.03711	3.05662	3.05765
30105	5	0.20	57.0	3.08722	3.00129	*
30105	10	0.10	54.0	3.14616	3.07031	3.08020
30105	13	0.20	54.0	3.06266	3.08236	3.05497
30105	13	0.20	54.7	3.07469	3.03807	3.05662
30106	1	0.10	52.8	3.05070	3.11954	3.07745
30106	2	0.10	54.7	3.13176	3.08722	3.12734
30106	3	0.10	53.0	3.00119	*	*
30106	16	0.10	55.0	3.10959	3.11841	3.11905
30106	16	0.10	55.0	3.12722	3.12217	3.10959
30107	11	0.30	54.3	3.02370	3.02852	3.04010
30107	13	0.10	54.4	3.07738	3.07683	3.03962
30107	16	0.10	55.0	3.11370	3.10412	3.11497
30107	17	0.70	58.6	3.09194	3.17195	3.14268
30107	19	0.10	53.5	2.96174	2.97086	2.96613
40101	11	0.30	54.3	2.92016	2.91498	2.91541
40101	13	0.10	53.8	2.93342	2.91971	2.97136
40101	16	0.10	55.0	3.00099	2.97212	2.98538
40101	17	0.70	58.6	3.01729	3.03904	2.99258
40101	19	0.10	53.5	2.85945	2.84124	2.85960
40102	6	1.00	52.0	2.81613	2.84898	2.83511
40102	8	0.10	56.0	2.94690	2.96887	2.99001
40102	12	0.10	60.0	3.07337	3.09874	3.09767
40102	17	0.20	56.2	2.95500	2.98453	2.99341
40102	17	0.70	58.6	3.01059	3.02115	3.00544
40103	9	0.30	57.0	3.09157	3.13096	3.11259
40103	11	0.30	53.8	2.94943	2.93945	2.90716
40103	11	0.30	54.3	2.94963	2.92133	2.95678
40103	15	0.20	52.5	2.96413	2.98201	2.98084
40104	18	0.10	53.9	2.94267	2.92786	2.99374
40104	19	0.10	53.5	2.84586	2.84586	2.86893
40105	4	0.10	61.4	2.93046	2.93959	2.92683
40105	5	0.20	57.0	2.97873	2.97632	*
40105	10	0.10	54.0	2.95643	2.94661	2.94703
40105	13	0.20	54.7	2.96053	2.93252	2.94204
40105	13	0.20	54.0	2.93124	2.95968	2.95994
40106	1	0.10	52.8	2.91881	3.00962	3.00005
40106	2	0.10	54.7	2.99650	2.98651	3.01389
40106	3	0.10	53.0	2.93358	2.93306	*
40106	16	0.10	55.0	2.99482	2.99512	3.00005

40106	16	0.10	55.0	2.98558	2.98042	2.99359
40107	11	0.30	54.3	2.88204	2.93731	2.93255
40107	13	0.10	54.4	2.96129	2.96081	2.95144
40107	16	0.10	55.0	3.01891	3.00966	3.02424
40107	17	0.70	58.6	2.88113	3.16897	3.05433
40107	19	0.10	53.5	2.87704	2.86330	2.86791
50101	11	0.30	54.3	3.52696	3.48858	3.48190
50101	13	0.10	53.8	3.52092	3.50716	3.54518
50101	16	0.10	55.0	3.57909	3.61445	3.58678
50101	17	0.70	58.6	3.46553	3.58180	3.59381
50101	19	0.10	53.5	3.42064	3.40452	3.40690
50102	6	1.00	52.0	3.36723	3.32441	3.36761
50102	8	0.10	56.0	3.53380	3.61436	3.56721
50102	12	0.10	60.0	3.61913	3.71709	3.72704
50102	17	0.20	56.2	3.55293	3.58527	3.56983
50102	17	0.70	58.6	3.59260	3.68472	3.61646
50103	9	0.30	57.0	3.73610	3.76438	3.72162
50103	11	0.30	53.8	3.53462	3.53314	3.51657
50103	11	0.30	54.3	3.54058	3.51634	3.51426
50103	15	0.20	52.5	3.54058	3.54980	3.53922
50104	18	0.10	53.9	3.56113	3.56841	3.59876
50104	19	0.10	53.5	3.40879	3.40879	3.40888
50105	4	0.10	61.4	3.48457	3.45597	3.47569
50105	5	0.20	57.0	3.51422	3.49955	*
50105	10	0.10	54.0	3.52162	3.51101	3.51701
50105	13	0.20	54.7	3.53830	3.47342	3.50043
50105	13	0.20	54.0	3.47903	3.50694	3.50554
50106	1	0.10	52.8	3.58426	3.54583	3.56103
50106	2	0.10	54.7	3.56824	3.57338	3.57742
50106	3	0.10	53.0	3.44662	*	*
50106	16	0.10	55.0	3.57947	3.60201	3.57930
50106	16	0.10	55.0	3.60071	3.59166	3.57804
50107	11	0.30	54.3	3.48208	3.46863	3.49799
50107	13	0.10	54.4	3.51737	3.51596	3.52056
50107	16	0.10	55.0	3.60211	3.59534	3.58710
50107	17	0.70	58.6	3.54056	3.53601	3.65768
50107	19	0.10	53.5	3.41442	3.42488	3.42024
110101	11	0.30	54.3	2.91676	2.92601	2.91676
110101	13	0.10	53.8	2.95736	2.95736	2.97117
110101	16	0.10	55.0	3.00568	3.01866	2.99052
110101	17	0.70	58.6	3.00972	3.01866	2.98687

110101	19	0.10	53.5	2.87180	2.87619	2.88495
110102	6	1.00	52.0	2.88070	2.84423	2.80848
110102	8	0.10	56.0	2.97269	3.00237	3.00483
110102	12	0.10	60.0	3.09488	3.12439	3.08219
110102	17	0.20	56.2	2.97751	3.01642	3.00639
110102	17	0.70	58.6	2.94112	3.07944	3.01782
110103	9	0.30	57.0	3.13847	3.13142	3.13341
110103	11	0.30	54.3	2.93507	2.96206	2.94937
110103	11	0.30	53.8	2.96708	2.94415	2.95823
110103	15	0.20	52.5	3.00341	2.99348	2.98649
110104	18	0.10	53.9	2.53476	2.52559	*
110104	19	0.10	53.5	2.85855	2.85424	2.85439
110105	4	0.10	61.4	2.95144	2.93883	2.95529
110105	5	0.20	57.0	2.95846	2.99109	*
110105	10	0.10	54.0	2.94153	2.93688	2.94153
110105	13	0.20	54.7	2.95032	2.93198	2.94593
110105	13	0.20	54.0	2.95267	2.96269	2.94485
110106	1	0.10	52.8	2.94620	2.99585	2.93836
110106	2	0.10	54.7	2.99071	2.98139	2.98469
110106	3	0.10	53.0	2.91099	2.92367	*
110106	16	0.10	55.0	3.01060	2.99771	3.00252
110106	16	0.10	55.0	3.00658	3.00252	2.97319
110107	11	0.30	54.3	2.94859	2.93081	2.94916
110107	13	0.10	54.4	2.89603	2.94010	2.94449
110107	16	0.10	55.0	3.00143	2.99551	2.99624
110107	17	0.70	58.6	2.91719	2.98452	3.02449
110107	19	0.10	53.5	2.88997	2.84598	2.85054
110201	11	0.30	54.3	2.22233	2.22453	2.23115
110201	13	0.10	53.8	2.23780	2.24221	2.26007
110201	16	0.10	55.0	2.28496	2.28393	2.25564
110201	17	0.70	58.6	2.23001	2.27097	2.28852
110201	19	0.10	53.5	2.16537	2.15580	2.17179
110202	6	1.00	52.0	2.13873	2.10716	2.11919
110202	8	0.10	56.0	2.22529	2.26530	2.27331
110202	12	0.10	60.0	2.33451	2.38495	2.35748
110202	17	0.70	58.6	2.26093	2.25319	2.29296
110202	17	0.20	56.2	2.25319	2.25126	2.27476
110203	9	0.30	57.0	2.37283	2.36042	2.36311
110203	11	0.30	53.8	2.24775	2.23004	2.25864
110203	11	0.30	54.3	2.23559	2.22674	2.25888
110203	15	0.20	52.5	2.27138	2.26329	2.25584

110204	18	0.10	53.9	2.68774	2.71329	2.69247
110204	19	0.10	53.5	2.16982	2.16221	2.18151
110205	4	0.10	61.4	2.23037	2.23598	2.22493
110205	5	0.20	57.0	2.22473	2.27314	*
110205	10	0.10	54.0	2.23265	2.21172	2.24813
110205	13	0.20	54.0	2.24885	2.26910	2.26471
110205	13	0.20	54.7	2.26028	2.24038	2.26366
110206	1	0.10	52.8	2.24245	2.28005	2.25613
110206	2	0.10	54.7	2.32172	2.26128	2.30721
110206	3	0.10	53.0	2.21061	*	*
110206	16	0.10	55.0	2.28955	2.28416	2.28170
110206	16	0.10	55.0	2.28170	2.26946	2.27630
110207	11	0.30	54.3	2.22788	2.25682	2.24265
110207	13	0.10	54.4	2.20287	2.25480	2.25919
110207	16	0.10	55.0	2.28306	2.27663	2.26837
110207	17	0.70	58.6	2.29474	2.32702	2.26077
110207	19	0.10	53.5	2.16613	2.19328	2.18031
120101	11	0.30	54.3	3.70632	3.70632	3.70557
120101	13	0.10	53.8	3.70745	3.69198	3.74238
120101	16	0.10	55.0	3.76453	3.74654	3.78019
120101	17	0.70	58.6	3.80071	3.76549	3.78547
120101	19	0.10	53.5	3.61115	3.58825	3.60995
120102	6	1.00	52.0	3.52076	3.49841	3.49243
120102	8	0.10	56.0	3.72129	3.73905	3.71813
120102	12	0.10	60.0	3.89357	3.90517	3.92305
120102	17	0.70	58.6	3.75529	3.86402	3.78175
120102	17	0.20	56.2	3.75229	3.76740	3.77443
120103	9	0.30	57.0	3.92000	3.93871	3.89287
120103	11	0.30	53.8	3.70557	3.72169	3.72232
120103	11	0.30	54.3	3.72169	3.69021	3.70105
120103	15	0.20	52.5	3.73588	3.75399	3.73960
120104	18	0.10	53.9	3.78255	3.68190	3.74142
120104	19	0.10	53.5	3.58746	3.60110	3.59685
120105	4	0.10	61.4	3.67451	3.66912	3.66823
120105	5	0.20	57.0	3.71144	3.71467	*
120105	10	0.10	54.0	3.68175	3.69902	3.69448
120105	13	0.20	54.0	3.67591	3.71146	3.68960
120105	13	0.20	54.7	3.69264	3.68445	3.68357
120106	1	0.10	52.8	3.69914	3.78070	3.79844
120106	2	0.10	54.7	3.74748	3.75676	3.72532
120106	3	0.10	53.0	3.62697	3.67170	*

120106	16	0.10	55.0	3.76454	3.79210	3.77413
120106	16	0.10	55.0	3.77617	3.75598	3.73514
120107	11	0.30	54.3	3.65490	3.69271	3.69001
120107	13	0.10	54.4	3.68547	3.69908	3.70360
120107	16	0.10	55.0	3.75196	3.73920	3.76447
120107	17	0.70	58.6	3.69353	3.85205	3.68090
120107	19	0.10	53.5	3.58078	3.59150	3.60387
120201	11	0.30	54.3	3.89005	3.84058	3.84507
120201	13	0.10	53.8	3.87200	3.87200	3.92408
120201	16	0.10	55.0	3.96732	3.94821	3.87512
120201	17	0.70	58.6	3.97062	3.99288	3.92062
120201	19	0.10	53.5	3.76536	3.76781	3.76088
120202	6	1.00	52.0	3.70593	3.64849	3.71133
120202	8	0.10	56.0	3.86081	3.91334	3.95991
120202	12	0.10	60.0	4.06767	4.10416	4.12080
120202	17	0.20	56.2	3.94013	3.94547	3.95894
120202	17	0.70	58.6	3.96287	3.96287	3.81282
120203	9	0.30	57.0	4.11354	4.09109	4.12507
120203	11	0.30	54.3	3.89457	3.86722	3.93223
120203	11	0.30	53.8	3.89884	3.90568	3.86948
120203	15	0.20	52.5	3.93538	3.93708	3.93623
120204	18	0.10	53.9	3.91786	3.88061	3.89108
120204	19	0.10	53.5	3.74105	3.76756	3.75403
120205	4	0.10	61.4	3.84610	3.85052	3.85277
120205	5	0.20	57.0	3.88861	3.95347	*
120205	10	0.10	54.0	3.89108	3.84829	3.90692
120205	13	0.20	54.0	3.87691	3.92910	3.88827
120205	13	0.20	54.7	3.87748	3.85500	3.88197
120206	1	0.10	52.8	3.91483	3.95407	3.94069
120206	2	0.10	54.7	3.95749	3.91893	3.93374
120206	3	0.10	53.0	3.82559	3.83685	*
120206	16	0.10	55.0	3.92758	3.93865	3.96541
120206	16	0.10	55.0	3.94244	3.91855	3.92726
120207	11	0.30	54.3	3.83716	3.83716	3.85055
120207	13	0.10	54.4	3.86854	3.88201	3.84833
120207	16	0.10	55.0	3.93214	3.89879	3.95055
120207	17	0.70	58.6	3.98582	4.01843	3.95213
120207	19	0.10	53.5	3.75215	3.75215	3.76573
120301	11	0.30	54.3	3.42589	3.49319	3.49905
120301	13	0.10	53.8	3.49597	3.49597	3.51676
120301	16	0.10	55.0	3.55401	3.55384	3.57519

120301	17	0.70	58.6	3.60433	3.60369	3.61876
120301	19	0.10	53.5	3.39674	3.38548	3.39343
120302	6	1.00	52.0	3.35881	3.28295	3.29295
120302	8	0.10	56.0	3.44139	3.58280	3.52000
120302	12	0.10	60.0	3.65772	3.69183	3.69330
120302	17	0.70	58.6	3.60115	3.68702	3.50149
120302	17	0.20	56.2	3.54720	3.54884	3.54284
120303	9	0.30	57.0	3.66841	3.67831	3.68096
120303	11	0.30	54.3	3.49106	3.48347	3.52811
120303	11	0.30	53.8	3.51779	3.49717	3.49132
120303	15	0.20	52.5	3.52950	3.53705	3.51783
120304	18	0.10	53.9	3.53401	3.52795	3.55571
120304	19	0.10	53.5	3.40257	3.43588	3.40257
120305	4	0.10	61.4	3.48527	3.49977	3.45186
120305	5	0.20	57.0	3.52821	3.54416	*
120305	10	0.10	54.0	3.50286	3.50735	3.50876
120305	13	0.20	54.0	3.54288	3.52353	3.51905
120305	13	0.20	54.7	3.53262	3.50146	3.51917
120306	1	0.10	52.8	3.55358	3.61789	3.52961
120306	2	0.10	54.7	3.59749	3.59962	3.60003
120306	3	0.10	53.0	3.47266	3.48442	*
120306	16	0.10	55.0	3.57627	3.59882	3.58470
120306	16	0.10	55.0	3.53678	3.58470	3.60452
120307	11	0.30	54.3	3.50673	3.50514	3.51693
120307	13	0.10	54.4	3.50941	3.53328	3.52733
120307	16	0.10	55.0	3.59538	3.56157	3.59792
120307	17	0.70	58.6	3.59864	3.60522	3.71599
120307	19	0.10	53.5	3.42364	3.42939	3.43390
120401	11	0.30	54.3	3.37070	3.40015	3.39118
120401	13	0.10	53.8	3.40253	3.39684	3.39802
120401	16	0.10	55.0	3.45059	3.43457	3.46678
120401	17	0.70	58.6	3.42050	3.39449	3.44543
120401	19	0.10	53.5	3.29620	3.27991	3.29620
120402	6	1.00	52.0	3.22888	3.25933	3.23032
120402	8	0.10	56.0	3.37555	3.43791	3.41280
120402	12	0.10	60.0	3.50511	3.58684	3.58203
120402	17	0.20	56.2	3.42907	3.43409	3.46964
120402	17	0.70	58.6	3.40869	3.45982	3.45982
120403	9	0.30	57.0	3.56980	3.60483	3.56843
120403	11	0.30	53.8	3.38267	3.40860	3.36586
120403	11	0.30	54.3	3.39844	3.39421	3.36006

120403	15	0.20	52.5	3.41465	3.42899	3.42648
120404	18	0.10	53.9	3.45059	3.48590	3.40650
120404	19	0.10	53.5	3.29055	3.28151	3.30052
120405	4	0.10	61.4	3.33329	3.32642	3.33773
120405	5	0.20	57.0	3.36320	3.37029	*
120405	10	0.10	54.0	3.36985	3.34405	3.36533
120405	13	0.20	54.0	3.37522	3.37305	3.36293
120405	13	0.20	54.7	3.37436	3.35306	3.37436
120406	1	0.10	52.8	3.36862	3.44971	3.41297
120406	2	0.10	54.7	3.42629	3.39707	3.45257
120406	3	0.10	53.0	3.34162	3.34266	*
120406	16	0.10	55.0	3.42448	3.44265	3.53485
120406	16	0.10	55.0	3.40843	3.40724	3.38786
120407	11	0.30	54.3	3.33373	3.33686	3.34585
120407	13	0.10	54.4	3.34556	3.37494	3.38170
120407	16	0.10	55.0	3.41369	3.38023	3.42487
120407	17	0.70	58.6	3.49035	3.42194	3.48758
120407	19	0.10	53.5	3.26154	3.25613	3.26609
210101	11	0.30	54.3	1.42175	1.42784	1.41474
210101	13	0.10	53.8	1.42903	1.42388	1.44354
210101	16	0.10	55.0	1.46775	1.45115	1.47287
210101	17	0.70	58.6	1.46069	1.44767	1.49512
210101	19	0.10	53.5	1.41206	1.36489	1.37443
210102	6	1.00	52.0	1.39378	1.33996	1.31953
210102	8	0.10	56.0	1.40771	1.38750	1.43450
210102	12	0.10	60.0	1.46852	1.51551	1.50043
210102	17	0.70	58.6	1.38991	1.46443	1.44675
210102	17	0.20	56.2	1.44973	1.43550	1.42298
210103	9	0.30	57.0	1.53016	1.50004	1.48251
210103	11	0.30	54.3	1.41713	1.37010	1.44020
210103	11	0.30	53.8	1.40536	1.40146	1.41256
210103	15	0.20	52.5	1.41452	1.41320	1.39509
210104	18	0.10	53.9	1.42360	1.44836	1.46585
210104	19	0.10	53.5	1.39350	1.37918	1.39079
210105	4	0.10	61.4	1.41261	1.41652	1.40485
210105	5	0.20	57.0	1.42759	1.39108	*
210105	10	0.10	54.0	1.42380	1.41532	1.41532
210105	13	0.20	54.0	1.42581	1.42605	1.43827
210105	13	0.20	54.7	1.42976	1.41532	1.47176
210105	31	0.10	*	1.45634	1.46702	*
210106	1	0.10	52.8	1.44842	1.44639	1.45710

210106	2	0.10	54.7	1.37464	1.41905	1.45274
210106	3	0.10	53.0	1.40359	1.41532	*
210106	16	0.10	55.0	1.46041	1.46329	1.45297
210106	16	0.10	55.0	1.44861	1.47257	1.46572
210107	11	0.30	54.3	1.37790	1.40799	1.41446
210107	13	0.10	54.4	1.41643	1.42996	1.41250
210107	16	0.10	55.0	1.46012	1.45851	1.45610
210107	17	0.70	58.6	1.43396	1.51592	1.46499
210107	19	0.10	53.5	1.38784	1.39048	1.36753
210201	11	0.30	54.3	1.84547	1.89910	1.88909
210201	13	0.10	53.8	1.87819	1.87904	1.92292
210201	16	0.10	55.0	1.90709	1.92304	1.92511
210201	17	0.70	58.6	1.91439	1.92570	1.94349
210201	19	0.10	53.5	1.83983	1.83577	1.85381
210202	6	1.00	52.0	1.75401	1.77198	1.78237
210202	8	0.10	56.0	1.88974	1.92809	1.88960
210202	12	0.10	60.0	1.94141	2.05423	1.98780
210202	17	0.70	58.6	1.93261	1.90537	1.90701
210202	17	0.20	56.2	1.91171	1.88150	1.89441
210203	9	0.30	57.0	1.96122	1.99166	1.97382
210203	11	0.30	53.8	1.85804	1.87356	1.85142
210203	11	0.30	54.3	1.84432	1.83901	1.87882
210203	15	0.20	52.5	1.90266	1.90258	1.90342
210204	18	0.10	53.9	1.90702	1.91740	1.89602
210204	19	0.10	53.5	1.83727	1.83727	1.81864
210205	4	0.10	61.4	1.83850	1.83850	1.87878
210205	5	0.20	57.0	1.83702	1.85456	*
210205	10	0.10	54.0	1.87335	1.87784	1.86885
210205	13	0.20	54.0	1.82883	1.83752	1.83036
210205	13	0.20	54.7	1.85079	1.84012	1.84253
210205	31	0.10	*	1.84429	1.83436	*
210206	1	0.10	52.8	1.86794	1.94269	1.93081
210206	2	0.10	54.7	1.89345	1.93421	1.88239
210206	3	0.10	53.0	1.81246	1.83032	*
210206	16	0.10	55.0	1.91529	1.86790	1.83586
210206	16	0.10	55.0	1.90810	1.90470	1.90504
210207	11	0.30	54.3	1.80767	1.82844	1.79991
210207	13	0.10	54.4	1.84089	1.86148	1.84354
210207	16	0.10	55.0	1.90060	1.89881	1.91417
210207	17	0.70	58.6	1.91662	1.98055	2.00715
210207	19	0.10	53.5	1.80896	1.83324	1.82865

210301	11	0.30	54.3	2.23219	2.28338	2.28876
210301	13	0.10	53.8	2.26761	2.28447	2.29812
210301	16	0.10	55.0	2.32546	2.33349	2.33384
210301	17	0.70	58.6	2.37569	2.40517	2.41856
210301	19	0.10	53.5	2.19034	2.20512	2.21494
210302	6	1.00	52.0	2.17246	2.18292	2.15580
210302	8	0.10	56.0	2.29032	2.32515	2.31334
210302	12	0.10	60.0	2.40187	2.42621	2.42621
210302	17	0.70	58.6	2.29729	2.37503	2.33988
210302	17	0.20	56.2	2.28638	2.31233	2.32413
210303	9	0.30	57.0	2.39961	2.42861	2.39166
210303	11	0.30	53.8	2.28778	2.26974	2.26954
210303	11	0.30	54.3	2.28545	2.25966	2.27201
210303	15	0.20	52.5	2.30061	2.30465	2.30360
210304	18	0.10	53.9	2.29844	2.33715	2.26306
210304	19	0.10	53.5	2.21385	2.19703	2.22583
210305	4	0.10	61.4	2.22616	2.23906	2.21150
210305	5	0.20	57.0	2.30372	2.28080	*
210305	10	0.10	54.0	2.24713	2.22375	2.22375
210305	13	0.20	54.0	2.25395	2.26279	2.24387
210305	13	0.20	54.7	2.24596	2.23932	2.23814
210305	31	0.10	*	2.30125	2.28391	*
210306	1	0.10	52.8	2.34682	2.26474	2.24725
210306	2	0.10	54.7	2.26474	2.27167	2.28336
210306	3	0.10	53.0	2.19153	2.19925	*
210306	16	0.10	55.0	2.27017	2.26601	2.28027
210306	16	0.10	55.0	2.30269	2.29697	2.26395
210307	11	0.30	54.3	2.21663	2.23953	2.24378
210307	13	0.10	54.4	2.23715	2.24947	2.23835
210307	16	0.10	55.0	2.26613	2.27285	2.27070
210307	17	0.70	58.6	2.32211	2.24204	2.29201
210307	19	0.10	53.5	2.17460	2.18522	2.15601
210401	11	0.30	54.3	2.81188	2.84265	2.82931
210401	13	0.10	53.8	2.82488	2.81603	2.86502
210401	16	0.10	55.0	2.89052	2.87782	2.89605
210401	17	0.70	58.6	2.85143	2.91858	2.96385
210401	19	0.10	53.5	2.78051	2.74112	2.74519
210402	6	1.00	52.0	2.74818	2.69994	2.71440
210402	8	0.10	56.0	2.81798	2.92716	2.89315
210402	12	0.10	60.0	2.97848	2.99688	3.01570
210402	17	0.70	58.6	2.89588	2.91945	2.89614

210402	17	0.20	56.2	2.87847	2.87884	2.88325
210403	9	0.30	57.0	2.99551	3.06222	2.96527
210403	11	0.30	53.8	2.81586	2.81586	2.82944
210403	11	0.30	54.3	2.84276	2.80231	2.82042
210403	15	0.20	52.5	2.85175	2.86970	2.85611
210404	18	0.10	53.9	2.87092	2.83086	2.85519
210404	19	0.10	53.5	2.75241	2.73171	2.75181
210405	4	0.10	61.4	2.73035	2.76982	2.74694
210405	5	0.20	57.0	2.80967	2.82706	*
210405	10	0.10	54.0	2.74775	2.73480	2.72613
210405	13	0.20	54.0	2.74132	2.76251	2.75822
210405	13	0.20	54.7	2.74755	2.72167	2.74775
210405	31	0.10	*	2.80586	2.80659	*
210406	1	0.10	52.8	2.79273	2.80489	2.72143
210406	2	0.10	54.7	2.76204	2.75102	2.75166
210406	3	0.10	53.0	2.70381	2.68268	*
210406	16	0.10	55.0	2.77943	2.77023	2.77535
210406	16	0.10	55.0	2.79627	2.79234	2.76155
210407	11	0.30	54.3	2.71359	2.75913	2.71975
210407	13	0.10	54.4	2.72001	2.73338	2.71581
210407	16	0.10	55.0	2.79085	2.77333	2.76894
210407	17	0.70	58.6	2.82544	2.83874	2.77345
210407	19	0.10	53.5	2.63554	2.64418	2.65736
210501	11	0.30	54.3	3.07580	3.07454	3.07944
210501	13	0.10	53.8	3.08478	3.10412	3.11409
210501	16	0.10	55.0	3.15028	3.15267	3.17098
210501	17	0.70	58.6	3.17027	3.21016	3.22962
210501	19	0.10	53.5	2.98932	2.98413	3.02197
210502	6	1.00	52.0	3.02338	3.01386	3.00850
210502	8	0.10	56.0	3.12723	3.16793	3.20601
210502	12	0.10	60.0	3.25326	3.29428	3.30240
210502	17	0.70	58.6	3.14970	3.18663	3.15415
210502	17	0.20	56.2	3.16611	3.16793	3.17059
210503	9	0.30	57.0	3.28088	3.30322	3.28260
210503	11	0.30	53.8	3.11331	3.08409	3.06899
210503	11	0.30	54.3	3.08630	3.05762	3.09170
210503	15	0.20	52.5	3.13551	3.12781	3.11573
210504	18	0.10	53.9	3.12394	3.11783	3.11698
210504	19	0.10	53.5	2.97788	2.99658	2.97879
210505	4	0.10	61.4	3.09074	3.08485	3.05682
210505	5	0.20	57.0	3.16935	3.12266	*

210505	10	0.10	54.0	3.09968	3.09918	3.09918
210505	13	0.20	54.0	3.13605	3.12269	3.10479
210505	13	0.20	54.7	3.10465	3.08978	3.09521
210505	31	0.10	*	3.19800	3.19319	*
210506	1	0.10	52.8	3.19634	3.13700	3.13534
210506	2	0.10	54.7	3.16608	3.16805	3.20457
210506	3	0.10	53.0	3.07235	*	*
210506	16	0.10	55.0	3.16911	3.16233	3.17415
210506	16	0.10	55.0	3.16739	3.15037	3.14910
210507	11	0.30	54.3	3.09030	3.10865	3.11203
210507	13	0.10	54.4	3.10917	3.10470	3.08536
210507	16	0.10	55.0	3.15861	3.16173	3.15670
210507	17	0.70	58.6	3.12971	3.19293	3.26825
210507	19	0.10	53.5	3.01812	3.04609	3.02723
210601	11	0.30	54.3	3.42517	3.41182	3.43219
210601	13	0.10	53.8	3.44241	3.46429	3.47460
210601	16	0.10	55.0	3.52652	3.51757	3.49688
210601	17	0.70	58.6	3.57812	3.51758	3.56051
210601	19	0.10	53.5	3.33675	3.32124	3.33336
210602	6	1.00	52.0	3.30489	3.28629	3.34954
210602	8	0.10	56.0	3.48968	3.53911	3.51831
210602	12	0.10	60.0	3.62407	3.65626	3.55176
210602	17	0.70	58.6	3.54799	3.50643	3.53735
210602	17	0.20	56.2	3.51682	3.49893	3.50780
210603	9	0.30	57.0	3.66591	3.68337	3.62398
210603	11	0.30	53.8	3.45733	3.43725	3.43200
210603	11	0.30	54.3	3.43725	3.40487	3.45418
210603	15	0.20	52.5	3.47319	3.47524	3.46967
210604	18	0.10	53.9	3.49955	3.50657	3.46656
210604	19	0.10	53.5	3.33454	3.33454	3.32319
210605	4	0.10	61.4	3.44103	3.40474	3.40563
210605	5	0.20	57.0	3.45576	3.42337	*
210605	10	0.10	54.0	3.44679	3.42631	3.42631
210605	13	0.20	54.0	3.45696	3.50215	3.45638
210605	13	0.20	54.7	3.45836	3.41611	3.41162
210605	31	0.10	*	3.56001	3.53043	*
210606	1	0.10	52.8	3.42793	3.45966	3.45256
210606	2	0.10	54.7	3.49281	3.49621	3.48172
210606	3	0.10	53.0	3.40496	3.40160	*
210606	16	0.10	55.0	3.50876	3.49977	3.50329
210606	16	0.10	55.0	3.50613	3.50286	3.50116

210607	11	0.30	54.3	3.39170	3.45435	3.45105
210607	13	0.10	54.4	3.41338	3.49154	3.41787
210607	16	0.10	55.0	3.50350	3.47853	3.49430
210607	17	0.70	58.6	3.47274	3.60426	3.61531
210607	19	0.10	53.5	3.33660	3.31998	3.34463
210701	11	0.30	54.3	3.78435	3.82381	3.86403
210701	13	0.10	53.8	3.82167	3.81694	3.82381
210701	16	0.10	55.0	3.87526	3.89080	3.89311
210701	17	0.70	58.6	3.87962	3.91796	3.99514
210701	19	0.10	53.5	3.68577	3.67767	3.67858
210702	6	1.00	52.0	3.73964	3.67371	3.74175
210702	8	0.10	56.0	3.83203	3.89492	3.92105
210702	12	0.10	60.0	4.04389	3.95395	4.08461
210702	17	0.70	58.6	3.86948	4.09080	3.90335
210702	17	0.20	56.2	3.92589	3.91280	3.88123
210703	9	0.30	57.0	4.03129	4.07272	4.07097
210703	11	0.30	53.8	3.80685	3.79117	3.82706
210703	11	0.30	54.3	3.82274	3.82274	3.79570
210703	15	0.20	52.5	3.85609	3.85178	3.84950
210704	18	0.10	53.9	3.82165	3.78517	3.86124
210704	19	0.10	53.5	3.67862	3.67323	3.67315
210705	4	0.10	61.4	3.76529	3.77733	3.73419
210705	5	0.20	57.0	3.81727	3.84949	*
210705	10	0.10	54.0	3.78588	3.80803	3.79694
210705	13	0.20	54.0	3.78615	3.83914	3.80756
210705	13	0.20	54.7	3.83028	3.81042	3.81886
210705	31	0.10	*	3.87721	3.89063	*
210706	1	0.10	52.8	3.87721	3.79038	3.83927
210706	2	0.10	54.7	3.86211	3.83243	3.91534
210706	3	0.10	53.0	3.72310	*	*
210706	16	0.10	55.0	3.83735	3.83959	3.86166
210706	16	0.10	55.0	3.86836	3.85263	3.87284
210707	11	0.30	54.3	3.77425	3.80297	3.76848
210707	13	0.10	54.4	3.77500	3.83288	3.76648
210707	16	0.10	55.0	3.88438	3.88427	3.87537
210707	17	0.70	58.6	3.85975	3.91391	3.87311
210707	19	0.10	53.5	3.68660	3.68751	3.69567
210801	11	0.30	54.3	4.22736	4.23199	4.25050
210801	13	0.10	53.8	4.23512	4.27399	4.27763
210801	16	0.10	55.0	4.33593	4.32797	4.33813
210801	17	0.70	58.6	4.52785	4.50290	4.51374

210801	19	0.10	53.5	4.09735	4.08987	4.10958
210802	6	1.00	52.0	4.09656	4.09020	4.10176
210802	8	0.10	56.0	4.26916	4.38038	4.37766
210802	12	0.10	60.0	4.51962	4.56424	4.55894
210802	17	0.20	56.2	4.37239	4.36540	4.35840
210802	17	0.70	58.6	4.41768	4.40153	4.45932
210803	9	0.30	57.0	4.54007	4.51552	4.51552
210803	11	0.30	53.8	4.28159	4.24968	4.24968
210803	11	0.30	54.3	4.19531	4.27781	4.22974
210803	15	0.20	52.5	4.28714	4.28627	4.28436
210804	18	0.10	53.9	4.28443	4.28237	4.13491
210804	19	0.10	53.5	4.10962	4.11152	4.09625
210805	4	0.10	61.4	4.21598	4.23896	4.23896
210805	5	0.20	57.0	4.28924	4.30603	*
210805	10	0.10	54.0	4.22656	4.22349	4.21412
210805	13	0.20	54.0	4.26344	4.26359	4.21154
210805	13	0.20	54.7	4.25627	4.22801	4.27210
210805	31	0.10	*	4.32546	4.31822	*
210806	1	0.10	52.8	4.31315	4.33369	4.29783
210806	2	0.10	54.7	4.36804	4.33795	4.28245
210806	3	0.10	53.0	4.18806	*	*
210806	16	0.10	55.0	4.30410	4.31001	4.28885
210806	16	0.10	55.0	4.31261	4.29813	4.27635
210807	11	0.30	54.3	4.24956	4.28277	4.24497
210807	13	0.10	54.4	4.22458	4.24809	4.25277
210807	16	0.10	55.0	4.31182	4.30582	4.32036
210807	17	0.70	58.6	4.42277	4.42997	4.45339
210807	19	0.10	53.5	4.13018	4.13214	4.11780
210901	11	0.30	54.3	4.63738	4.60676	4.65444
210901	13	0.10	53.8	4.63223	4.64453	4.69272
210901	16	0.10	55.0	4.70271	4.69001	4.71165
210901	17	0.70	58.6	4.74620	4.79071	4.78628
210901	19	0.10	53.5	4.53745	4.53887	4.57112
210902	6	1.00	52.0	4.57929	4.56805	4.54271
210902	8	0.10	56.0	4.66123	4.64092	4.74408
210902	12	0.10	60.0	4.89959	5.03057	4.95560
210902	17	0.70	58.6	4.70198	4.71931	4.75032
210902	17	0.20	56.2	4.75004	4.75905	4.78148
210903	9	0.30	57.0	5.12151	5.16149	5.20532
210903	11	0.30	54.3	4.72149	4.59641	4.56255
210903	11	0.30	54.3	4.73031	4.76139	4.82868

210903	15	0.20	52.5	4.89366	4.88311	4.88373
210904	18	0.10	53.9	4.69325	4.78559	4.69490
210904	19	0.10	53.5	4.40138	4.41720	4.43855
210905	4	0.10	61.4	4.75215	4.66747	4.74770
210905	5	0.20	50.0	4.64637	4.54633	*
210905	10	0.10	54.0	4.80105	4.86464	4.76088
210905	13	0.20	54.0	4.79480	4.76385	4.77282
210905	13	0.20	54.7	4.75614	4.73401	4.74734
210905	31	0.10	*	4.77282	4.71069	*
210906	1	0.10	52.8	4.71189	4.74315	4.78804
210906	2	0.10	54.7	4.80236	4.75685	4.78677
210906	3	0.10	53.0	4.78360	4.81076	*
210906	16	0.10	55.0	4.79607	4.86510	4.82185
210906	16	0.10	55.0	4.88662	4.89100	4.87394
210907	11	0.30	54.3	4.73701	4.63182	4.56692
210907	13	0.10	54.4	4.73309	4.70647	4.71531
210907	16	0.10	55.0	4.80403	4.84807	4.84849
210907	17	0.70	58.6	4.82439	4.77724	4.75935
210907	19	0.10	53.5	4.62236	4.57498	4.60543
740209	6	1.00	52.0	0.93610	0.87690	0.82687
740209	8	0.10	56.0	0.92170	0.92125	0.94449
740209	12	0.10	60.0	0.98723	0.98329	0.99797
740209	17	0.20	56.2	0.94365	0.94061	0.93592
740209	17	0.70	58.6	0.96977	0.93418	0.96609
740311	1	0.10	52.8	1.33640	1.33856	1.37188
740311	2	0.10	54.7	1.36102	1.34568	1.29802
740311	3	0.10	53.0	1.31965	*	*
740311	16	0.10	55.0	1.37748	1.37605	1.38271
740311	16	0.10	55.0	1.35885	1.38432	1.37954
740311	18	0.10	53.9	1.36138	1.37157	1.35832
740311	19	0.10	53.5	1.30374	1.30107	1.31964
740511	1	0.10	52.8	1.77965	1.78549	1.80545
740511	2	0.10	54.7	1.80854	1.75149	1.83422
740511	3	0.10	53.0	1.72963	*	*
740511	16	0.10	55.0	1.80867	1.79739	1.79739
740511	16	0.10	55.0	1.80176	1.79923	1.80247
740511	18	0.10	53.9	1.76689	1.78507	1.77952
740511	19	0.10	53.5	1.70607	1.71975	1.72966
740609	6	1.00	52.0	2.26115	2.24867	2.23718
740609	8	0.10	56.0	2.37086	2.39531	2.37386
740609	12	0.10	60.0	2.47190	2.50675	2.49078

740609	17	0.20	56.2	2.39096	2.44761	2.39167
740609	17	0.70	58.6	2.35411	2.42658	2.41274
740809	6	1.00	52.0	3.51402	3.57586	3.45279
740809	8	0.10	56.0	3.73944	3.82078	3.82078
740809	12	0.10	60.0	3.94590	4.00274	3.99679
740809	17	0.20	56.2	3.82857	3.82130	3.79994
740809	17	0.70	58.6	3.77117	3.74536	3.84590
741011	1	0.10	52.8	2.32975	2.31619	2.27116
741011	2	0.10	54.7	2.29386	2.22332	2.29731
741011	3	0.10	53.0	2.23537	*	*
741011	16	0.10	55.0	2.33373	2.34627	2.35064
741011	16	0.10	55.0	2.32608	2.33210	2.32507
741011	18	0.10	53.9	2.33711	2.31382	2.30367
741011	19	0.10	53.5	2.20438	2.19142	2.22273
741211	1	0.10	52.8	2.75174	2.76465	2.79895
741211	2	0.10	54.7	2.77775	2.77302	2.80488
741211	3	0.10	53.0	2.69567	*	*
741211	16	0.10	55.0	2.79089	2.81307	2.80391
741211	16	0.10	55.0	2.80373	2.81315	2.80382
741211	18	0.10	53.9	2.73593	2.74597	2.82278
741211	19	0.10	53.5	2.63435	2.65873	2.64203
741310	4	0.10	61.4	2.80110	2.82715	2.82308
741310	5	0.20	57.0	2.90355	2.87826	*
741310	9	0.30	57.0	3.06401	3.07010	3.07189
741310	10	0.10	54.0	2.94124	2.87715	2.88616
741310	11	0.30	53.8	2.87334	2.85511	2.89154
741310	11	0.30	54.3	2.86401	2.88259	2.86282
741310	13	0.20	54.0	2.86768	2.85814	2.86373
741310	13	0.20	54.7	2.86359	2.86784	2.85846
741310	15	0.20	52.5	2.89894	2.88841	2.89154
741410	4	0.10	61.4	2.06405	2.03617	2.06892
741410	5	0.20	57.0	2.08088	2.05438	*
741410	9	0.30	57.0	2.20725	2.22139	2.20401
741410	10	0.10	54.0	2.10165	2.06844	2.06844
741410	11	0.30	53.8	2.06844	2.07254	2.09033
741410	11	0.30	54.3	2.07555	2.07614	2.06125
741410	13	0.20	54.0	2.08159	2.08463	2.09072
741410	13	0.20	54.7	2.06081	2.08767	2.09033
741410	15	0.20	52.5	2.09775	2.09857	2.10316
741510	4	0.10	61.4	2.68360	2.65793	2.64557
741510	5	0.20	57.0	2.69954	2.69026	*

741510	9	0.30	57.0	2.85667	2.88427	2.86589
741510	10	0.10	54.0	2.71082	2.67662	2.68971
741510	11	0.30	53.8	2.68157	2.69138	2.66399
741510	11	0.30	54.3	2.65563	2.67202	2.73042
741510	13	0.20	54.7	2.67202	2.68971	2.69497
741510	13	0.20	54.0	2.69138	2.68545	2.67084
741510	15	0.20	52.5	2.70982	2.71514	2.70650
741609	6	1.00	52.0	2.70419	2.74982	2.71919
741609	8	0.10	56.0	2.80597	2.84565	2.82733
741609	12	0.10	60.0	2.91428	2.96050	2.96502
741609	17	0.20	56.2	2.82771	2.81870	2.91824
741609	17	0.70	58.6	2.85041	2.95098	2.82327
741709	6	1.00	52.0	3.05872	3.06639	3.02795
741709	8	0.10	56.0	3.21498	3.24188	3.23969
741709	12	0.10	60.0	3.41149	3.44401	3.41841
741709	17	0.20	56.2	3.27251	3.26194	3.24627
741709	17	0.70	58.6	3.33383	3.36701	3.27439
742011	1	0.10	52.8	2.56544	2.56373	2.57491
742011	2	0.10	54.7	2.59011	2.60319	2.60319
742011	3	0.10	53.0	2.48751	*	*
742011	16	0.10	55.0	2.60751	2.59795	2.60337
742011	16	0.10	55.0	2.59157	2.59469	2.61474
742011	18	0.10	53.9	2.59129	2.54604	2.59043
742011	19	0.10	53.5	2.46169	2.47805	2.48810
742210	4	0.10	61.4	3.62858	3.65339	3.67106
742210	5	0.20	57.0	3.70178	3.61501	*
742210	9	0.30	57.0	3.91487	3.91906	3.97995
742210	10	0.10	54.0	3.79436	3.72077	3.71004
742210	11	0.30	53.8	3.70178	3.72555	3.70467
742210	11	0.30	54.3	3.65999	3.71093	3.71147
742210	13	0.20	54.0	3.69842	3.71136	3.69494
742210	13	0.20	54.7	3.70856	3.71922	3.69303
742210	15	0.20	52.5	3.71982	3.73994	3.73484
742309	6	1.00	52.0	1.54635	1.53984	1.47828
742309	8	0.10	56.0	1.51578	1.55405	1.61825
742309	12	0.10	60.0	1.69996	1.72381	1.69888
742309	17	0.20	56.2	1.59306	1.58448	1.59103
742309	17	0.70	58.6	1.53886	1.56249	1.57141
742410	4	0.10	61.4	1.76132	1.76325	1.73748
742410	5	0.20	57.0	1.70306	1.77403	*
742410	9	0.30	57.0	1.82054	1.69872	1.69315

742410	10	0.10	54.0	1.80447	1.70913	1.74139
742410	11	0.30	53.8	1.73926	1.73595	1.71746
742410	11	0.30	54.3	1.69239	1.72371	1.61952
742410	13	0.20	54.0	1.64528	1.73979	1.69993
742410	13	0.20	54.7	1.73156	1.67928	1.69277
742410	15	0.20	52.5	1.65268	1.75532	1.62091
742509	6	1.00	52.0	1.79537	1.80115	1.86470
742509	8	0.10	56.0	1.95490	1.93225	1.93784
742509	12	0.10	60.0	2.07382	2.08109	2.06755
742509	17	0.70	58.6	1.96250	2.00401	1.97249
742509	17	0.20	56.2	1.96404	1.95941	1.92429
742611	1	0.10	52.8	1.87374	1.77894	1.88887
742611	2	0.10	54.7	1.86258	1.88907	1.93342
742611	3	0.10	53.0	1.86784	*	*
742611	16	0.10	55.0	1.93628	1.93415	1.94035
742611	16	0.10	55.0	1.92119	1.93299	1.92490
742611	18	0.10	53.9	1.91515	1.90313	1.90245
742611	19	0.10	53.5	1.83491	1.81546	1.89195
747211	1	0.10	52.8	3.27458	3.20855	3.22037
747211	2	0.10	54.7	3.23709	3.26281	3.21424
747211	3	0.10	53.0	3.15541	*	*
747211	16	0.10	55.0	3.24670	3.23678	3.25754
747211	16	0.10	55.0	3.22639	3.25299	3.26936
747211	18	0.10	53.9	3.23667	3.24744	3.27406
747211	19	0.10	53.5	3.09441	3.10343	3.11024
747610	4	0.10	61.4	1.77654	1.75004	1.80048
747610	5	0.20	57.0	1.76828	1.78436	*
747610	9	0.30	57.0	1.90586	1.91975	1.91084
747610	10	0.10	54.0	1.84874	1.79095	1.78911
747610	11	0.30	53.8	1.78768	1.78443	1.79312
747610	11	0.30	54.3	1.76892	1.78610	1.79311
747610	13	0.20	54.0	1.77961	1.78768	1.77334
747610	13	0.20	54.7	1.78656	1.77961	1.78401
747610	15	0.20	52.5	1.79569	1.80718	1.77140
747710	4	0.10	61.4	2.43467	2.41336	2.41410
747710	5	0.20	57.0	2.49194	2.44588	*
747710	9	0.30	57.0	2.60962	2.60436	2.59454
747710	10	0.10	54.0	2.50172	2.45474	2.45404
747710	11	0.30	53.8	2.45030	2.41764	2.41764
747710	11	0.30	54.3	2.41001	2.43610	2.46409
747710	13	0.20	54.0	2.45100	2.43911	2.45780

747710	13	0.20	54.7	2.43839	2.43911	2.45850
747710	15	0.20	52.5	2.46913	2.47561	2.45443

* Missing data

APPENDIX B. ABSOLUTE ANALYSIS DATA

INGOT	LAB	OXYGEN (μg/g)
0101	21	2.83
0101	21	2.85
0101	22	3.6
0101	23	2.6
0101	25	2.56
0101	26	3.22
0101	26	2.92
0101	28	1.8
0201	21	7.56
0201	21	7.67
0201	23	7.6
0201	24	6.1
0201	25	7.06
0201	26	8.48
0201	26	10.65
0201	26	8.12
0201	28	5.8
0301	21	11.63
0301	21	11.69
0301	22	11.0
0301	23	10.8
0301	25	9.99
0301	26	12.30
0301	26	11.47
0301	26	10.87
0301	28	8.2
0401	21	11.09
0401	21	11.07
0401	22	8.8
0401	23	10.0
0401	23	7.0
0401	24	10.3
0401	25	9.82
0401	26	10.75
0401	26	9.64
0401	26	10.49
0401	28	8.9

0501	21	12.98
0501	21	13.27
0501	22	9.6
0501	23	12.9
0501	24	12.6
0501	25	11.90
0501	26	13.48
0501	26	12.95
0501	26	13.07
0501	28	10.2
1101	21	10.34
1101	21	10.05
1101	22	10.3
1101	23	11.7
1101	24	9.5
1101	25	9.96
1101	26	11.28
1101	26	10.90
1101	26	11.24
1101	28	9.8
1102	21	7.94
1102	21	7.90
1102	22	7.3
1102	24	8.5
1102	25	7.38
1102	26	8.77
1102	26	8.31
1102	26	8.39
1102	28	8.1
1201	21	12.95
1201	21	12.56
1201	22	13.5
1201	23	12.6
1201	26	13.85
1201	26	13.16
1201	26	13.39
1202	21	14.54
1202	21	14.19
1202	22	11.3
1202	23	15.0
1202	23	14.7

1202	26	14.57
1202	26	13.92
1202	26	14.29
1203	21	12.63
1203	21	12.41
1203	22	10.2
1203	23	13.3
1203	23	11.9
1203	26	12.99
1203	26	12.38
1203	26	13.30
1204	21	12.40
1204	21	12.22
1204	22	9.6
1204	23	11.7
1204	23	11.3
1204	26	13.28
1204	26	12.77
1204	26	11.51
2101	21	4.62
2101	21	5.35
2101	21	5.01
2101	22	5.7
2101	24	3.7
2101	25	4.64
2101	28	3.8
2102	21	6.89
2102	21	6.66
2102	22	8.9
2102	23	7.2
2102	24	4.6
2102	25	5.57
2102	26	6.65
2102	26	7.17
2102	26	7.26
2102	28	4.8
2103	21	8.42
2103	21	8.12
2103	22	7.7
2103	23	7.7
2103	25	7.13

2103	26	8.79
2103	26	8.73
2103	26	8.85
2103	28	6.5
2104	21	10.04
2104	21	9.69
2104	21	10.17
2104	22	9.2
2104	24	8.4
2104	25	9.27
2104	28	8.6
2105	21	10.87
2105	21	11.01
2105	22	6.5
2105	23	11.5
2105	23	11.2
2105	25	9.49
2105	26	11.52
2105	26	11.22
2105	26	12.09
2105	28	10.8
2106	21	11.94
2106	21	12.17
2106	21	12.92
2106	22	8.6
2106	24	9.7
2106	25	11.22
2106	26	13.67
2106	26	12.95
2106	26	12.91
2106	28	10.6
2107	21	13.07
2107	21	13.69
2107	21	13.56
2107	22	11.1
2107	23	14.0
2107	23	10.8
2107	24	11.5
2107	25	12.27
2107	26	14.43
2107	26	13.63

2107	26	14.22
2107	28	11.6
2108	21	15.59
2108	21	16.24
2108	22	11.4
2108	24	11.7
2108	25	13.65
2108	28	15.9
2109	21	16.62
2109	21	16.59
2109	22	13.2
2109	24	12.0
2109	25	15.31
2109	26	16.21
2109	26	16.38
2109	28	15.4
2110	21	0.0454
2110	21	0.0462
2110	23	0.02
2110	23	0.03
2110	25	0.06
7402	21	2.53
7402	21	2.99
7402	21	3.16
7402	21	2.73
7402	22	2.6
7402	23	2.22
7402	27	3.23
7402	27	3.25
7402	27	2.95
7402	27	2.87
7402	27	3.90
7406	21	8.24
7406	21	7.94
7406	22	5.7
7406	23	9.41
7406	27	8.71
7406	27	7.95
7408	21	13.39
7408	21	14.02
7408	21	13.40

7408	21	12.58
7408	23	11.41
7408	27	13.89
7408	27	13.09
7416	21	10.42
7416	21	10.53
7416	22	12.0
7416	23	8.67
7416	27	9.85
7416	27	9.86
7417	21	11.41
7417	21	11.18
7417	21	11.97
7417	21	11.19
7417	22	13.2
7417	23	10.10
7417	27	11.40
7417	27	11.19
7423	21	5.90
7423	21	5.07
7423	21	5.66
7423	21	5.94
7423	22	10.5
7423	23	5.53
7423	27	6.19
7423	27	5.24
7425	21	7.29
7425	21	7.19
7425	21	6.87
7425	21	7.65
7425	22	7.4
7425	23	7.19
7425	27	7.89
7425	27	6.88

APPENDIX C.

Interlaboratory Determination of the Calibration Factor for the Measurement of the Interstitial Oxygen Content of Silicon by Infrared Absorption‡

A. Baghdadi,* W. M. Bullis,† M. C. Croarkin,§ Yue-zhen Li,¶
R. I. Scace,# R. W. Series,ᶻ P. Stallhofer,ʸ and M. Watanabeᶻ

Abstract

We report an international interlaboratory dual experiment to determine the calibration factor used to calculate the interstitial oxygen content of silicon from room-temperature (300 K) infrared (IR) absorption measurements. We conducted round robins for both the infrared and the absolute measurements on the same or equivalent specimens. The calibration factor for computing the oxygen content of silicon in parts per million atomic (ppma) from a room-temperature measurement of the absorption coefficient at 1107 cm^{-1} was determined to be 6.28 ± 0.18 ppma/cm^{-1}. The IR round robin showed a reproducibility on the order of 3%.

1. Introduction

This paper is a report of a world-wide interlaboratory experiment to determine the calibration factor used to calculate the interstitial oxygen content of silicon from room-temperature infrared (IR) absorption measurements. The basic approach taken for this experiment was to conduct both the infrared measurements and the absolute oxygen concentration measurements at many different laboratories on the same or similar specimens. The infrared measurements were carried out at 18 laboratories in China, Europe, Japan, and the United States (see Table I), using either dispersive infrared (DIR) or Fourier transform infrared (FTIR) spectrometers. The absolute measurements were carried out at eight laboratories in Europe, Japan, and the United States (see Table II), using charged-particle

---

‡ Contribution of the National Institute of Standards and Technology (formerly National Bureau of Standards). Not subject to copyright.

* Semiconductor Electronics Division, National Institute of Standards and Technology, Gaithersburg, MD

† Siltec Silicon, Menlo Park, California

§ Statistical Engineering Division, National Institute of Standards and Technology

¶ Shanghai Institute of Metallurgy, Shanghai, People's Republic of China

Center for Electronics and Electrical Engineering, National Institute of Standards and Technology

ᶻ Royal Signals and Radar Establishment, Great Malvern, United Kingdom

ʸ Wacker Chemitronic, Burghausen, West Germany

ᶻ Toshiba Research and Development, Tokyo, Japan

activation analysis (CPAA), photon activation analysis (PAA), or inert gas fusion analysis (IGFA).

Since Kaiser and Keck[1] first showed a linear relationship between the oxygen content of semiconductor silicon and IR absorption at 9.1 μm (1107 cm^{-1}), there have been numerous experiments which have attempted to establish a definitive value for the calibration factor.[2] The results of these experiments are summarized in Table III. The values proposed for the calibration factor range from 4.9 ± 0.3 to 12.0 ± 1.4 ppma/cm^{-1} [1,3–15]. Note that even the most recent determinations disagree by about 20%. At present, there are at least four values in commercial use: the "old ASTM" value of 9.63,[16] the "DIN" and "new ASTM" value of 4.9,[17,18] the "JEIDA" value of 6.06,[12] and the Guo Biao†-designated value of 6.2.[11]

The present study differs from all the previous work in that both the IR and the absolute determinations were obtained from a substantial number of interlaboratory measurements. Thus we could estimate the reproducibility of both types of measurements on a statistical basis rather than rely on estimates of measurement errors provided by individual laboratories.

This work had three goals. The first was to provide an accurate and well-established value for the calibration factor, using equivalent samples and up-to-date radio-analytical methods. The second was to provide a basis for calculating the uncertainty in the value of the calibration factor and to explain the sources of error for that uncertainty. The third, and arguably the most important, goal was to provide a universally acceptable value for the calibration factor. The present study includes participation by groups from the American Society for Testing and Materials (ASTM), Deutsches Institut für Normung (DIN), the Japan Electronic Industry Development Association (JEIDA), and the Academia Sinica, as well as contributions from all of the laboratories which have published recent measurements of the calibration factor.

Two other multilaboratory experiments and their relationship to this work should be mentioned. The JEIDA work,[12] which was conducted from 1979 to 1982, was intended to accomplish the same goals as the present experiment. Unexpected difficulties were encountered in part from axial variations in the oxygen content of the parent crystals, which caused the IR absorption data on neighboring slices to vary in a way which was difficult to account for properly in the analysis. The original data were made available by JEIDA to NBS for statistical examination. This analysis completely supported the JEIDA decisions on exclusion of aberrant data but also revealed a hitherto unsuspected bimodal distribution of the data. This distribution appears to have resulted from variations in the procedures used by the infrared laboratories.[19]

JEIDA generously made available 18 of the specimens from their experiment plus three others from a standard reference set calibrated from that experiment. Data on these specimens can be used to tie the present work back to the JEIDA experiment and thus to

† Guo Biao designates the State Standards of China.

improve the basis for calibration of the JEIDA reference specimens. However, the JEIDA specimens were not used in the calculation of the calibration factor: only the data obtained on the specimens prepared especially for this study were used to compute the calibration factor.

The second multilaboratory experiment, by the European Community Bureau of Reference (BCR), is underway to provide calibrated reference specimens. The BCR kindly arranged for absolute analyses of subsets of material from the present experiment by two laboratories participating in their work. In addition, several of the IR laboratories in this experiment are also involved in the BCR effort.

In this paper, we describe the silicon samples and the test matrix, the statistical analyses of the data, and the determination of the conversion coefficient. The analyses and discussions of the data presented here are necessarily brief: we present only a synopsis of the statistical methods and the resulting conclusions. A more extensive description of the statistical analyses, together with the complete data base and a more detailed description of the experimental procedures used by the absolute laboratories, is being published concurrently as a National Institute of Standards and Technology Special Publication.[20]

2. Experimental Plan

2.1 Test Samples

The silicon samples were produced specially for this project by eight leading producers of semiconductor silicon. The samples were cut from 20 different 100-mm diameter silicon crystals with room-temperature free carrier concentrations less than 2×10^{15} cm^{-3}. The determination of the oxygen content of silicon crystals is not significantly affected by the presence of free carriers at these concentrations.[21] The crystals were grown so that the IR absorption coefficient at 9.1 μm due to oxygen for all the slices ranged from about 0.9 cm^{-1} to about 5 cm^{-1}, with a relatively uniform distribution of values throughout the entire range.

Each laboratory contributing specimens cut a 120-mm long section from each crystal. Two 2-mm thick slices polished on both sides, a 10-mm thick slug, and then two more 2-mm slices were cut from the end of this section, as shown in Figure 1a. The 10-mm thick slug was reserved for PAA or IGFA measurements. Samples for the destructive PAA and IGFA measurements were cut from the 10-mm slugs as they were needed. Two of the four 2-mm slices were used for the IR and CPAA measurements. The remainder of each crystal was set aside for future or follow-up experiments.

The nominal oxygen concentration was measured, by the silicon producers, as the average of at least three separate IR measurements, at each of four positions on each slice, 90 degrees apart located 18.5 $\pm$ 1.0 mm from the center of the slice, with one measurement on each of the four radii at 45 degrees to the bisector of the primary flat. The maximum

spread in the IR absorption coefficient due to oxygen in slices cut from either side of the 10-mm slug was less than 0.06 cm^{-1}.

Four squares, 25 ± 1 mm on a side, were cut from the center of each of two slices from each crystal, as shown in Figure 1b. Each square was laser marked or scribed in the corner nearest the center of the slice with a three-part code which identified the preparing organization, the set number from that organization, and the square number. There were 8 squares, marked 1 through 8, prepared from each crystal, yielding 8 equivalent test sets of 20 squares each. In addition to these 8 sets of 20 squares, 3 sets of 7 samples each were supplied by JEIDA. Each of these samples had either been used in the JEIDA round robin experiment[12] or was part of JEIDA reference set 44.[22] The eight test sets prepared for this study were designated Test Sets 1 through 8, and the JEIDA test sets were designated JEIDA Sets 1 through 3. Test sets 2 through 6 also included an oxygen-free float-zoned reference square and a sapphire filter to be used in an instrumental check.

The thicknesses of the test and reference squares were measured at the National Institute of Standards and Technology (formerly National Bureau of Standards), Toshiba Ceramics, Wacker, and the Shanghai Institute of Metallurgy. All replicate thickness measurements agreed to within ±0.05%.

2.2 Test Matrix

Measurements were carried out in five separate geographic regions: The People's Republic of China; Germany; Japan; United Kingdom, France and Italy; and the United States. Table I lists the IR laboratories that participated in this study; a coordinating laboratory for each region is listed in boldface. The coordinating laboratories in Germany, Japan, and the United States represented DIN, JEIDA, and ASTM, respectively, as noted in parentheses in Table I. The coordinating laboratory in China represented the Academia Sinica. The coordinating laboratories played a central role in the experimental plan. One of the test sets was assigned to each region. The coordinating laboratories made the first IR measurements on that test set, passed them on for measurement by the other laboratories in the region, and then made a second set of measurements after the other laboratories in their region completed their IR measurements. Test set 2 was assigned to Japan, test set 3 to the United States, test set 4 to Germany, test set 5 to the United Kingdom, France and Italy, and test set 6 to China. Test sets 1 and 7 were circulated among the coordinating laboratories and were measured by IR at the same time as the initial measurements on the set assigned to that region. Test set 8 was reserved to check whether the silicon crystals contained significant amounts of precipitated oxygen. Since samples subjected to CPAA are no longer suitable for IR analysis, each CPAA measurement was scheduled following the IR analyses for that set of samples. Test sets 2 and 3 were measured by CPAA at laboratories 21 and 22, respectively. Test set 4 was measured by CPAA at laboratories 23 and 26. Samples cut from the 10-mm slugs were subjected to PAA in the U.K. and in Germany, and to IGFA in Germany.

JEIDA set J-1 was measured at all the Japanese IR laboratories, and then circulated for

CPAA measurements in Japan, the United States, Germany, and Belgium at the same time as the assigned test sets were measured. JEIDA set J-2 was circulated for IR measurements in the United States and the U.K., and JEIDA set J-3 was circulated for IR measurements in Germany and China.

2.3 Sources of Error

The sources of error that were examined in this study are due to material inhomogeneity and to laboratory performance. The dependence of the oxygen absorbance band on the specimen temperature is not a significant source of error, as discussed in section 4.1. Material stability and freedom from precipitated oxygen are not significant; these points are verified in section 4.2. The factors of laboratory performance which are discussed in sections 4.1 and 4.2 include within-laboratory repeatability, between-laboratory reproducibility, and nonlinear behavior of the absolute laboratories relative to the IR laboratories.

The within-laboratory repeatability for individual IR laboratories was estimated from three repetitions over a three-day period. The spread of the relative biases among IR laboratories, which was minimized by specifying the IR measurement procedure, was estimated from differences among the 18 IR laboratories.

The experimental plan for absolute measurements did not specify repetitions on individual specimens. Laboratory repeatability was estimated by the residual standard deviation of the fit of absolute measurements to a linear function of the IR measurements.[23] Bias among laboratories was a dominant source of error because of the lack of a specified operating procedure. Failure of the measurements to conform to the linear model proved to be another source of error for some absolute laboratories.

The error due to material inhomogeneity could only be partially quantified because of time constraints on the experimental plan. Oxygen concentrations could be directly compared only for test sets 1 and 7 because these were the only test sets measured by the same IR laboratories. The possible effect of material inhomogeneity on the conversion factor was included as a contribution to its uncertainty.

3. Measurement Procedures

A standard measurement procedure was specified for the IR measurements. This procedure is described in the following sub-section. However, we did not specify a standard procedure for the absolute measurements. Each absolute laboratory followed its own internally developed procedures. This approach was necessary because there is no single generally accepted procedure for the absolute measurements.

3.1 Infrared Measurements

The participating laboratories obtained the infrared spectra of the test squares according to the specified procedure. Roughly two-thirds of the participating IR laboratories used FTIR spectrophotometers. The remaining laboratories used DIR spectrophotometers, some of

which were computerized. Each laboratory conducted a series of instrumental checks in addition to obtaining the spectra on the test squares:

1. The 100% base line was obtained to measure the "noise" level. On double beam instruments, the transmittance spectrum was recorded with both the sample and reference beams empty. On single-beam instruments, the transmittance spectrum was obtained as the ratio of two spectra taken with the reference specimen in the sample beam. The 100% base line was plotted over a wavenumber range covering 900 to 1300 cm^{-1}.

2. A 0% line was established, for DIR instruments only, by blocking the sample beam, and recording the instrument zero over the range from 900 to 1300 cm^{-1}.

3. The presence of stray light was detected by obtaining an air-reference transmittance spectrum of the sapphire square provided with the test sets. The resulting spectrum was plotted over the range from 900 cm^{-1} to 1300 cm^{-1}. Sapphire is a cut-off filter below 1180 cm^{-1}, so that any signal detected in the region of the oxygen peak would be due to light which did not pass through the sample.

4. The mid-scale linearity of each spectrophotometer was determined by obtaining an air-reference spectrum of the silicon reference square over the wavenumber range from 450 to 4000 cm^{-1}. Since the transmittance of a silicon specimen which is polished on both sides can be calculated from the reflectivity of silicon,† the observed transmittance in regions of the spectrum where silicon is transparent can be used to evaluate the linearity of the instrument at mid-scale.

5. The throughput characteristics of each FTIR spectrophotometer were reported by plotting a single-beam spectrum, obtained with the sample beam empty, over the wavenumber range from 450 to 4000 cm^{-1}.

6. The temperature in the laboratory and the temperature in the spectrophotometer chamber were recorded with an accuracy of $\pm 0.5°C$.

A test method for determining the interstitial oxygen content of silicon wafers similar to this method has been recommended to the ASTM for adoption.

Immediately prior to the initial measurement in any laboratory, all specimens, including the reference specimen, were etched in hydrofluoric acid to remove any surface oxide. Infrared transmittance spectra were obtained with a resolution, at 1107 cm^{-1}, of 4 cm^{-1} for the FTIR instruments and 5 cm^{-1} or better for the DIR instruments over (at least) the range from 900 to 1300 cm^{-1}. The squares were positioned so that the IR beam was centered on the test squares. The test squares were measured three separate times over a three- (or more) day period. On some double-beam DIR instruments, the transmittance spectra were obtained with the oxygen-free reference square in the reference beam, and the test square in the sample beam. On single-beam instruments, and on some computerized DIR

† The transmittance of a silicon specimen polished on both sides should be 53.8%.

instruments, the transmittance spectra were computed as the ratio of the spectrum of the test square to the spectrum of the reference square.

The data reported by each IR laboratory on the performance of its spectrophotometer will be included in the National Institute of Standards and Technology Special Publication mentioned above.[20]

The original data, in the form of transmittance spectra, were sent to the National Bureau of Standards for evaluation and data reduction. The base line transmittance at approximately 1107 cm^{-1} was obtained by drawing a straight line from 900 cm^{-1} to 1300 cm^{-1}, and the peak and base line transmittances were recorded. All of the spectra were read by the same person. The absorption coefficient was calculated from the base line and peak transmittances. The transmittance spectra obtained according to the procedure described above can be derived as the ratio of two equations, one for the transmittance of each specimen:[24]

$$T_{s/r} = \frac{(1-R)^2 e^{-\alpha_t x_t}(1-R^2 e^{-2\alpha_r x_r})}{(1-R)^2 e^{-\alpha_r x_r}(1-R^2 e^{-2\alpha_t x_t})}, \tag{1}$$

where $T_{s/r}$ is the ratio of the spectrum of the IR source with the sample in the IR beam to the spectrum of the IR source with the reference specimen in the IR beam, α_t is the absorption coefficient of the test crystal, α_r is the absorption coefficient of the reference crystal, x_t is the thickness of the test crystal, x_r is the thickness of the reference crystal, and R is the reflectivity of the semiconductor. In the wavenumber region of interest, R = 0.30 for silicon. Note that T and α are functions of wavenumber.

Assuming that the absorption in the test crystal is due only to the host lattice, α_L, to interstitial oxygen, α_o, and to unknown instrumental effects, α_{us},

$$\alpha_t = \alpha_L + \alpha_o + \alpha_{us}.$$

The term α_{us} arises because actual instruments differ from the ideal instrument in several significant respects. For example, the detector system may not be absolutely linear. Also, in many instruments, the insertion of the sample into the sample beam results in a series of extraneous reflections between the sample surfaces and the spectrometer components. In double-beam instruments, it is very difficult to completely balance the two beams of the spectrometer throughout the spectrum. The effect of these instrumental problems is to shift the base line of the instrument. This will result in a change in the apparent absorption spectrum.

Since the reference crystal does not contain a measurable concentration of oxygen, the absorption in the reference crystal is due only to the host lattice and to the unknown instrumental effects, so that

$$\alpha_r = \alpha_L + \alpha_{ur}.$$

Note that α_{ur}, although small, may be different from α_{us}. $\alpha_L = 0.85$ cm^{-1} was used as the value of the lattice absorption coefficient at 1107 cm^{-1}. This value was measured directly at the National Bureau of Standards from the spectrum of a 4.7-mm thick polished float-zoned silicon crystal. However, the calculation of the absorption coefficient due to oxygen is very insensitive to this value. For example, a change of 10% in this parameter would result in a change of 0.25% in the calculated value of the absorption coefficient.

For convenience, we can define

$$A = e^{-[(\alpha_L + \alpha_{ur})x_r]}$$

$$B = e^{-[\alpha_L + (\alpha_{ur}\frac{x_r}{x_t})]x_t},$$

and

$$X = e^{-[\alpha_o + \alpha_{us} - (\alpha\frac{x_r}{x_t})x_t]}.$$

Then eq. (1) can be rewritten as

$$T_{s/r} \cdot R^2 \cdot B^2 \cdot X^2 + \frac{B}{A} \cdot [1 - R^2 A^2] \cdot X - T_{s/r} = 0.$$

Solving for X

$$X = \frac{-\frac{B}{A}(1 - R^2 \cdot A^2) + \sqrt{\frac{B^2}{A^2} \cdot [1 - R^2 A^2]^2 + 4 \cdot R^2 \cdot B^2 \cdot T_{s/r}^2}}{2T_{s/r} \cdot R^2 \cdot B^2}.$$

If $x_r \approx x_t$, if $\alpha_{ur} << \alpha_L$, and assuming that α_{ur} and α_{us} are small and varying slowly with wavenumber, the net absorption coefficient due to interstitial oxygen can be calculated from the peak and base line values of X by

$$\alpha_o = -\frac{lnX_p - lnX_b}{x_t},$$

where X_p and X_b refer to X calculated using the peak and base line values of the transmittance at 1107 cm^{-1}, respectively.

3.2 Absolute Measurements

As noted above, each laboratory measuring the oxygen content of the silicon samples by an absolute method used its own internally developed procedures. This was necessary because there is no *a priori* basis for asserting that any particular procedure is fundamentally superior to any other procedure for this particular impurity (oxygen) in this particular matrix (silicon) at this particular concentration level ($\approx$ 5 to 30 ppma). Moreover, by using this approach, the expertise which had been developed at each of the laboratories could be brought to bear on this project.

Table II lists five laboratories that used CPAA, two laboratories that used PAA, and one laboratory which used IGFA. The latter two techniques require separation of the impurity from the silicon matrix prior to the final measurement. All five CPAA laboratories used the same nuclear reaction $\left({}^{16}O({}^{3}He,p) \rightarrow {}^{18}F\right)$, removed roughly the same amount of surface material by etching, and used roughly the same nominal energy for the ${}^{3}He$ ions. However, the calibration technique varied among the laboratories, as did the number of samples measured, and the number of times each sample was measured. The two PAA laboratories also differed mainly in the calibration technique, in the number of samples measured and in the number of repeated measurements.

4. Statistical Analysis

The calibration factor reported in section 5 was computed from the data base of IR and absolute measurements which satisfy certain statistical criteria as outlined in this section. Isolated aberrant measurements and complete results from certain laboratories were excluded. Estimates of precision were generated for both the IR and the absolute measurements. Also considered was whether the assumptions about the uniformity and quality of the sample sets are supported by the experimental results.

Two performance criteria for the absolute laboratories were tested: conformance to a linear model with a zero intercept, and goodness of fit to the linear model. These conditions ensure that a proportionality constant describes the relationship between IR absorbance and oxygen concentration. Laboratories which failed either condition were excluded in the computation of the conversion factor.

4.1 Infrared Data

To validate the data base that was used to compute the net absorption coefficients from the spectral plots, the range or difference between the largest and the smallest of each of the triplicate absorption coefficients was examined for each specimen, and for each laboratory. Coefficients with ranges greater than 0.1 cm^{-1} were checked for mis-recordings, and the data were accordingly corrected or verified as being correct. Coefficients that still showed a range greater than 0.1 cm^{-1} after verification were flagged as "outliers". Twelve measurements out of 1450 were flagged in this manner. A check on the consistency of IR measurements from different laboratories on the same specimens identified three additional

measurements as outliers. All the outliers in the IR measurements were excluded from further analyses. This data exclusion is consistent with the practices for dealing with outliers described in ASTM E 691, Standard Practice for Conducting an Interlaboratory Test Program to Determine the Precision of Test Methods.[25]

The IR data base was restricted to the data obtained for test sets 2, 3, 4, 5, and 6, in order to avoid biasing the results towards the coordinating laboratories (which also measured test sets 1 and 7).

We can test whether the sample sets were substantially identical for the purposes of the experiment. Based upon the measurements on test sets 1 and 7, which were measured by all the coordinating laboratories, the typical variation between test sets could be determined for each oxygen concentration. Note that test sets 1 and 7 are geometrically the farthest apart of any two test sets (see Figure 1b). Since these test sets were measured by the same laboratories, on the same days, the difference between the oxygen content measured on these test sets is a measure of the homogeneity of the crystals' oxygen content. The results, averaged over the five IR laboratories which measured both test sets, are shown in column 3 of Table IV. Figure 2 shows the percentage difference between test set 7 and test set 1, as measured by the IR absorption averaged over all five coordinating laboratories.

We cannot directly test how close the oxygen concentrations of the 10-mm thick slugs were to the oxygen concentrations of the test wafers. Most of the test wafers were taken from either side of the 10-mm slug. Thus the variation between test sets 1, 2, 3, and 4 (which were taken from one side of the slug), and test sets 5, 6, and 7 (which were generally taken from the other side), is an indication of the maximum likely difference in oxygen content between the wafers and the 10-mm slugs.

We show that the test sets did not change as they were circulated among the different IR laboratories. The coordinating laboratories measured each test set circulated in their region both before and after all the other laboratories in the region made their measurements. Thus the differences in the "before" and "after" measurements can be tested for significance. Only seven of the eighty specimens given both "before" and "after" measurements showed a significant apparent change in their oxygen concentration at the 95% probability level. This is hardly more than would be expected to occur at random. Thus, we conclude that the specimens were unchanged with respect to their oxygen concentrations during the time they circulated among the IR laboratories.

The intensity of the oxygen band maximum absorbance is dependent upon the temperature of the specimen. The temperature dependence at about room temperature can be estimated from the data presented in Figure 1a of Hrostowski and Kaiser's classic paper on the infrared absorption of oxygen in silicon.[26] The temperature dependence is roughly linear near 300 K, with a slope of –0.09%/degree. Both the mean and the median temperatures in the spectrophotometer chambers in this round robin were 300 K. The range of temperatures was from 293 to 309 K. Therefore, the warmest laboratory would be in error, due to the temperature difference, by 0.8%, and the coldest by –0.6%. However, since the

temperature dependence is linear, the errors introduced by laboratories above the mean temperature, 300 K, are canceled by the errors introduced by laboratories below the mean temperature. The temperature differences may contribute to the dispersion among the IR laboratories, but will not introduce a bias in the value of the calibration factor.

Finally, we conclude that the test sets did not contain a significant concentration of precipitated oxygen. Test set 8 was used to test this assumption. The absorption coefficients of all the specimens in this test set were measured at the National Bureau of Standards. The test set was then annealed at 1300°C in nitrogen for one hour and then rapidly quenched to room temperature. The absorption coefficients were then measured again on the same spectrometer at NBS. The results of the before-anneal and after-anneal measurements of the oxygen concentration are shown in Table V. These results show that the concentration of noninterstitial oxygen in the specimens was not detectable by this test.

The precision of the infrared measurements was defined at two levels in this study. The first is the ability of a given IR laboratory to make repeatable measurements in the short run (over three days, for most of the data obtained for this study). Table VI shows the standard deviations reflecting the within-laboratory repeatability for each laboratory. The second column shows the results in units of absorption coefficients (cm^{-1}). The absorption coefficients for the 20 crystals range from 0.8 to 4.7, and the average absorption coefficient for the 20 crystals is roughly 3.01. A measure of the within-laboratory precision expressed as the ratio of the standard deviation for each laboratory to the average IR absorption coefficient is listed as a percentage in the third column of Table VI. The within-laboratory precision ranges from 0.4% to 1.2% for all 18 IR laboratories.

The second level of precision is the ability of IR laboratories to agree with one another when making measurements on the same set of samples, as measured by an interlaboratory standard deviation. For each oxygen concentration, these standard deviations were pooled over the seven test sets. Table VII shows the standard deviations reflecting the interlaboratory reproducibility. The third column of this table shows the interlaboratory reproducibility in percentage terms over all the crystals. Systematic differences among IR laboratories exist at the 2% to 3% level, but by using a large number of IR laboratories for this study, a representative result has been obtained. Note that the crystals with the greatest nonuniformity did not show poorer interlaboratory reproducibility for the IR measurements.

As a parenthetical note, we would like to observe that these results, obtained by comparing the best efforts of many infrared laboratories around the world, have clear implications vis-à-vis oxygen measurements at the supplier/user interface. Even under the best of circumstances, a lack of reproducibility on the order of 3% may occur between two different IR laboratories.

4.2 Absolute Data

To validate the absolute data base, two questions must be answered: which individual data points must be excluded as outliers, and how should the overall results from each of

the individual absolute laboratories be evaluated? Large outliers in the absolute analysis data can be identified by ranking the specimens in the order of their infrared absorption coefficients, and then comparing that ranking to the order in which the specimens are ranked by each individual absolute laboratory. This procedure was used to exclude four data points as outliers.

To evaluate the overall results of individual absolute laboratories is more difficult. The measurement of oxygen concentration by an individual absolute laboratory should be related to IR measurement by a linear function with zero intercept. Given that the conditions of linearity and zero intercept hold, the slope of this line defines the calibration factor estimated from the data for this particular laboratory.

Table VIII lists the results of a least squares fit to the absolute data as a function of the IR data, averaged over all IR laboratories. The t statistics[27] in the table are used to judge whether or not a given absolute laboratory has a nonzero intercept. A large value for the t statistic is indicative of a nonzero intercept. Laboratories 22 and 28 show nonzero intercepts which are significant at the 95% probability level. The intercept terms for all other laboratories are not statistically significant. Thus data from laboratories 22 and 28 are excluded from this study based upon their failure to agree with the model requirement for a zero intercept.

The linearity of the data from each absolute laboratory was then tested. Regression analysis was carried out for each absolute laboratory with the IR measurement regarded as the dependent variable and the absolute measurement regarded as the independent variable. This approach takes advantage of the repetitions across IR laboratories on each specimen and evaluates the aptness of the linear model for each absolute laboratory.

If the linear model correctly describes the data, the total mean-squared error will be attributable to replication error, i.e. the replication across IR laboratories as pooled over all specimens. The other possible source of error is the "lack-of-fit" error, i.e., the failure of the average IR values per specimen to fall close to the fitted line. The statistical device for assessing the contribution from lack of fit is an F-test.[28] A large F-statistic indicates a large component for lack of fit, indicating that the linear model does not adequately describe the relationship between IR and absolute measurements.

For the first four entries of Table VIII, only IR data on the test set measured by a given CPAA laboratory were used in the F-test so as not to contaminate the result by inhomogeneities or differences among test sets. For the PAA and IGFA laboratories which measured the 10-mm slugs, the combined IR data from test sets 2, 3, 4, 5, and 6 were used in the analysis.

The F-statistics are listed in Table VIII. The F-statistic for laboratory 25 was computed by excluding anomalous results for two specimens (taken from crystals 2102 and 2105). Exclusion of the data from these two crystals reduced the F-statistic to 12.8. To decide whether this value is reasonable, we compare it with the F-statistic for laboratories 21, 23,

and 26 using the **same** IR data set that we used for laboratory 25. These F-statistics are shown as the last three entries in Table VIII, and are of comparable size. For laboratories 24 and 28, the exclusion of possibly anomalous data for a few crystals failed to reduce the F-statistic to a satisfactory level. Figure 3 is the data from laboratory 28, plotted against the absorption coefficient averaged over all IR laboratories.

The F-statistics, which are listed in Table VIII, are extremely large for laboratories 22, 24, and 28 indicating an egregious lack of fit. Thus, for the purpose of computing the final calibration factor, the absolute data base is restricted to measurements by CPAA laboratories 21, 23, and 26 and PAA laboratory 25. Absolute measurements by CPAA laboratory 22, PAA laboratory 24, and IGFA laboratory 28 are excluded because they failed either the test for linearity or the test for zero intercept or both tests.

The data for laboratory 27 also fit the zero-intercept linear model, as shown by the *t*-statistic and F-statistic for that laboratory in Table VIII. The data from laboratory 27, which measured only the JEIDA specimens, is in excellent agreement with the data on the same specimens from laboratories 21, 23, and 26. Thus, laboratory 27 provided important confirmation of the results of other CPAA laboratories.

5. Calculation of the Calibration Factor

There are two issues which must be resolved before a calibration factor can be calculated from the data in this study. The first issue is whether the calibration factor should be calculated by averaging the IR data over test sets 2, 3, 4, 5, and 6, or by restricting the IR data to the same test sets as the absolute data. If the crystals are sufficiently homogeneous, the first approach is preferable because it includes a wider variety of IR spectrophotometers. This approach was used and includes in the uncertainty of the final calibration factor an allowance for systematic error due to the possible lack of absolute homogeneity in the crystals.

The second issue is how to calculate the final calibration factor. We combined the data from the equivalent absolute laboratories (i.e., laboratories 21, 23, 25, and 26) by fitting the data to the linear model, weighted to account for the dependence of precision on oxygen content, and take the resulting slope as the best estimate of the conversion factor.† This approach assumes that the measurements by all laboratories are consistent and without bias, i.e., a zero intercept and a single slope characterize the relationship between the IR measurements and the absolute measurements.

The least-squares fit confirms that the intercept term is nonsignificant (0.12 ppma with a standard deviation of 0.14 ppma). CPAA laboratories 21 and 23 were the only laboratories

† In fact, because the absolute measurements and the IR measurements are subject to random error, the least-squares estimate of the slope is biased towards zero[29]. However, for this data set, the estimate of the slope is only biased by -0.005 ppma/cm^{-1} which is not significant for this study.

which reported detectable concentrations of oxygen in the "oxygen-free" reference specimens. The average of the oxygen concentrations they reported was 0.06 ppma. This value is very small. For example, it is almost an order of magnitude smaller than the absolute uncertainty in the CPAA measurements reported by laboratory 26, or calculated from the repeated measurements for laboratory 21. Thus it is consistent with the zero intercept model. Moreover, such a small oxygen concentration in the reference specimen would only shift the straight line parallel to itself. It would have no effect on the slope, i.e. no effect on the calibration factor itself.

The final calibration factor is calculated from the linear model restricted to have a zero intercept, using data from all the IR laboratories and data from the absolute laboratories 21, 23, 25, and 26, excluding data taken on the JEIDA test sets. The F statistic for this fit is 0.67, indicating the appropriateness of the restricted linear model. Figure 4 is a plot of the absolute data points used for the determination of the final calibration factor, plotted against the average of the IR laboratory results. The straight line in this figure shows the fit of the data to the restricted linear model.

6. The Calibration Factor

The calibration factor for computing the interstitial oxygen content in parts per million atomic (ppma) from a measurement of the absorption coefficient at about 1107 cm^{-1}, calculated from the data base which includes all 18 participating IR laboratories and the four absolute laboratories whose data fit the restricted linear model, is 6.28 ± 0.18 ppma/cm^{-1}. Absolute laboratories with large biases or nonlinear behavior were excluded. Differences among the remaining laboratories are reflected in the standard deviation of the slope from the fit. The random component of the uncertainty in the conversion factor is taken to be twice the standard deviation of the estimate in the calibration factor, or 0.08 ppma/cm^{-1}. A systematic component to the overall uncertainty is due to the lack of absolute homogeneity in the silicon crystals. This factor is estimated to be 0.10 ppma/cm^{-1}, as explained in the next paragraph. The overall uncertainty is the sum of the random and systematic uncertainties.

The systematic uncertainty was assessed to account for the effect of possible crystal inhomogeneity. This was a potentially important effect, even though all the laboratories measured samples obtained from the same set of 20 crystals. The data from laboratories 21, 23, and 26 provide a means of assessing the contribution to uncertainty from inhomogeneity. For each laboratory, the conversion factor as calculated from the total IR data base was compared to the conversion factor calculated from the IR data base restricted to the same test set subjected to CPAA measurement. On the average, this restriction increased the calibration factor by 0.10 ppma. This increase is due to the inhomogeneity in the ingot, as well as to differences due to the much smaller set of IR laboratories which were included in the restricted data set. The increase can be used as an estimate of the effect of inhomogeneity that contributes a systematic uncertainty of $\pm$ 0.10 ppma/cm^{-1} to the uncertainty in the determination. Note that this estimate is consistent with the finding

of differences in the oxygen content between test set 1 and test set 7 of 1% to 2% for the majority of crystals.

It is recommended that when an oxygen content determination is based upon the use of the calibration factor obtained in this work, 6.28 ± 0.18 ppma/cm^{-1}, its use be denoted by the acronym IOC-88 (International Oxygen Coefficient 1988). The use of this calibration factor should be limited to the range of oxygen concentrations investigated in this paper, 0 to 30 ppma. Oxide precipitation may affect the validity of the calibration factor at higher concentrations.

7. Acknowledgments

The authors of this work wish to express their appreciation for the successful completion of this project to a great number of organizations and individuals. The silicon crystals used for this study were generously supplied by Japan Silicon, Komatsu Electronic Materials, Monsanto Electronic Materials, Osaka Titanium Corporation, Shin-Etsu Handotai, Siltec Silicon, Toshiba Ceramics, and Wacker Chemitronic. Union Carbide supplied the sapphire squares used in the instrumental verification procedure. The authors would like to thank the individual researchers at the IR laboratories: Dr. D. Andrews (General Electric Co., Ltd.), P. Ashby (Mullards, Ltd.), Dr. M. Domenici (Dynamit Nobel Silicon), Dr. K. Graff (Telefunken), Dr. N. Inoue (Nippon Telegraph & Telephone), Li Guang Ping (Tianjin Electronic Materials Research Institute), Lin Yu Ping (Zhejiang University), E. Ohashi (Komatsu Electronic Materials), Dr. B. Pajot (Ecole Normale Supérieure), Dr. L. Shive (Monsanto Electronic Materials), H. Suzuki (Hitachi), and Ye Yu Zong (Shanghai Second Smelting Plant). We would also like to thank those responsible for making the very difficult absolute measurements of the oxygen content of the silicon specimens: Dr. K. Bethge (Institut für Kernphysik, Wolfgang Goethe Universität, Frankfurt), Dr. E. Grallath (Max-Planck-Institut für Metallforschung, Dortmund), Dr. T. Nozaki (Institute of Physical and Chemical Research (RIKEN), Wako, Saitama), Dr. B. Schmitt (Bundesanstalt für Materialprüfung, Berlin), Dr. E. Schweikert (Center for Chemical Characterization and Analysis, Texas A & M University), Dr. J. Stoquert (Centre de Recherches Nucleaires, Strasbourg), Dr. K. Strijckmans (Institute for Nuclear Sciences, Rijksuniversiteit Gent), and Drs. D. Wood and J. Hislop (AERE Harwell, Oxfordshire).

The cooperation of Dr. H. Marchandise and the Community Bureau of Reference (BCR) was very important, as it enabled us to include results obtained at four additional highly skilled laboratories on this project. We would like to give special thanks to Dr. John Mandel, statistician for the National Measurement Laboratory of the National Institute of Standards and Technology, for his contributions to the analysis of the data base.

References

1. W. Kaiser and P.H. Keck, *J. Appl. Phys.* **28**, 882 (1957).
2. W. M. Bullis, M. Watanabe, A. Baghdadi, Li Yue-zhen, R.I. Scace, R.W. Series, and P. Stallhofer, in *Semiconductor Silicon 1986*, H.R. Huff, T. Abe, and B. Kolbesen, editors, The Electrochemical Society (Pennington, New Jersey, 1986), p. 166.
3. M.I. Iglitsin, G.P. Kekelidze, and G.V. Lazareva, Soviet Physics-Solid State **6**, 2508 (1965).
4. G.I Alexandrova, A.M. Demidov, G.A. Kotel'nikov, G.P. Pleshakova, G.V. Suhov, D.Y. Choporov, and G.I. Shmanenkova, *Atomnaya Energiya* **23**, 106 (1967).
5. H.L. Rook and E.A. Schweikert, *Anal. Chem.* **41**, 958 (1969).
6. C.K. Kim, *Radiochem. Radioanal. Lett.* **2**, 53 (1969).
7. J.A. Baker, *Solid State Electronics* **13**, 1431 (1970).
8. C. Gross, G. Gaetano, T.N. Tucker, and J.A. Baker, *This Journal* **119**, 7 (1972).
9. Y. Yatsurugi, N. Akiyama, Y. Endo, and T. Nozaki, *This Journal* **120**, 975 (1973).
10. K. Graff, E. Grallath, S. Ades, G. Goldbach, and T. Tölg, *Solid State Electronics* **16**, 887 (1973).
11. H. He, Y. Li, G. Xhao, R. Yan, Q. Lu, and M. Qi, *Talanta* **30**, 761 (1983); Li Yuezhen and Wang Qimin, *Review of Progress in Quantitative Nondestructive Evaluation*, Vol. 5, 957 (1986).
12. T. Iizuka, S. Takasu, M. Tajima, T. Arai, T. Nozaki, N. Inoue, and M. Watanabe, *Defects in Silicon*, ECS Proceedings Vol. 83-9, p. 265 (1983); ——, *This Journal* **132**, 1707 (1985).
13. H.J. Rath, P. Stallhofer, D. Huber, and B.F. Schmitt, *J. Electrochem. Soc.* **131**, 1920 (1984).
14. K.G. Barraclough, R. W. Series, J.S. Hislop, and D.A. Wood, *This Journal* **133**, 187 (1986).
15. J.L. Regolini, J.P. Stoquert, C. Ganter, and P. Siffert, *This Journal* **133**, no. 10, 2165 (1986).
16. ASTM *Standard Test Method F 121-79 for Interstitial Atomic Oxygen Content of Silicon by Infrared Absorption*, 1979 Annual Book of ASTM Standards, Part 43.
17. DIN Standard 50 438/1, *Determination of Impurity Content in Silicon by Infrared Absorption: Oxygen*, Beuth Verlag GmbH, Burggrafenstrasse 4-10, D-1000 Berlin 30, Federal Republic of Germany.
18. ASTM Method *F 121-83, Standard Test Method for Interstitial Atomic Oxygen Content of Silicon by Infrared Absorption*, 1987 Annual Book of ASTM Standards,

Vol. 10.05.

19. T. Iizuka, private communication.

20. National Institute of Standards and Technology Special Publication 400-82 (July 1989), *Semiconductor Measurement Technology: Data, Procedures, and Statistical Analyses of the Interlaboratory Determination of the Calibration Factor for the Measurement of the Interstitial Oxygen Content of Silicon by Infrared Absorption*, edited by A. Baghdadi, R.I. Scace, and E.J. Walters.

21. W.K. Gladden and A. Baghdadi, in *Emerging Semiconductor Technology*, D.C. Gupta and P.H. Langer, editors (American Society for Testing and Materials, Philadelphia, Pennsylvania, 1987), p. 353.

22. N. Inoue, T. Arai, T. Nozaki, K. Endo, and K. Mizuma, *ibid*, p. 365.

23. N.R. Draper and H. Smith, *Applied Regression Analysis, Second Edition* (John Wiley & Sons, New York, N.Y., 1981), pp. 1-69.

24. ASTM Standard Practices *F 120, Infrared Absorption Analysis of Impurities in Single Crystal Semiconductor Materials*, 1987 Annual ASTM Book of Standards, Vol. 10.05.

25. ASTM Standard Practice *E 691, Conducting an Interlaboratory Test Program to Determine the Precision of Test Methods*, 1987 Annual ASTM Book of Standards, Vol. 14.02.

26. H.J. Hrostowski and R.H. Kaiser, *Phys. Rev.* **107**, 966-972 (1957).

27. N.R. Draper and H. Smith, *Applied Regression Analysis, Second Edition* (John Wiley & Sons, New York, N.Y., 1981), p. 28.

28. *Ibid*, p. 33-40.

29. See W.A. Fuller, *Measurement Error Models* (John Wiley & Sons, New York, N.Y., 1987), p. 13-27.

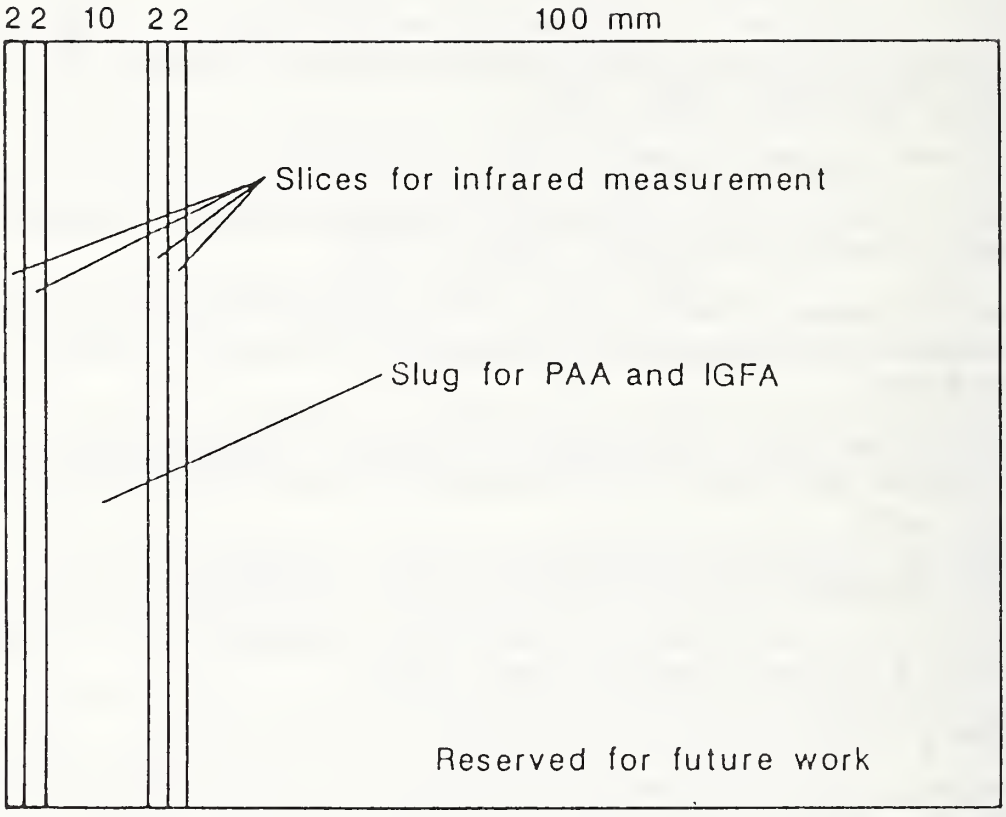

Figure 1a: Schematic of 100-mm diameter silicon crystal showing four 2-mm thick slices for infrared absorption and CPAA measurements, a 10-mm thick slug for PAA and IGFA measurements, and the 100-mm wide section reserved for future work.

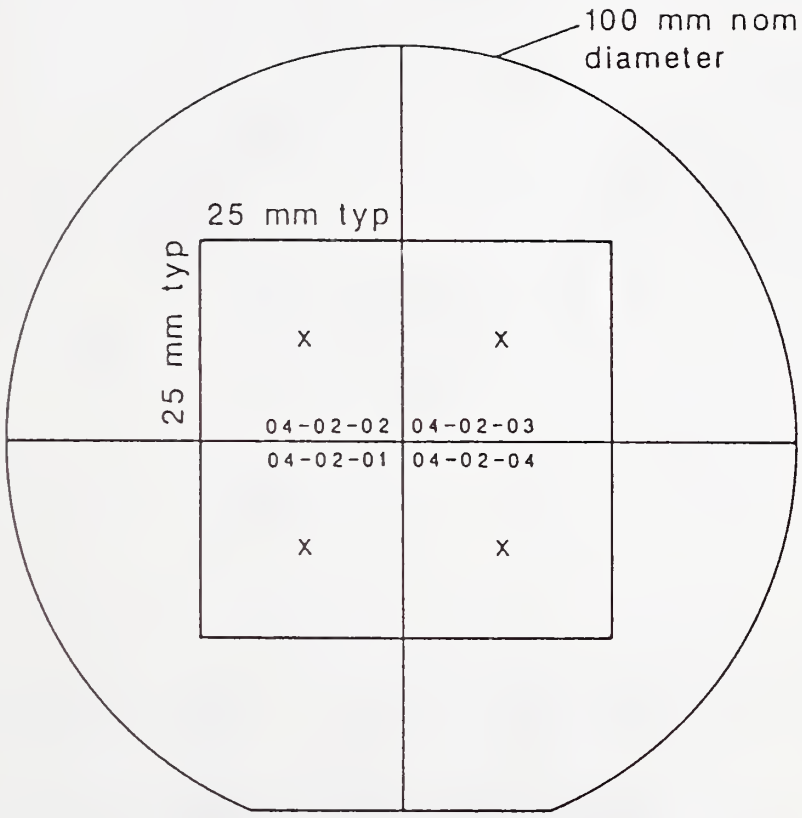

Figure 1b: Diagram of 2-mm thick slice, showing test squares 1 to 4, 25 mm on a side; identification markings (04-02-0x); and the location of the infrared measurements (x). A second similar slice contains tests squares 5 to 8.

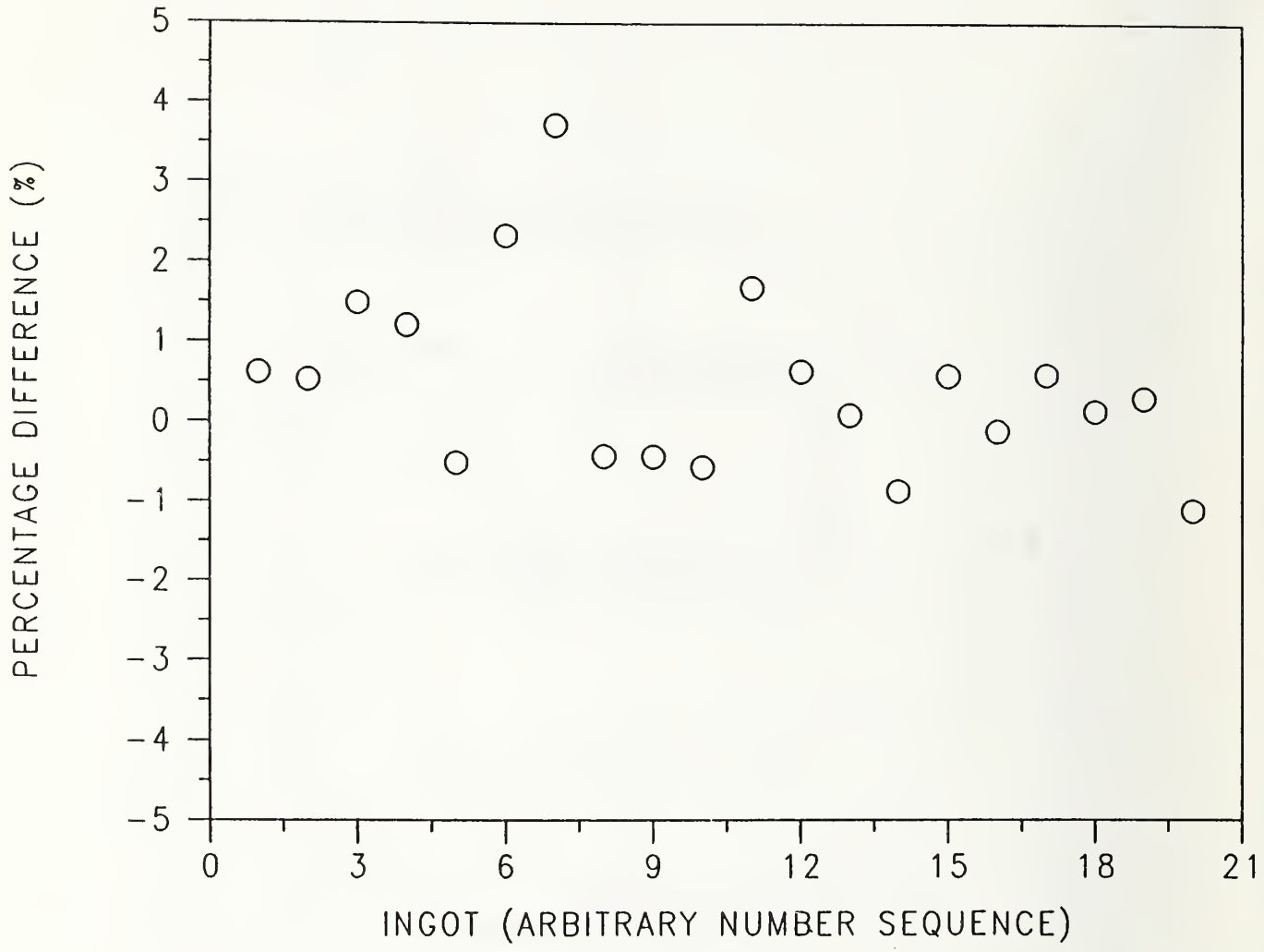

Figure 2: Percentage difference in absorption coefficient between test set 7 and test set 1.

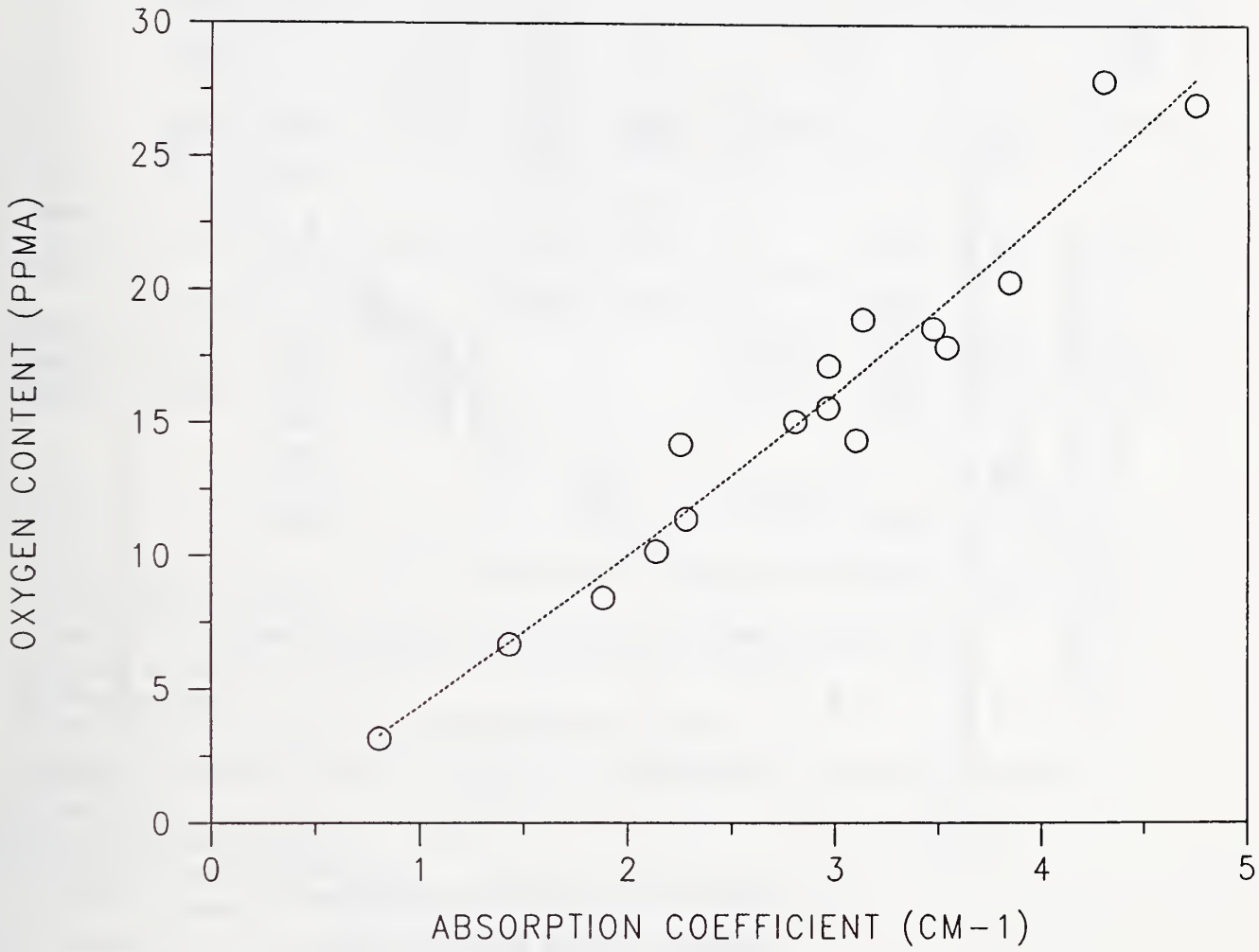

Figure 3: Oxygen content determined by laboratory 28 plotted against the the average of the infrared absorption coefficient for test sets 2, 3, 4, 5, and 6. The dashed line in the figure is a least-squares fit of a second-order polynomial to the data, showing that the data have a nonzero intercept and are not quite linear.

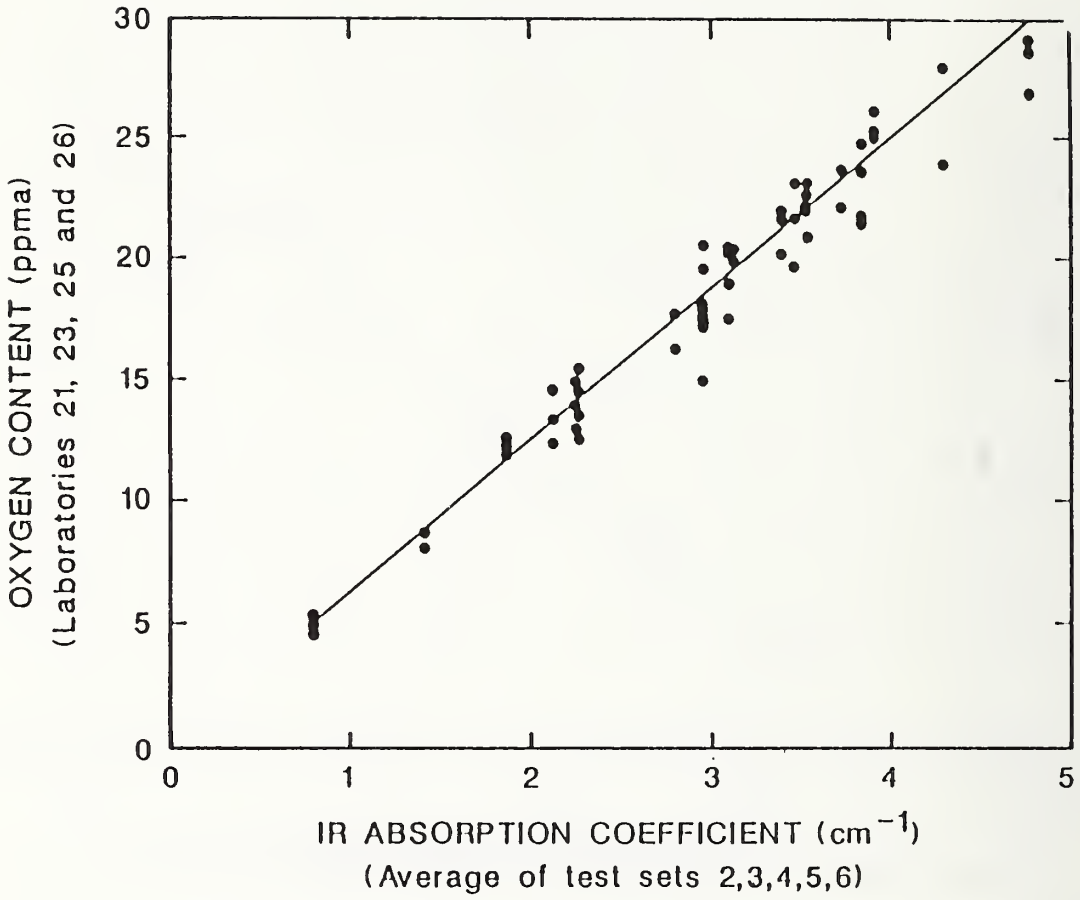

Figure 4: Oxygen content determined by laboratories 21, 23, 25, and 26 plotted against the average of the infrared absorption coefficient for test sets 2, 3, 4, 5, and 6.

TABLE I: EXPERIMENTAL PLAN‡

JEIDA SETS			TEST SETS†						
J-1	J-2	J-3	1	2	3	4	5	6	7
TOS			TOS	TOS					TOS
NTT	NBS		NBS	NTT	NBS				NBS
KOM				KOM					
HIT	MON	WAC	WAC	HIT	MON	WAC			WAC
TOS	SIL			TOS	SIL				
CPAA		TFK		CPAA		TFK			
NBS#	NBS				NBS				
CPAA	RSR		RSR	TOS#	CPAA		RSR		RSR
WAC#		WAC				WAC			
	MUL			NBS@	NBS@		MUL		
CPAA	GEC	SIM	SIM			CPAA	GEC	SIM	SIM
WAC#	RSR	DNS				WAC#	RSR		
CPAA	TOS@	TEM	NBS@			CPAA	DNS	TEM	NBS@
		ZJU					ENS♮	ZJU	
		SSS						SSS	
		SIM				CPAA		SIM	
TOS@		TOS@				NBS@	NBS@	NBS@	

‡ 10-mm slugs cut from ingots were used for destructive PAA measurements in UK and Germany, as well as for IGFA in Germany

† Test set 8 was reserved for high-temperature anneal and remeasure for total oxygen

\# Transit only, no measurements

@ Home location

♮ ENS measured only specimens from ingots 2101-05 to 2109-05

Participating laboratories (Regional coordinators in boldface followed by standards organization):

HIT Hitachi
KOM Komatsu Electronic Metals
NTT Nippon Telegraph and Telephone
TOS **Toshiba Ceramics, JEIDA**
NBS **National Bureau of Standards (U.S.), ASTM**
MON Monsanto
SIL Siltec Silicon
TFK Telefunken
WAC **Wacker Chemitronic, DIN**
DNS Dynamit Nobel Silicon
ENS École Normale Superiéure, Université Paris VII, France
GEC General Electric Company, Ltd.
RSR Royal Signals and Radar Establishment (U.K.)
MUL Mullards, Ltd.
SIM **Shanghai Institute of Metallurgy (Academia Sinica)**
SSS Shanghai Second Smelting Plant
TEM Tianjin Electronic Materials Research Institute
ZJU Zhejiang University

TABLE II: ABSOLUTE MEASUREMENT TECHNIQUES

Laboratory	Method	Separation	Reaction	# Samples	# Meas/sample	Etching	# Calibration Materials	Nominal Energy
Texas A&M	CPAA	no	$^{16}O(^3He,p) \rightarrow ^{18}F$	25	1	18μm	Prev. calib.	14.3 MeV
Frankfurt	CPAA	no	$^{16}O(^3He,p) \rightarrow ^{18}F$	12	1	16μm	SiO_2 Al_2O_3	10 MeV
RIKEN	CPAA	no	$^{16}O(^3He,p) \rightarrow ^{18}F$	27	2-4	23μm	SiO_2	15 MeV
Ghent	CPAA	no	$^{16}O(^3He,p) \rightarrow ^{18}F$	7	2-5	24μm	SiO_2	20 MeV
Strasbourg	CPAA	no	$^{16}O(^3He,p) \rightarrow ^{18}F$	18	3	15μm	Al_2O_3	20 MeV
Harwell	PAA	yes	$^{16}O(\gamma,n) \rightarrow ^{15}O$	12	1	40μm (no sep)	$Li_2B_4O_7$ (incident)	32 MeV
Berlin	PAA	yes	$^{16}O(\gamma,n) \rightarrow ^{15}O$	16	8	60-100μm	BeO	30 MeV
Dortmund	IGFA	yes	—	16	1	25μm	CO	—

TABLE III: SUMMARY OF CALIBRATION FACTOR EXPERIMENTS

Ref	Author	Year	Chem. Analysis Method (a)	No. of Data Pts	Stated Error (Infrared)	Stated Error (Chemical) (b)	Sensitivity Limit (Chem, ppma)	Range of Absorp Coef (cm^{-1}) or Oxygen Conc (ppma) (c)	Calibration Factor (ppma·cm) (c)
1	Kaiser & Keck	1957	VFA	12	(d)	±4	(d)	**0.2–6.4**	5.5 (e)
3	Iglitsyn et al.	1965	LD	8	(d)	(d)	(d)	**0.5–12.4**	12.0±1.4
4	Alexandrova et al.	1967	CPAA	3				**5–10**	(f)
5	Rook & Schweikert	1969	CPAA	4	(d)	±10%	0.01	**4.8–9.4**	5.8±0.5
6	Kim	1969	CPAA	6	(d)	20%	(d)	**6–22**	7.6±1.5
7	Baker	1970	IGA	99	±5%	±3	3	0.3–3.5	9.63±2.29
8	Gross et al.	1972	CPAA	4	(d)	< 10%	0.02	**0.6–20**	7.7±0.4
9	Yatsurugi et al.	1973	CPAA	(g)	(h)	< 10%	0.01	0.1–1.5	6.0 (i)
10	Graff et al.	1973	VFA	12	(d)	±1–4	8	2–4	4.9±0.3
11	He et al.	1983	IGA	67	(d)	(d)	2	0.3–2.8	6.2±0.1
11	He et al.	1983	CPAA	7	(d)	(d)	0.07	0.1–3.3	6.2±0.4
12	Iizuka et al.	1983	CPAA	22	0.5%	±3	10^{-3}	0.8–3.5	6.06±0.05
13	Rath et al.	1984	PAA	8	±2%	±15%	0.1	2–4.6	6.0±0.4
14	Barraclough et al.	1986	PAA	21	< 5%	< 15%	0.6	0.8–3.8	5.2±0.6
15	Regolini et al.	1986	CPAA	7	(d)	(d)	(d)	2-4	6.0±0.4

Notes:

(a) VFA = Vacuum fusion analysis
LD = Lithium diffusion
CPAA = Charged particle activation analysis
IGA = Inert gas fusion analysis
PAA = Photon activation analysis

(b) In ppma unless otherwise stated.

(c) If range is given in ppma (boldface entry), the calibration factor was calculated from infrared absorption results which were reported to be based on the calibration of reference 1. However, since the numerical value of the calibration factor used was not stated, it was taken to be 5.5 ppma·cm.

(d) None stated.

(e) Scaled from published graph. Other values from this work appear in the literature. For example the value scaled from the graph in ASTM F 45 is 5.45 ppma·cm; the value quoted in references 10 and 11 is 5.65 ppma·cm, while reference 6 quotes 5.76 ppma·cm.

(f) Oxygen concentrations derived from CPAA are one-half those derived from infrared measurements with an unspecified calibration factor.

(g) 10 points within range stated used for calibration curve determination; 29 points from 0.1 to 7.5 cm^{-1} shown.

(h) Better than CPAA.

(i) Scaled from published graph.

TABLE IV: PERCENTAGE DIFFERENCE IN THE IR ABSORPTION COEFFICIENT BETWEEN TEST SET 7 AND TEST SET 1, AS MEASURED BY THE COORDINATING LABORATORIES

Oxygen Content (ppma)	Ingot	Average	11	13	16	17	19
4.99	101	0.618	−1.905	0.835	0.614	1.671	1.874
8.76	2101	0.527	1.500	0.874	0.388	−0.259	0.133
11.88	2102	1.113	3.508	2.363	0.724	−2.088	1.059
13.36	201	0.910	0.188	1.012	0.850	1.437	1.062
13.90	1102	−0.507	−0.739	0.345	−0.052	−1.370	−0.720
14.52	2103	2.436	1.534	1.828	2.619	4.768	1.431
17.50	2104	3.719	3.434	3.959	3.823	3.392	3.989
17.90	1101	0.433	−0.788	1.185	0.240	0.988	0.538
19.20	2105	−0.348	−0.880	0.040	−0.033	0.199	−1.067
19.45	401	−0.560	−0.015	−0.556	−1.053	−0.614	−0.560
20.47	301	1.686	1.606	2.174	1.037	2.618	0.994
21.61	1204	0.638	1.433	0.933	1.286	−1.359	0.897
21.66	2106	0.093	−0.272	0.564	0.613	−0.339	−0.099
21.98	1203	−0.854	−1.062	−0.584	−0.672	−0.860	−1.094
22.40	1201	0.587	0.725	0.482	0.316	1.103	0.307
23.05	501	−0.107	0.464	0.183	−0.039	−0.875	−0.269
23.59	2107	0.598	1.103	0.768	0.130	1.238	−0.251
25.23	1202	0.143	0.439	0.593	0.078	−0.608	0.213
27.95	2108	0.304	−0.531	0.479	0.492	1.760	−0.678
28.28	2109	−1.161	−0.267	−1.327	−2.809	−0.264	−1.138

TABLE V: THE EFFECT OF HIGH-TEMPERATURE ANNEALING ON THE MEASURED INFRARED ABSORPTION COEFFICIENT
(at 1107 cm^{-1})

ID	Post1 α (cm^{-1})	Post2 α (cm^{-1})	Post3 α (cm^{-1})	Pre1 α (cm^{-1})	Pre2 α (cm^{-1})	Pre3 α (cm^{-1})	Post/ Pre (cm^{-1})
210108	1.4288	1.3735	1.3800	1.3618	1.4041	1.3854	1.0075
210208	1.8270	1.9310	1.8641	1.8239	1.8743	1.9124	1.0021
210308	2.2072	2.2459	2.3120	2.2040	2.2117	2.2786	1.0106
210408	2.7782	2.7650	2.6718	2.7048	2.7249	2.7210	1.0079
210508	3.1787	3.1737	3.2144	3.1011	3.1281	3.1465	1.0204
210608	3.3974	3.4150	3.4091	3.4086	3.4485	3.4691	0.9899
210708	3.8922	3.9206	3.9050	3.8508	3.8043	3.8430	1.0191
210808	4.2430	4.2942	4.2632	4.2793	4.2680	4.3030	0.9961
210908	4.7098	4.7381	4.6664	4.7109	4.8121	4.8043	0.9851
110108	2.9882	2.9927	2.8955	2.9433	2.9576	2.9395	1.0041
110208	2.2115	2.2595	2.2017	2.2631	2.2568	2.2612	0.9840
120108	3.7064	3.7576	3.7568	3.6809	3.6982	3.7235	1.0106
120208	3.9940	3.9807	4.0064	3.9156	3.9411	3.8977	1.0193
120308	3.4531	3.5191	3.5380	3.5020	3.5213	3.5392	0.9950
120408	3.3934	3.3932	3.3706	3.3172	3.3727	3.4142	1.0053
10108	0.7940	0.7705	0.7683	0.7884	0.7911	0.8026	0.9793
20108	2.0787	2.0645	2.1321	2.1144	2.1180	2.1198	0.9879
30108	3.0921	3.0956	3.1082	3.0391	3.0527	3.0751	1.0141
40108	2.9476	2.9455	2.9308	2.9089	2.9656	2.9514	0.9998
50108	3.5803	3.5680	3.6012	3.4802	3.5131	3.5449	1.0200

(The disagreement between the post- and pre-anneal absorption coefficients ranges from −2% to +2%, with an overall average of 0.3%).

TABLE VI: POOLED STANDARD DEVIATIONS REFLECTING THE WITHIN-LABORATORY REPEATABILITY OF THE MEASUREMENT OF THE IR ABSORPTION COEFFICIENT

Laboratory	Standard Deviation	Ratio of S.D. to Average (%)	Degrees of Freedom
1	0.03265	1.1	52
2	0.02552	0.8	54
3	0.01313	0.4	12
4	0.01824	0.6	54
5	0.02736	0.9	26
6	0.02942	1.0	54
8	0.03642	1.2	54
9	0.02761	0.9	54
10	0.02352	0.8	54
11	0.02225	0.7	184
12	0.03144	1.0	52
13	0.01809	0.6	188
15	0.01552	0.5	54
16	0.01518	0.5	188
17	0.03446	1.1	176
18	0.02802	0.9	48
19	0.01293	0.4	184
31	0.01749	0.6	9

TABLE VII: TOTAL STANDARD DEVIATIONS REFLECTING DISPERSION AMONG THE IR LABORATORIES

Crystal	Total Standard Deviation		Degrees of Freedom*
	Absorption Coefficient (cm^{-1})	Percentage	ν
2101	0.0376	2.6	21
2102	0.0543	2.9	21
2103	0.0559	2.4	21
2104	0.0678	2.4	21
2105	0.0712	2.2	21
2106	0.0823	2.4	21
2107	0.0881	2.3	20
2108	0.1081	2.5	20
2109	0.1451	3.0	17
1101	0.0619	2.1	19
1102	0.0523	2.3	19
1201	0.0905	2.4	19
1202	0.0944	2.4	19
1203	0.0866	2.4	19
1204	0.0787	2.3	20
0101	0.0255	3.1	20
0201	0.0470	2.2	20
0301	0.0760	2.4	20
0401	0.0669	2.2	19
0501	0.0858	2.4	20

* Note that formulas have been adjusted for missing data and/or outliers.

TABLE VIII. RESULTS OF FIT OF IR DATA AS A LINEAR FUNCTION OF THE ABSOLUTE DATA FOR EACH ABSOLUTE LABORATORY

Absolute Laboratory	Absolute Test Set	IR Test Set	Intercept	t Statistic	F Statistic
21	2	2	−0.037	−0.27	1.9
22	3	3	2.391	3.32[a]	155.3
23	4	4	−0.151	−0.23	5.9
26	4	4	0.239	1.50	1.6
24[c]	10-mm slug	2,3,4,5,6	−0.268	−0.26	285.9
25[b]	10-mm slug	2,3,4,5,6	−0.009	−0.08	12.8
28[c]	10-mm slug	2,3,4,5,6	−1.302	−2.95[a]	164.6
27	J-1	J-1	−0.037	−0.21	3.9
21	2	2,3,4,5,6	−0.022	−0.15	15.9
23	4	2,3,4,5,6	−0.161	−0.25	70.6
26	4	2,3,4,5,6	0.370	1.86	26.0

[a] Values of the t statistic which show a significant nonzero intercept at the 95% probability level.

[b] Crystals 2102 and 2105 were excluded from this analysis.

[c] Crystal 1102 was excluded from this analysis.

NBS-114A (REV. 2-8C)

U.S. DEPT. OF COMM. BIBLIOGRAPHIC DATA SHEET (See instructions)	1. PUBLICATION OR REPORT NO. NIST/SP-400/82	2. Performing Organ. Report No.	3. Publication Date July 1989

4. TITLE AND SUBTITLE

Semiconductor Measurement Technology: Database for and Statistical Analysis of the Interlaboratory Determination of the Conversion Coefficient for the Measurement of the Interstitial Oxygen Content of Silicon by Infrared Absorption

5. AUTHOR(S)

A. Baghdadi, R. I. Scace, and E. J. Walters, editors

6. PERFORMING ORGANIZATION (If joint or other than NBS, see instructions)

NATIONAL INSTITUTE OF STANDARDS AND TECHNOLOGY
(formerly NATIONAL BUREAU OF STANDARDS)
U.S. DEPARTMENT OF COMMERCE
GAITHERSBURG, MD 20899

7. Contract/Grant No.

8. Type of Report & Period Covered

Final

9. SPONSORING ORGANIZATION NAME AND COMPLETE ADDRESS (Street, City, State, ZIP)

Same as Item #6

10. SUPPLEMENTARY NOTES

Library of Congress Catalog Card Number: 89-600739

☐ Document describes a computer program; SF-185, FIPS Software Summary, is attached.

11. ABSTRACT (A 200-word or less factual summary of most significant information. If document includes a significant bibliography or literature survey, mention it here)

This Special Publication contains the data collected for the worldwide, double-round-robin determination of the conversion coefficient used to calculate the interstitial oxygen content of silicon from infrared absorption measurements. It also contains detailed statistical analyses of those data. A paper describing the results of this study has been accepted for publication by the Journal of the Electrochemical Society. It should be considered the official result of the study. The approach taken to determine the conversion coefficient was to conduct interlaboratory round robins for both the infrared measurements and the absolute measurements. The infrared measurements were carried out at 18 laboratories in China, Europe, Japan, and the United States, using either dispersive infrared (DIR) or Fourier transform infrared (FTIR) spectrometers. The absolute measurements were carried out at eight laboratories in Europe, Japan, and the United States, using either charged-particle activation analysis, photon activation analysis, or inert gas fusion analysis.

12. KEY WORDS (Six to twelve entries; alphabetical order; capitalize only proper names; and separate key words by semicolons)

charged-particle activation analysis; conversion coefficient; IR database; inert gas fusion analysis; infrared spectroscopy; oxygen in silicon; photon activation analysis; statistical analysis

13. AVAILABILITY

☒ Unlimited

☐ For Official Distribution. Do Not Release to NTIS

☒ Order From Superintendent of Documents, U.S. Government Printing Office, Washington, D.C. 20402.

☒ Order From National Technical Information Service (NTIS), Springfield, VA. 22161

14. NO. OF PRINTED PAGES

179

15. Price

USCOMM-DC 6043-P80

☆U.S. GOVERNMENT PRINTING OFFICE: 1989-242-311/04070

NIST Technical Publications

Periodical

Journal of Research of the National Institute of Standards and Technology—Reports NIST research and development in those disciplines of the physical and engineering sciences in which the Institute is active. These include physics, chemistry, engineering, mathematics, and computer sciences. Papers cover a broad range of subjects, with major emphasis on measurement methodology and the basic technology underlying standardization. Also included from time to time are survey articles on topics closely related to the Institute's technical and scientific programs. Issued six times a year.

Nonperiodicals

Monographs—Major contributions to the technical literature on various subjects related to the Institute's scientific and technical activities.

Handbooks—Recommended codes of engineering and industrial practice (including safety codes) developed in cooperation with interested industries, professional organizations, and regulatory bodies.

Special Publications—Include proceedings of conferences sponsored by NIST, NIST annual reports, and other special publications appropriate to this grouping such as wall charts, pocket cards, and bibliographies.

Applied Mathematics Series—Mathematical tables, manuals, and studies of special interest to physicists, engineers, chemists, biologists, mathematicians, computer programmers, and others engaged in scientific and technical work.

National Standard Reference Data Series—Provides quantitative data on the physical and chemical properties of materials, compiled from the world's literature and critically evaluated. Developed under a worldwide program coordinated by NIST under the authority of the National Standard Data Act (Public Law 90-396). NOTE: The Journal of Physical and Chemical Reference Data (JPCRD) is published quarterly for NIST by the American Chemical Society (ACS) and the American Institute of Physics (AIP). Subscriptions, reprints, and supplements are available from ACS, 1155 Sixteenth St., NW., Washington, DC 20056.

Building Science Series—Disseminates technical information developed at the Institute on building materials, components, systems, and whole structures. The series presents research results, test methods, and performance criteria related to the structural and environmental functions and the durability and safety characteristics of building elements and systems.

Technical Notes—Studies or reports which are complete in themselves but restrictive in their treatment of a subject. Analogous to monographs but not so comprehensive in scope or definitive in treatment of the subject area. Often serve as a vehicle for final reports of work performed at NIST under the sponsorship of other government agencies.

Voluntary Product Standards—Developed under procedures published by the Department of Commerce in Part 10, Title 15, of the Code of Federal Regulations. The standards establish nationally recognized requirements for products, and provide all concerned interests with a basis for common understanding of the characteristics of the products. NIST administers this program as a supplement to the activities of the private sector standardizing organizations.

Consumer Information Series—Practical information, based on NIST research and experience, covering areas of interest to the consumer. Easily understandable language and illustrations provide useful background knowledge for shopping in today's technological marketplace.

Order the **above** *NIST publications from: Superintendent of Documents, Government Printing Office, Washington, DC 20402.*

Order the **following** *NIST publications—FIPS and NISTIRs—from the National Technical Information Service, Springfield, VA 22161.*

Federal Information Processing Standards Publications (FIPS PUB)—Publications in this series collectively constitute the Federal Information Processing Standards Register. The Register serves as the official source of information in the Federal Government regarding standards issued by NIST pursuant to the Federal Property and Administrative Services Act of 1949 as amended, Public Law 89-306 (79 Stat. 1127), and as implemented by Executive Order 11717 (38 FR 12315, dated May 11, 1973) and Part 6 of Title 15 CFR (Code of Federal Regulations).

NIST Interagency Reports (NISTIR)—A special series of interim or final reports on work performed by NIST for outside sponsors (both government and non-government). In general, initial distribution is handled by the sponsor; public distribution is by the National Technical Information Service, Springfield, VA 22161, in paper copy or microfiche form.

U.S. Department of Commerce
National Institute of Standards and Technology
(formerly National Bureau of Standards)
Gaithersburg, MD 20899